# Chapter 1 Introduction

Zinc oxide (ZnO) was a II-VI group semiconductor with a hexagonal wurtzite structure (Fig1-1). Zinc oxide (ZnO) is a wide direct band gap (3.37eV) and large exciton binding energy (60meV) material. It attracts much attention for many application, like ultraviolet (UV) laser devices [1], transparent conduction thin films, field emission display [2], solar cells [3] and etc..

There are many methods to fabricate the ZnO nanowires, like Vapor-Liquid-Solid (VLS) [4], chemical vapor deposition (CVD), molecular beam epitaxy (MBE) [5], pulsed laser deposition (PLD) [6] and hydrothermal methods [7]. Some of them need catalysts, high temperature and good air flow. And as the times advances , the energy resources are more and more important. In order to reduce the power consumption and easy method to fabricate the ZnO nanowires, the hydrothermal method is employed.

ZnO is the powerful material for ultraviolet (UV) laser devices. By the thermal process after fabricating, the optical properties of ZnO nanowires can be improved. It also can make the defect of ZnO nanowires less. And by the effect of doping some elements , the band gap of ZnO nanowires can be tuned and the intrinsic propertities may be changed. As the band gap changes , the optical properties of cathodluminescence (CL) spectrum will change. It affects not only in the ultraviolet (UV) region , but also in the visible light region. So the doping ZnO nanowires can be applied for the tunable ultraviolet (UV) laser devices .

# Chapter 2 Reviews of zinc oxide

Since the carbon nanotubes (CNTs) were discovered in 1991, the worldwide nanotechnology research has been quite extensive on the one-dimensional (1D) nanostructures, such as CNTs , oxide nanobelts (or nano ribbons) , and nanowires .

In recent years, nanotechnology is very important. There are many kinds of materials are used in the nanodevice , like carbon , ZnO and GaAs , etc . The III-VI group semiconductor are most used for the light emittering diodes (LED) . As new materials are found , the II-VI group semiconductor is noticed .

Current trends in nanotechnology and nanomaterials play an important role in the potential applications of photonic, electrooptical and electronic devices because of their unique physical and chemical properties .

## 2.1 The properties of zinc oxide

Zinc oxide (ZnO) was a II-VI group semiconductor with a hexagonal wurtzite structure . It has high melting point (1975℃) and high thermal stability . Its molecular mass is 81.39 . Its specific heat is 0.125 cal/gm . And its thermal conductivity is 0.006 cal/cm/K . The hexagonal wurtzite structure is composed of Bravais lattice and basis . The bravais lattices of hexagonal wurtzite structure are t1 = a/2 (1, $3^{1/2}$, 0), t2 = a/2 (-1, $3^{1/2}$, 0), t3 = c (0, 0, 1) . The basis of hexagonal wurtzite structure are d1 = (0, 0, 0) , d2 = (0, 0, uc) , d3 = (0, a/$3^{1/2}$, c/2) , d4 = (0, a/$3^{1/2}$, uc+c/2) , where a and c are the lattice

constants, (The lattice constants of ZnO are : a = 3.25 Å, c = 5.21 Å) and u is a dimensionless parameter (u = 0.345 for ZnO) . The lattice ZnO structure was seen in figure 2-1 . The ratio of c/a is 1.633 which is nearly perfect . The hexagonal wurtzite structure is a composite crystal structure because there are four atoms in the primitive unit cell ( primitive unite cell contains just one lattice point ) . [9]

Zinc oxide (ZnO) had wide direct band gap (3.37eV) and large excitonic binding energy (60 meV) at room temperature . So zinc oxide (ZnO) was extensively used in short wavelength light emitting diode , ultraviolet laser and transparent conducting electrodes . The large excitonic binding energy (60 meV) leads to extreme stability of excitons , and enables devices to function at a low threshold voltage. A lower threshold optical pumping density for lasing is due to the carrier confinement effect in 1D nanowires. Therefore, it has great potential applications for short wavelength photonic devices.

Because of the large excitonic binding energy (60 meV) , the light efficiency of zinc oxide (ZnO) was higher than other general materials . Due to its superior conducting properties based on oxygen vacancies, ZnO has been investigated as transparent conducting and piezoelectric materials for fabricating solar cells, electrodes, and sensors. Aligned ZnO nanowires could be used as good field electron emitters because they have high aspect ratios, negative electron affinity and high chemical stability. The high aspect ratio of these materials makes them genuine candidates of election field emission due to the tip geometry and the apex structure, which are essential to the field emission properties .

## 2.2 The doped-properties of the zinc oxide

To enhance the electrical and optical properties , ZnO was frequently doped with the group III, IV, and V elements (e.g., Al, Ga, In, Sn, and Sb ) . The Al doping increases the

conductivity without impairing the optical transmission and is regarded as a potential alternative candidate for indium-tin-oxide (ITO) materials . The Ga is another excellent dopant in increasing the conductivity , and the source is less reactive and more resistive to oxidation . In-doped ZnO films show similar electrical conductivity and better transparency in both the visible and the infrared regions as compared to ITO , so they can be widely used as transparent conductors in many applications . The Sn-doping increases rather the resistivity of ZnO film and induces an emission at blue wavelength region . The grain size and resistivity of ZnO were controlled by the doping levels of Sb [8].

## 2.3 The growth method of the ZnO nanowires

Various kinds of ZnO nanostructures such as nanorods, nanowires, nanobelts, nanotubes, nanobridges, nanonails, nanowalls, nanorings , etc. have been realized using several techniques including VLS (vapor-liquid-solid) method , metalorganic chemical vapor deposition , thermal evaporation , template method , and hydrothermal method .

### 2.3.1 VLS (vapor-liquid-solid) method

The VLS (vapor-liquid-solid) method was that the equal amounts of ZnO powder and graphite were milled, then loaded into an alumina boat and placed in the center of a quartz tube . And then used $N_2$ and Ar as the carrier gas . As the temperature is increased to the reaction temperature, the ZnO was reduced by graphite and CO(g) . The gaseous products produced by reactions (1) and (2) would adsorb and condense on the catalytic droplets. And then grew to ZnO nanowires . Subsequently, The following reaction (3) is catalyzed by the metal droplets at solid–liquid interface. The corresponding chemical reaction can be shown in figure 2-2 .

$$ZnO(s) + C(s) \rightarrow Zn(g) + CO(g)\,, \quad (1)$$

$$CO(g) + ZnO(s) \rightarrow CO_2(g) + Zn(g)\,. \quad (2)$$

$$Zn(g) + CO(g) \rightarrow ZnO(s) + C(s)\,, \quad (3)$$

$$C(s) + CO_2(g) \rightarrow 2CO(g)\,. \quad (4)$$

Various vapor-phase methods such as the vapor-liquid-solid epitaxial (VSLE) , pulsed laser deposition (PLD) , and metal-organic chemical vapor deposition (MOCVD) have been successfully used to grow oriented ZnO nanowire arrays at temperatures of 800-900°C. In order to lower the temperature of the growth , the ZnO nanowire can dope some impurity like tin (Sn) and indium (In) . It can low the temperature of the growth about 500-600℃. The VLS (vapor-liquid-solid) method needed catalysts like aurum (Au) and copper (Cu) . The control of the flow rate was very important . It affected the length, diameter and the density of the ZnO nanowires.

The introduction of catalysts or templates to the reaction system involves a much more complicated process and may result in impurity in the final product. Besides, the ZnO nanorods or nanowires obtained by the VLS growth process are usually interwoven together and formed bundles with some junctions. The poor dispersion of ZnO nanorods or nanowires synthesized by the VLS process may limit their practical applications .

## 2.3.2 The template method

The template method [35] uses the porous $Al_2O_3$ substrate be the template of the ZnO nanowires . It can use many methods like CVD , sol-gel , hydrothermal method to fill the hole of the $Al_2O_3$ template . The structure is the polycrystal . And the diameter and the length of the ZnO nanowires is the the diameter of the hole and the thickness of the Al thin film , respectively . After filling , use the solution of NaOH to remove the $Al_2O_3$ template . It is also used extensively .

## 2.3.3 The hydrothermal method [29,30,31,34]

The hydrothermal method was the cheapest method to grow zinc oxide (ZnO) nanowires . The hydrothermal process has several advantages over other growth processes such as catalyst-free growth, low cost, large area uniform production, environmental friendliness, and low reaction temperature to integrate into the microelectronics and plastic electronics . The common growth temperature of the ZnO nanowires was below 100℃. It did not think over the air flow. The template with ZnO seeding layer was put into an aqueous solution of the zinc nitrate hexahydrate ( $Zn(NO_3)_2 \cdot 6H_2O$ (99.9% purity) ) and the hexa-methylenetetramine ( HMT; $C_6H_{12}N_4$, (99.9% purity) )in a sealed vessel . The growth process is shown in figure 2-3 .

The hydrothermal method is based on the formation of solid phase from a solution , which involves two steps as nucleation and growth . In the nucleation , the clusters of molecules formed undergo rapid decomposition and particles combine to grow up to a certain thickness of the film by heterogeneous reactions at the substrate surface.

For our deposition of ZnO film, zinc nitrate hexahydrate ( $Zn(NO_3)_2 \cdot 6H_2O$ (99.9% purity) ) is used as source of zinc. When hexamethylenetetramine ( HMT ; $C_6H_{12}N_4$, (99.9% purity) ) was added to the solution, no precipitate occurs as they were mixed together initially. With the increase of temperature, the HMT begins to decompose into ammonia and then Zn $(OH)_2$ occurred . For this solution was heated , precipitation on the substrate forms ZnO nuclei , thus ZnO film grows from the nuclei on the substrate. These can be represented by the following reactions:

$$(CH_2)_6N_4 + 6H_2O \rightarrow 6HCHO + 4NH_3 \quad (1)$$

$$NH_3 + H_2O \leftrightarrow NH_4^+ + OH^- \quad (2)$$

$$2OH^- + Zn^{2+} \rightarrow Zn(OH)_2 \quad (3)$$

$$Zn(OH)_2 \rightarrow ZnO_{(S)} + H_2O \quad (4)$$

So the synthesis of one-dimensional ZnO nanostructures by wet chemical approach without involving catalysts or templates provides a promising option for the large-scale production of well-dispersed one-dimensional nanostructured materials .

## 2.4 The optical properties of the zinc oxide

Recently, Huang *et al.* demonstrated a UV nanolaser at room temperature using highly oriented ZnO nanowire arrays. ZnO generally reveals *n*-type conduction with a typical carrier concentration of $10^{17}$ /$cm^3$, which is smaller than the carrier concentration of $10^{18}$ to $10^{20}$ /$cm^3$ in laser diode applications.

The strong exciton binding energy of ZnO (~60 meV) is much larger than that of ZnSe (~22 meV) and GaN (~25 meV), also larger than the thermal energy of ZnO (~26 meV) , which are favorable for obtaining an efficient excitonic laser action at room temperature. So ZnO is a good candidate for blue-UV emission optoelectronic devices. The optical spectrum is shown in figure 2-4.

Zinc oxide (ZnO) generally had two kinds of emission manner. One was the ultraviolet emission (UV emission) , the other was the green emission. The ultraviolet emission (UV emission) was related to the conduction band and valence band of zinc oxide (ZnO) . The mechanism of the emission is shown in figure 2-5 . The green emission was related that the electron transition from valence band to the energy band of impurity . If the component , structure and defects changed , the characterization of emission changed .[33]

The green emission [36] (519 nm) originates from the oxygen vacancies according to the result of Vanheusden et al. [10]. By full-potential linear muffin-tin orbital method , the green emission of ZnO is because that the oxygen interstitials (Oi) occupy the zinc vacancies ($V_{Zn}$) to form the defect of antisite oxide ($O_{Zn}$) . The kind of defect is easily formed because the antisite oxide has relatively low formation energy . It is shown in

figure 2-6 . All the prepared films are n-type and the majority donors are oxygen vacancies (Vo) and zinc interstitials (Zni). It is proved that the singly ionized oxygen vacancy is responsible for the green emission and this emission results from the recombination of a photogenerated hole with a singly ionized charge state of this defect. The more are singly ionized oxygen vacancies are, the stronger the luminescence intensity is. [11]

Figure 2-5 shows the mechanism of the photoluminescence . The excitation of zinc oxide (ZnO) was the photon excite the electrons from valence band to excited state . And use the combination of electrons and holes to release the photon , heat or another form of energy . The exciting energy which was higher than the energy level of ZnO make the electrons of the sample absorb the illuminant energy and then jump to higher level . After that it would spontaneously jump to the low level . And then release the energy in the form of light . When there exists another energy state between excited state and the valence band , for example : donor level or accepter level . The excited form was from the valence band to the excited state and then from the excited state to donor level or accepter level and the last to the valence band . The form would make the FWHM value increase . Besides , as the carrier concentration increases , the excited state would approach the conduction band . At last , it would form the degeneration phenomenon . The luminescence efficiency of the compound may be inversely proportional to the number of the defect . When the electron is excited to the excited state , if have too many defects between the excited state and the valence band , the electron is easy to be absorbed in the defect , the part electrons can not combine with the holes in the valence band . So they make luminescence efficiency reduce and influence the power of intensity .

Oxygen vacancies in ZnO can occur in three different charge states：the $V_{\Phi}$ state which has captured two electrons and is neutral relative to the lattice, the singly ionized

$V_O^{\bullet}$ state, and the $V_O^{\bullet\bullet}$ state which did not trap any electron and is doubly positively charged with respect to the lattice. The $V_\Phi$ state is assumed to be a very shallow donor [12]. The description is shown in figure 2-7 .

# Chapter 3 Experiments

## 3.1 The process of experiment

### 3.1.1 The process of the pure ZnO nanowires

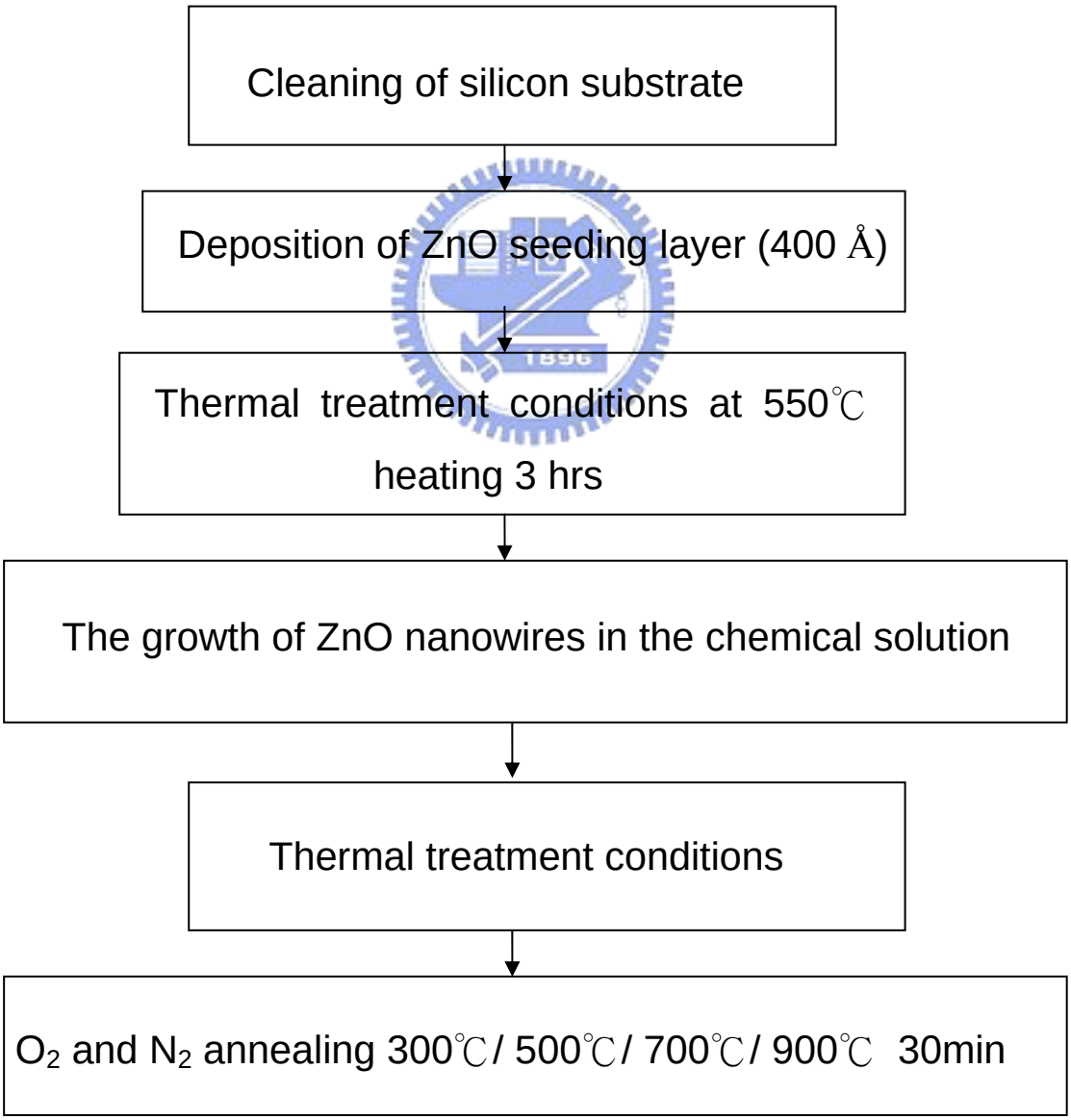

### 3.1.2 The process of the Al-doped ZnO nanowires

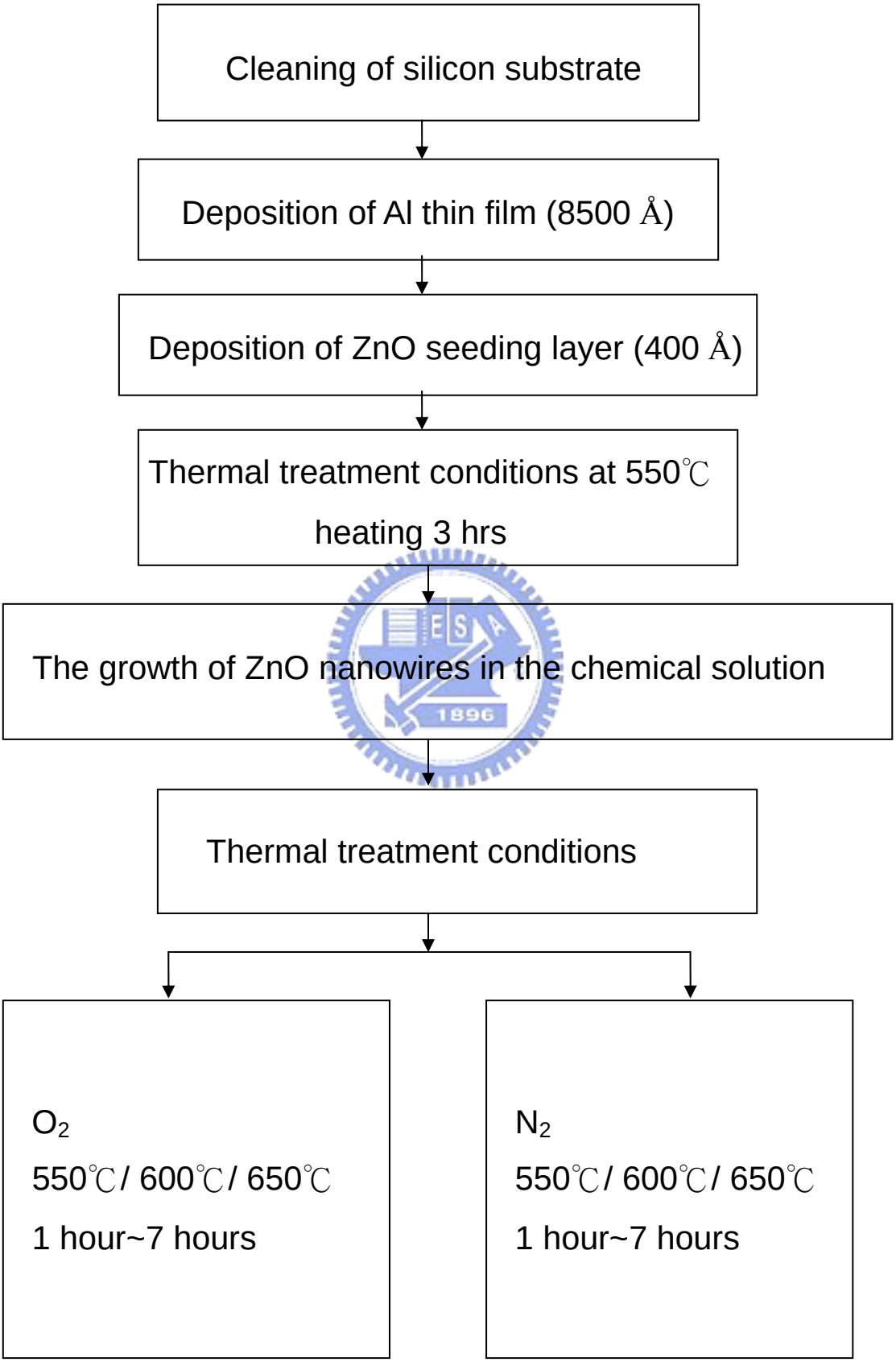

## 3.2 Preparation of the Si substrate and the ZnO target

In the experiment, the p-type Si (100) substrate was cleaned by a standard Radio Corporation of America (RCA) cleaning method and rinsed in acetone for 30 min. to remove native oxide from the surface of Si substrate.

The pure ZnO target was made by the ZnO powders . The ZnO powders were first dry ball-milled for thirty minutes and wet ball-milled in alcohol for 24 hours to ensure the powders were uniform . After the milling, put the binder into the ZnO powders and mill again . After the milling, put it in the 2.5 inch pattern and press the pattern to 15000 p.s.i. for 1 min . Finally , the stressed powders were put into the oven to sinter at 1300℃ for 4 hours . After sintering, grind the target into 2 inch in diameter . Then plaster the ZnO target and copperplate with Ag glue . After that put into the oven to sinter for 1 day .

## 3.3 Deposition of the ZnO seeding layer

The ZnO seeding layer was deposited by the radio frequency (RF) magnetron sputtering system (30W at $2x10^{-2}$ torr for 40 min ) and in-situ annealing at 550℃ for 3hrs . The thickness of the ZnO seeding layer was about 400 Å . The annealing ambient was nitrogen and oxygen . The epitaxial ZnO seeding layer had a dominant orientation along (002) . The structure was as below ：

| ZnO seeding layer (400 Å) |
| --- |
| Silicon substrate |

## 3.4 Synthesized of the pure ZnO nanowires on Si wafer

After the thermal process , the Si substrate with ZnO seeding layer was put into an

aqueous solution of zinc nitrate hexahydrate ( $Zn(NO_3)_2 \cdot 6H_2O$ ( 99.9% purity ) ) and hexamethylenetetramine ( HMT ; $C_6H_{12}N_4$, ( 99.9% purity ) ) in a sealed vessel at 95℃ heating for 3 hours. The concentration of zinc and amine were fixed at 0.1mol/dm3 (0.1M). The pH value of the concentration was about 6.6 . The structure was as below :

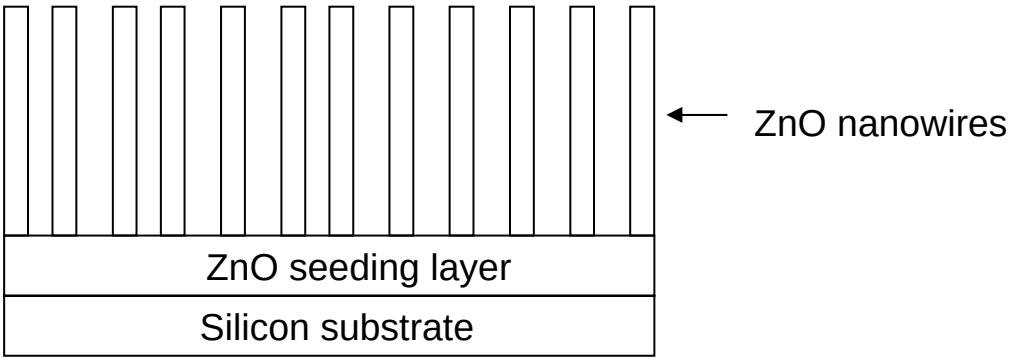


## 3.5 Synthesized of Al-doped ZnO nanowires on Si

The aluminum thin film was deposited on the silicon wafer by the thermal coater method . The thickness of aluminum thin film was about 8500 Å . After deposition of aluminum thin film , the ZnO seeding layer was deposited on the aluminum thin film .The ZnO seeding layer was deposited by rf-sputtering (30W at $2x10^{-2}$ torr for 40 min ) and in-situ annealing at 550℃ for 3 hrs . The thickness of the ZnO seeding layer was 400 Å . The Si substrate with aluminum thin film and the ZnO seeding layer was put into an aqueous solution of zinc nitrate hexahydrate ( $Zn(NO_3)_2 \cdot 6H_2O$ (99.9% purity ) ) and hexamethylenetetra- mine ( HMT; $C_6H_{12}N_4$, (99.9% purity) ) in a sealed vessel at 95℃ heating for 3 hours . The concentration of zinc and amine were fixed at 0.1mol/dm3 (0.1M ). The pH value of the concentration was about 6.6 . After the ZnO nanowires was formed , use the diffusion method to make aluminum diffuse from the aluminum thin film to ZnO nanowires . The diffusion temperature was from 550℃ to 650℃ . The

diffusion time was from 1 hour to 7 hours . The diffusion atmosphere was oxygen and nitrogen . The structure was shown in figure 3-1 .

## 3.6 The experimental equipment

### 3.6.1 RF Magnetron Sputter System

RF magnetron Sputter was a kind of equipment used for thin film process . Utilize the electric field to produce electrons between the two poles , the accelerate electrons collide with the inert gas and make the inert gas take positive electricity . These particles with positive electricity will be attracted to strike the negative pole by the negative pole (target) , the incidence ion (usually with the argon ) gets momentums by the electric field to strike the atoms of the target surface, these atoms are shifted by the momentum that the collision of the straight ionization son get the incidence ion, because the momentum which accepts the incidence ion of target material surface atom struck , put atoms and lead to the fact to the target material surface that it makes it shift to extrude, this target material multi-layer atom pinch , will produce vertical target effort , material of surface collide out the surface atom under the surface, these collide into atom (on the way in line to is it lead positive electricity to collide neutral argon atom ) that go out, deposit and form the membrane on the base plate (positive pole ) at last .

### 3.6.2 Thermal coater

The thermal coater relatively is easy by principle . The metal that used for the melting evaporation directly is hung in heating the tungsten filament by way of line material , as soon as heated melting, because of the liquid surface tension , will seek connections with heating the tungsten filament , then steaming slowly it for four weeks (include brilliant and round) . Because heat the heat-resisting ability of the tungsten

filament and for the metal to melt the liquid to seek connections with the space limitedly , the metal only used in the low point is plated, such as the aluminium , and it is limited to steam the thickness . Have the so-called ladder that is covered and wrapped to plate the law basically to steam (step coverage ) shortcoming not good . Function to put argon for let metal atom in steam in plating colliding with argon member, and then reduce the kinetic energy of the metal and atom, lower its speed which becomes membrane, it is smaller particle when and can make into the membrane , increase into the membrane and cause the density .

### 3.6.3 Oven

In order to grow the ZnO nanowire , the oven is used . The setting temperature is 92.5 ± 2.5℃ .

## 3.7 The measured equipment and parameters

### 3.7.1 FE-SEM

The surface structural and morphology analysis of the ZnO nanowires and the Al-doped ZnO nanowires was observed by field emission scanning electron microscopy ( FE-SEM, Hitachi S-4700I, Japan ) . The measured pressure was at 2 x $10^{-6}$ Torr. The working voltage was 15 KeV. The working current was 10μA..

### 3.7.2 TEM and EDX

The structure and morphology analysis of ZnO nanowires was measured by the high resolution transmission electron microscopy ( HR-TEM, JEOL JEM-2010 ) . The TEM is the equipment which produces the diffractive and scattering electrons by the interaction

between substances and electrons . And by the selected area electron diffraction (SAED) , it shows the crystalline structure of the ZnO nanowires , The HR-TEM shows that the lattice constants of the ZnO nanowires . In order to measure the aluminum content in the Al-doped ZnO nanowires , the EDX of the TEM is used . The fixed quantity analysis of the EDX is also used for the quantity of Zn , Al and O .

Ths preparation of the TEM samples are put in the ultrasonic vibration . The rate of the vibration is about 14000 rpm . The vibration time is 3~5 minutes . And then put it on the copper ring .

### 3.7.3 Cathodluminescence (CL)

The optical properties are measured by the Cathodluminescence spectrum ( CL, JEOL JSM6500F, Japan ) with an electron beam as an excitation source (15 KV) at room temperature . Cathodluminescence was a kind of nonsubversive optical measurement. By the analysis of Cathodluminescence (CL) spectrum , it can measure the band gap of solid materials and devices , and the defects and impurity of the materials . Different materials had different excitation source . When the light illuminates the sample , the photon energy makes the electron of atom jump from ground state to excited state. Because the excited state was very unstable , the electron would subsequently jump to ground state. Between the transition of electron , the redundant energy would release in the form of heat energy or photon energy. The released energy was called the photoluminescence.

The Cathodluminescence spectrum is mainly used for measuring the optical spectrum. The excitation source is 15 KV. And the value of the photomultiplier tube (PMT) is -800V. The sweeping range is from 350nm to 700nm. The sweeping rate was 2nm per second.

### 3.7.4 X-ray Diffraction (XRD)

The crystal structure of the ZnO nanowires and the Al-doped ZnO nanowires was observed by the X-ray diffraction ( XRD, MAC Science, MXP18, Japan ). X-ray diffraction (XRD) was the equipment most used for identifying the crystal structure. If the included angle θ (Bragg`s angle) between the crystal plane and the incident light matched the Bragg`s law ($n\lambda=2d\sin\theta$) , the incident light was diffracted by the crystal plane .By using Bragg`s law for diffraction , the reflected x-rays from the respective atomic planes can be measured by the detector .In the Bragg`s law ($n\lambda=2d\sin\theta$) , $n\lambda$ is an integral number of wavelengths , and d is the distance between two successive crystal planes .

The X-ray diffraction measurement with Cu Kα radiation ($\lambda=1.5418$ Å ) was operated at 30KV and 20mA . In order to avoid the peak of silicon at about 70° , the angle 2θ of the measurement was from 30° to 60° . The sweeping rate was 4° per minute .

# Chapter 4 Results and discussion

## 4.1 The pure ZnO nanowires

### 4.1.1 Characterization of the ZnO seeding layer

The thickness and the qualities of the ZnO (002) seeding layer must be suitable . As long as the ZnO seeding layer deposited on any substrate , the ZnO nanowires can grow on it .

If the thickness of the ZnO (002) seeding layer was too thick , it offered enough seeds for ZnO nanowires to grow , but the thick ZnO (002) seeding layer may be have low adsorption . So the the thick ZnO (002) seeding layer was easy to be washed away by the D.I. water . If the thickness of the ZnO (002) seeding layer was too thin , it can not offer enough seeds for ZnO nanowires to grow . So the ZnO nanowires can not grow on the ZnO (002) seeding layer.

The epitaxial ZnO seeding r layer was deposited by the rf-sputtering (30W at $2x10^{-2}$ torr for 40 min at room temperature ) . The thickness of the epitaxial ZnO seeding layer was about 40 nm , which had a dominant orientation along (002) . Figure 4-1 shows the SEM image of the ZnO seeding layer grown on the Si substrate .

After the epitaxial ZnO seeding layer was deposited , anneal the the epitaxial ZnO seeding layer at 550℃ for 3 hours . The flow rate of the annealing atmosphere was about 30 sccm . Because the epitaxial ZnO (002) seeding layer was deposited at room temperature , the quality of the epitaxial ZnO seeding layer was not good enough . Figure

4-2 shows the XRD patterns of the ZnO seeding layer after annealing at 550℃ for 3hr . It implied that the crystallinity of the ZnO thin film has good orientation along (002) after annealing at 550℃ for 3hr.

## 4.1.2 Characteristic analysis of the pure ZnO nanowires

The ZnO nanowires was synthesized by the hydrothermal method . The variable of the hydrothermal method was the concentraton of the solution , the growth temperature and the growth time . Because the the environment of the hydrothermal method was in the chemical solution , the pH value is very important . The source of the hydrothermal method was zinc nitrate hexahydrate ( $Zn(NO_3)_2 \cdot 6H_2O$ (99.9% purity) ) and hexamethylenetetramine ( HMT ; $C_6H_{12}N_4$, (99.9% purity) ) . The chemical solution was mixed with the ratio of 1:1 . In order to check the formation of the compound in the chemical solution , the relation between pH value and the kind of compound was shown in figure 4-3 . The figure 4-3 was the pourbaix diagram for zinc. From the pourbaix diagram , the pH value of the solution must control between 6 and 14 . If the pH value of the solution was not between 6 and 14 , there were many other compounds produced . The compounds included $Zn^{2+}_{(aq)}$ , $Zn_{(s)}$ and $Zn(OH)_4^{2-}{}_{(aq)}$ .

## (1) The pH value of the solution.

In order to check the formation of $Zn(OH)_2$ in different concentration of the solution , the pourbaix diagram was used . In the experiment , the concentration of chemical solution was from 0.08M to 0.16M . In order to check to pH value of the growth concentration fit it with the formation of $Zn(OH)_2$ . The pH value was measured by the HANNA M-5-23 . From the Table 4-1 , the pH value of the concentration from 0.08M to 0.16M before growing is between 6 and 14 . So in the experiment , they can grow ZnO

nanowires . The pH value of the concentration after growing is lower than that before growing . The growth time may be arrived the maximum value . And exceed the the maximum growth time , the ZnO nanowires can not grow .

## (2) The chemical solution concentration

As raising the concentration of the chemical solution under the same growth time , the density of the ZnO nanowires become higher and higher . When the concentration of the chemical solution was 0.16M , the density of the ZnO nanowires was high to nearly become the ZnO thin film . And as raising the concentration of the chemical solution , the length of the ZnO nanowires was almost the same . It can be explained that the ZnO source in chemical solution was enough for the ZnO nanowires to grow in 3 hours . The surface morphologies of the ZnO nanowires in different concentration of the chemical solution under the same growth time were shown in figure 4-4. Figure 4-5 shows the crystallinity of the ZnO nanowires in different concentration of the chemical solution under the same growth time . From the figure 4-5 , it implies that the ZnO nanowires in different concentration of the chemical solution under the same growth time still had the maximum peak of orientation along (002) .

## (3) The growth time

Different ZnO seeding layer had different ZnO nanowires growth time . In the experiment , the growth time of the ZnO nanowires was above 2 hours . From 2 hours to 3 hours, the density of the ZnO nanowires become more and more . The morphologies of the ZnO nanowires in the same concentration of the chemical solution under different growth time were shown in figure 4-6 . Figure 4-7 shows the growth rate [32] of the ZnO nanowires . From the figure 4-7 , it shows that the ZnO nanowires grow rapidly after 90

mins . Figure 4-8 shows the crystallinity of the ZnO nanowires in the same concentration of the chemical solution under different growth time. From the figure 4-8 , it implies that the growth time of ZnO nanowires from 1 hour to 1.5 hours had weak peak of (002) . And the growth time of ZnO nanowires from 2 hour to 3 hours had strong peak of (002) .

## (4) The TEM analysis

Figure 4-9 displays cross-sectional TEM images of the ZnO nanowires grown on Si template . Figure 4-9(b) shows HRTEM image of the ZnO nanowires , illustrating the growth orientation . As shown in the figure 4-9(b) , the ZnO nanowires grew uniformly along the [002] lattice frings of the ZnO nanowires is 2.60 Å . The corresponding selected area electron diffraction (SAED) pattern of the hydrothermally grown ZnO nanowires is shown in figure 4-9(c) . It shows that the ZnO nanowires is a single-crystalline structure . Figure 4-9(d) is the EDX spectrum of the ZnO nanowire . In the spectrum , Zn and O was the signal of the ZnO nanowires . The C and Cu was the signal of the cupper ring .

## (5) The optical properties

Figure 4-10 shows the cathodluminescence (CL) spectra of the ZnO nanowires . From figure 4-10 , the peak of UV was at about 376 nm . By the equation 4-1 , the band gap was 3.30 eV . It is different that the ZnO band gap was 3.37 eV . Because the 3.37 eV was the band gap between the valence band and the conduction band . And the 3.30 eV was the band gap between the valence band and the excited state . The cathodluminescence (CL) mainly measured the signal from the valence band to the excited state .

When the ZnO nanowires formed , the surface of the ZnO nanowires was very

unstable . It is easy to adsorb the steam and the impurities in the air to passivate the surface of the ZnO nanowires to the stable state . In the macroscope , the surface of the ZnO nanowires was smooth , but in the microscope , the surface of the ZnO nanowires was rough . And the steam and the impurities in the air adsorbed on the surface of the ZnO nanowires were called the surface defects . The defects of the ZnO nanowires are the radiative defects and the nonradiative defects . The radiative defects were Vo , $Zn_i$ , $V_{Zn}$ , $O_i$ and $O_{Zn}$ . The nonradiative defects were the surface defects , the lattice defects and etc. . And the detected signal of the cathodluminescence (CL) included the surface state and the inner defects . And the steam and the impurities in the air may decrease the UV peak and increase the luminescence intensity .

By the hydrothermal method , the chemical component of the ZnO nanowires was nonstoichiometric , and usually consisted of excess Zn atoms and oxygen vacancies . They also make the UV intensity lower and luminescence higher .

From figure 4-10 , it can find that the signal of the UV peak is lower than that of the visible light region . It means that the defects in the ZnO nanowires are very much . In order to check what kind of defects in the ZnO nanowires , the figure 2-6 is used . The main peak of the visible light region is at about 575 nm (2.16 eV ) . By the figure 2-6 , the deep-level emission is caused by the energy interval between the Vo level (1.62 eV ) and the $O_i$ level (2.28 eV) .

### 4.1.3 The optical properties of the pure ZnO nanowires after the thermal treatment under different atmospheres

In order to decrease the defects of the ZnO nanowires , the thermal process is needed . Figure 4-11 shows the cathodluminescence (CL) spectra of the ZnO nanowire under the different annealing temperature in oxygen atmosphere . The annealing time is

30 min . When the thermal process temperature rises from 300℃ to 700℃ , the intensity of the UV peak rises slowly . At the 900℃ , the intensity of the UV peak rises fast . The luminescence of the ZnO nanowires is shown in figure 4-12 . By the thermal process , the intensity of the luminescence is the same as the background signal . But the intensity of the luminescence at 900℃ is higher than another . By the figure 2-6 , it was induced by the effect of the $O_{Zn}$ .

Figure 4-13 shows the cathodluminescence (CL) spectra of the ZnO nanowire under the different annealing temperature in nitrogen atmosphere . The annealing time is also 30 min . When the thermal process temperature rises from 300℃ to 700℃ , the intensity of the UV peak rises slowly . It is the same as that in the oxygen atmosphere . At the 900℃ , the intensity of the UV peak rises fast . The luminescence of the ZnO nanowires is shown in figure 4-14 . By the thermal process , the intensity of the luminescence is the same as the background signal . But the intensity of the luminescence at 900℃ is higher than another . By the figure 2-6 , it was also induced by the effect of the $O_{Zn}$ . But the intensity of the $O_{Zn}$ was lower than that in the oxygen atmosphere . And the intensity of the luminescence in the oxygen is lower than that in the nitrogen atmosphere . It is due that the quantity of the oxygen vacancies in the oxygen atmosphere is less than that in the nitrogen atmosphere .

The ratio of $I_{UV}/I_{DLE}$ after annealing in oxygen atmosphere and nitrogen atmosphere is shown in Figure 4-15 . As the thermal process temperature increases in the oxygen stmosphere , the $I_{UV}/I_{DLE}$ ratio also increases . It can be explained that the oxygen vacancies can be repaired in the oxygen atmosphere . But at 900℃ , the optical properties of the ZnO nanowires increase slowly because of the formation of $O_{Zn}$ . In the nitrogen atmosphere , the $I_{UV}/I_{DLE}$ ratio also increases with the thermal process temperature . It can be explained that the surface state is repaired by the nitrogen ions and the Vzn , Vo , Zni , Oi and $O_{Zn}$ restructure as the annealing temperature . But at 900℃ ,

the optical properties of the ZnO nanowires increase slowly because of the formation of $O_{Zn}$ .

From the figure 4-15 , it shows that the ratio of $I_{UV}/I_{DLE}$ in the oxygen atmosphere is higher than that in the nitrogen atmosphere . It is because that the formation rate of the oxygen ions is higher than that of the nitrogen ions and the oxygen vacancies in oxygen atmosphere are lower than in the nitrogen atmosphere . As the annealing temperature increases , the quantity of the oxygen ions increases .

Figure 4-16 shows the cathodluminescence (CL) spectra of the ZnO nanowires under the different annealing temperature in oxygen atmosphere in the visible light region . From the figure 4-16 , the peak position shifts from 575 nm to 625 nm . From the figure 2-6 , the energy level of 2.16 eV was between the Vo level (1.62 eV ) and the $O_i$ level (2.28 eV) . And the energy level of 1.99 eV was also between the Vo level (1.62 eV ) and the $O_i$ level (2.28 eV) . But it is near the Vo level . It may mean that after the thermal process , the quantities of Vo are more than that of Oi . The Oi may replace the Vo and the oxygen ions repair the oxygen vacancies after the thermal process . So the quantilities of Oi decrease and the oxygen vacancies decrease .

Figure 4-17 shows the cathodluminescence (CL) spectra of the ZnO nanowires under the different annealing temperature in nitrogen atmosphere in the visible light region . From the figure 4-17 , the peak position also shifts from 575 nm to 625 nm . From the figure 2-6 , the energy level of 2.16 eV was between the Vo level (1.62 eV ) and the $O_i$ level (2.28 eV) . And the energy level of 1.99 eV was also between the Vo level (1.62 eV ) and the $O_i$ level (2.28 eV) . But it is near the Vo level . It may mean that after the thermal process , the quantities of Vo are more than that of Oi . The Oi may replace the Vo and the oxygen ions repair the oxygen vacancies after the thermal process . So the quantilities of Oi decrease and the oxygen vacancies decrease .

## 4.2 The Al-doped ZnO nanowires

### 4.2.1 The hydrothermal method to form Al-doped ZnO nanowires

The source of the ZnO nanowires was the deposition of $Zn(OH)_{2\,(s)}$ and the source of Al was $Al(OH)_{3\,(s)}$ . So the hydrothermal method to form Al-doped ZnO nanowirs must think over the solubility product constant (Ksp) . The solubility product constant is shown as follows :

$Zn(OH)_2$ : $Ksp=1.6x10^{-16} = [Zn^{+}]\,[OH^{-}]^{\,2}$

$Al(OH)_3$ : $Ksp=1.6x10^{-34} = [Al^{3+}]\,[OH^{-}]^{\,3}$

The solubility product constant (Ksp) was related to the deposition rate . The lower Ksp value represents the faster deposition rate . Because the difference of the solubility product constant (Ksp) is very much , it make the deposition rate of the $Al(OH)_3$ faster than that of the $Zn(OH)_2$ . And the solution of the $Al(OH)_3$ also affects formation of the ZnO nanowires . The ionic radius of Al is 0.057nm and the ionic radius of Zn is 0.083 nm . The difference of the ionic radius between Al and Zn is more than 15 % , so it is hard to substitute . And the different valance of the two elements , different structures of the two elements and no appreciable difference in the electronegativities of the two elements also cause the Al is hard to substitute for Zn .

### 4.2.2 The formation and the diffusion mechanism of Al-doped ZnO nanowires

In order to ensure the structure of the ZnO nanowires formed , the ZnO nanowires

must grow first by hydrothermal method . Because the hydrothermal method is hard to form the structure of Al-doped ZnO nanowires , the diffusion method of aluminum was used . The diffusion precess was shown in figure 4-18 .

First , the aluminum thin film was deposited on Si substrate . The thickness of the aluminum thin film was about 8500 Å . The aluminum thin film was the source of the Al-doped ZnO nanowires . The principle of the diffusion method utilizes that the ionic radius of aluminum is smaller than the grain boundary size of the ZnO seeding layer and the diffusion takes place more rapidly along grain boundaries than in the grain matrix .

Aluminum ions can move in crystal lattices from one ionic site to another if there is enough activation energy provided by the thermal vibration of the aluminum ions and if there are vacancies or other crystal defects in the lattice for aluminum ions to move into . As the diffusion temperature of the aluminum increases , more vacancies are present and more thermal energy is available , and so the duffusion rate is higher at higher temperature . The aluminum ions move radiatively under the high temperature . And as the annealing time become longer , the aluminum ions have enough energy move to the ZnO nanowires . But because of the solid solubility of aluminum in the ZnO , the content of the aluminum in the ZnO nanowire was very little . In the experiment , the maximum thermal process temperature was 650℃ , because the melting point of aluminum was 660℃ .

The ZnO nanowire is the single crystal structure . By the semiconductor process , after the ion implantation , the metal ions may radiatively diffuse to the silicon by the thermal process . The diffusion quantity of the aluminum may rest with the ZnO and the aluminum . As the thermal process time increases , the diffusion quantity that aluminum diffuse into the ZnO nanowires may not increase . But the aluminum which has been in the ZnO nanowires can diffuse more far as the thermal process time increases .

The lattice constants of ZnO nanowire are a=b=3.23 Å and c=5.21 Å . The ion

radius of zinc is 0.083 nm , the ion radius of oxygen is 0.132 nm and the ion radius of aluminum is 0.057 nm . The covalent bond of the Zn-O is 0.197 nm . Because the difference of the ionic radius between Al and Zn is more than 15 % , so it is hard to substitute . Although it is hard to substitute , the substitution may happen as the thermal process temperature or time increases . The primitive unit cell of the ZnO structure was shown in figure 4-19 .

### 4.2.3 The various thermal treatment in oxygen atmosphere

After the growth of ZnO nanowires , the sample was put into the 2-inch ceramic furnace . The carrier gas was oxygen . The air flow was 10 sccm . The thermal process temperature was 550℃ , 600℃ and 650℃ . The thermal process time was 1 hour , 3 hours , 5 hours and 7 hours .

#### 4.2.3.1 The optical properties of the Al-doped ZnO nanowires

The UV emission is due to the band edge emission of the ZnO nanowires . The UV photo photoluminescence characteristic reveals the Stoke`s shift of the solid solution [14] . The ultraviolet (UV) emission peak of ZnO is generally attributed to the exciton-related activity [22] , and the deep level emission may be due to the transitions of native defects such as oxygen vacancies and zinc interstitials [23] . The imperfect boundaries and stacking faults of ZnO nanowires would cause the unstable surface states to trap impurities and further damage the optical property, especially as the diameter of ZnO nanowires was down to nano scale [24] .

Figure 4-20 shows the the cathodluminescence (CL) spectra of Al-doped ZnO nanowires at 550℃ under different thermal process time in the oxygen atmosphere . From figure 4-20 , the ZnO nanowires emit a strong emission at 376 nm . By the equation

4-1 , the band gap of the ZnO was 3.30 eV .

The equation 4-1 was shown as follows :

$$E = hv = hc / \lambda = 6.626 \times 10^{-34} \times 3 \times 10^{17} / \lambda \quad ( J )$$

$$\therefore E = 1.242375 \times 10^{3} / \lambda \quad (eV) \qquad \textbf{(eq.4-1)}$$

where E is the energy , h is the planck`s constant , and v is the frequency .

From figure 4-20 , when the ZnO nanowires was formed , the intensity of the UV peak is lower than that of the luminescence peak . By the hydrothermal method , the chemical component of the ZnO nanowires was nonstoichiometric , and usually consisted of excess Zn atoms and oxygen vacancies . It can be explained that the quantities of the defects in the ZnO nanowires are very much . The defects include the radiative defects and nonradiative defects . The radiative defects are Vo , $Zn_i$ , $V_{Zn}$ , $O_i$ and $O_{Zn}$ . The nonradiative defects are the surface defects , the lattice defects and etc. . The surface defects of the ZnO nanowires include the steam and the impurities in the air . The peak position of the luminescence is at 575 nm . By full-potential linear muffin-tin orbital method, Sun [20] calculated the energy levels of the intrinsic defect in ZnO films . Figure 2-6 shows the result . It can find that the peak of the deep-level emission is caused by the energy interval between the Vo level (1.62 eV ) and the $O_i$ level (2.28 eV) .[21]

When the thermal process time is 1 hour , the UV peak of the Al-doped ZnO nanowires was at about 376 nm and the intensity of the UV peak is higher than the ZnO nanowires . It is because that the defects of the surface state are reduced and the oxygen vacancies are repaired . The defects of the surface state are repaired by the oxygen ions . By the thermal process , the steam and the impurities on the surface of the ZnO nanowires can be removed . And the oxygen ions can adsorb the surface of the ZnO nanowires . But the quantities of the oxygen ions are not very much at 550℃ heating 1 hour . After the thermal process finish , the steam and the impurities in the air will adsorb

the surface of the ZnO nanowires again . So the surface of the ZnO nanowires includes the oxygen ions , steam and the impurities in the air . But the repaired results improve the intensity of the UV peak . The shift of the UV peak was not noticeable . It is because the content of Al in the ZnO nanowires was not very much and the resolution of the cathodluminescence (CL) spectra was hard to detect .

Figure 4-21 shows the magnification of figure 4-20 from 450 nm to 700 nm . The intensity of the luminescence in the visible light region is lower than the ZnO nanowires . It is due to that when the thermal process time was 1 hour in the oxygen atmosphere , the oxygen vacancies decrease and the defects of the surface state corporately contribute to the lower intensity of the luminescence in the visible light region . Although the Al in the ZnO nanowires may be taken as the defects , it affects the intensity of the luminescence lightly .

And in the visible light region , the luminescence sfifts from 575 nm to 625 nm (from 2.16 eV to 1.99 eV ) . From the figure 2-6 , the energy level of 2.16 eV was between the Vo level (1.62 eV ) and the $O_i$ level (2.28 eV) . And the energy level of 1.99 eV was also between the Vo level (1.62 eV ) and the $O_i$ level (2.28 eV) . But it is near the Vo level . It may mean that after the thermal process , the quantities of Vo are more than that of Oi . The Oi may replace the Vo and the oxygen ions repair the oxygen vacancies after the thermal process . So the quantilities of Oi decrease and the oxygen vacancies decrease .

When the thermal process time is 3 hours , the intensity of the UV peak is higher than that the thermal process time was 1 hour . It is due to that the defects of the surface state and the oxygen vacancies are repaired more completely . The intensity of the luminescence is lower than that the thermal process time was 1 hour . It is demonstrated that the more oxygen vacancies are also repaired in the oxygen atmosphere . Although the quantities of the Al in the ZnO nanowires also increase , it affects the intensity of the

luminescence lightly .

When the thermal process time is 5 hours , the nonradiative defects forms . And when the thermal process time increases , the grain size decreases and the content of Al in the ZnO nanowires increases [25] . The smaller grain size has larger nonradiative relaxation rates over the surface states [26]. Although the oxygen ions also repair the defects of the surface state , the formation of the nonradiative defects decrease the UV intensity more . So they reduce the intensity of the UV peak . In the visible light region , the luminescence is still lower than that the thermal process time is 3 hours . It is because that the defects of the surface state and the oxygen vacancies decrease in the oxygen atmosphere . So it makes the luminescence in the visible light region lower than 3 hours . Although the Al in the ZnO nanowires may be taken as the defects , it affects the intensity of the luminescence lightly .

When the thermal process time is 7 hours , the intensity of UV peak is lower than 5 hours . It is because the nonradiative defects increase . And when the thermal process time increases , the grain size decreases and the content of Al in the ZnO nanowires increases . The smaller grain size has larger nonradiative relaxation rates over the surface states . Although the oxygen ions repair the defects of the surface state , the formation of the nonradiative defects decrease the UV intensity more . So they reduce the intensity of the UV peak . In the visible light region , the luminescence is still lower than 5 hours . It is because that the defects of the surface state and the oxygen vacancies decrease in the oxygen atmosphere . So it makes the luminescence in the visible light region lower than 5 hours . Although the quantities of the Al in the ZnO nanowires also increase , it affects the intensity of the luminescence lightly .

Figure 4-22 shows the the cathodluminescence (CL) spectra of Al-doped ZnO nanowires at 600℃ under different thermal process time in the oxygen atmosphere . From figure 4-22 , when the thermal process time is 1 hour , the UV peak of the

Al-doped ZnO nanowires was still at about 376 nm and the intensity of the UV peak is higher than the ZnO nanowires . It is also because that the quantities of the oxygen ions were more than that at 550℃ . The defects of the surface state are reduced more completely . Figure 4-23 The magnification of figure 5-22 from 450 nm to 700 nm . From figure 4-23 , in the visible light region , the luminescence also shifts from 575 nm to 625 nm . And the intensity of the luminescence was lower than the ZnO nanowires . It is the same that when the diffusion temperature increases , the oxygen vacancies decrease and the repaired defects of the surface state also corporately contribute to the intensity of the luminescence in the visible light region lower than ZnO nanowires . Although the Al in the ZnO nanowires may be taken as the defects , it affects the intensity of the luminescence lightly .

When the thermal process time is 3 hours , the intensity of the UV peak is lower than that the thermal process time was 1 hour . The luminescence is lower than that the thermal process time was 1 hour . It is demonstrated that the defects of the surface state decrease with the diffusion temperature . But when the diffusion temperature increases , the formation time of the nonradiative defects is faster . It is due that the high diffusion temperature provides high energy to form the nonradiative defects in the oxygen atmosphere . And the formation probability of the nonradiative defects in the oxygen atmosphere was higher than that in the nitrogen atmosphere . Because the decay time in the oxygen atmosphere is lower than that in nitrogen atmosphere [27] . For temperature higher than 450℃ , more defects responsible for the nonradiative transition will be introduced into the films [28] .

When the thermal process time is from 5 hours to 7 hours , the quantities of the nonradiative defects increase , so the intensity of UV peak decrease as the thermal process time . And the formation of the nonradiative defects at 600℃ was faster than that at 550℃ . Although the oxygen ions also repaired the surface of the ZnO nanowires , the

formation of the nonradiative defects decrease the UV intensity more . The visible light region shows that the intensity of luminescence emission at 600℃ is lower than that at 550℃ . It can be explained that when the diffusion temperature increases , the oxygen vacancies and the defects of the surface state decrease in the oxygen atmosphere . So it makes the luminescence in the visible light region lower .

Figure 4-24 shows the the cathodluminescence (CL) spectra of Al-doped ZnO nanowires at 650℃ under different thermal process time in the oxygen atmosphere . From figure 4-24 , when the thermal process time is 1 hour , the UV peak of the Al-doped ZnO nanowires was still at 376 nm and the intensity of the UV peak is higher than the ZnO nanowires . When the thermal process time and temperature was 1 hour and 650℃ , the nonradiative defects were also formed and the defects of the surface state were also reduced . The quantities of the oxygen ions at 650℃ were more than that at 600℃ . And the nonradiative defects may be saturated . So they make the intensity of the UV peak rising . But the intensity of the UV peak was lower than that at 550℃ and 600℃ heating 1 hour . Figure 4-25 shows the magnification of figure 4-24 from 450 nm to 700 nm . In the visible light region , the luminescence also sfifts from 575 nm to 625 nm . It is the same that when the diffusion temperature increases , the oxygen vacancies decrease and the nonradiative defects also corporately contribute to the intensity of the luminescence in the visible light region lower than ZnO nanowires .

When the thermal process time is 3 hours , the intensity of the UV peak is higher than that the thermal process time was 1 hour . The luminescence is lower than that the thermal process time was 1 hour . It is demonstrated that the defects of the surface state decrease with the diffusion time . The quantities of the oxygen ions in 3 hours were more than that in 1 hour . And the nonradiative defects may be saturated . So they make the intensity of the UV peak rising . But the intensity of the UV peak was lower than that at 550℃ and 600℃ heating 3 hours .

When the thermal process time is from 5 hours to 7 hours , the quantities of the nonradiative defects increase and the repaired the defects of the surface state decrease . But the the quantities of the nonradiative defects may be saturated . The repaired the defects of the surface state decease as the thermal process temperature . So it makes the UV intensity increases . The visible light region shows that the intensity of luminescence emission at 650℃ is lower than that at 550℃ and 600℃ . It can be explained that when the diffusion temperature increases , the oxygen vacancies decrease .

The CL intensity ratio of the UV emission to the deep-level emission is shown in figure 4-26 . The figure 4-26 represents the optical properties of ZnO nanowires and the Al-doped ZnO nanowires after thermal process . The principle of the optical properties is based on the $I_{UV}$ / $I_{DLE}$ ratio . $I_{UV}$ is the intensity of the UV emission and $I_{DLE}$ is the intensity of the deep level emission [14] . In the figure 4-26 , the $I_{UV}$ / $I_{DLE}$ ratio of ZnO nanowires was 0.73 . It results from the oxygen deficiency in the growth process .

At 550℃ and 600℃ , as the thermal process time rises from 1 hour to 3 hours , the optical properties are improved more noticeably . When the thermal process time is 5 hours , the optical properties achieve the maximum value . At 550℃ , after the thermal process time is 5 hours , the optical properties start to reduce from 5.43 to 4.92 . At 600℃ , after the thermal process time is 5 hours , the optical properties start to reduce from 5.97 to 4.72 . It is due that the nonradiative defects increases as the diffusion time increases . Although the defects of the surface state also repaired the surface of the ZnO nanowires , the formation of the nonradiative defects decrease the UV intensity more . As the diffuson time increases , the quantities of the nonradiative defects may be saturated . At 650℃ as the thermal process time rises from 1 hour to 3 hours , the nonradiative defects makes the UV intensity low , but the surface defects repaired by the oxygen ions makes the UV intensity high at 650℃ . When the thermal process time rises from 5 hours to 7 hours , the quantities of the nonradiative defects may be saturated . But the oxygen

ions repaired the surface defects as the thermal process temperature increases . So the optical properties increases as the thermal process time .

### 4.2.3.2 The surface morphology and the structure of the Al-doped ZnO nanowires

The surface morphology of the Al-doped ZnO nanowires at 550℃ under different thermal process time in the oxygen atmosphere is shown in figure 4-27 . When the thermal process time was from 1 hour to 3 hours , the surface of the ZnO nanowires was repaired by the oxygen ions . From the figure 4-27 , the change of the surface morphology was not noticeable . When the thermal process time was 5 hours , the nonradiative defects in the Al-doped ZnO nanowires are formed in the oxygen atmosphere . This kind of the nonradiative defects might be in the inner structure of the ZnO nanowires . From the figure 4-27 , the nonradiative defects in the inner structure of the ZnO nanowires were also not noticeable . And the crystal structure of ZnO may be distorted by the high temperature and long time . From the figure 4-27 , the change of the surface morphology was also not noticeable . And the mismatch between the ZnO seeding layer and the aluminum oxide ($AlO_x$) layer makes the Al-doped ZnO nanowires have random direction .

The surface morphology of the Al-doped ZnO nanowires at 600℃ under different thermal process time in the oxygen atmosphere is shown in figure 4-28 . When the thermal process time was 1 hour , the surface of the ZnO nanowires was repaired by the oxygen ions . From the figure 4-28 , the change of the surface morphology was not noticeable . When the thermal process time was from 3 hours to 5 hours , the nonradiative defects in the Al-doped ZnO nanowires are formed in the oxygen atmosphere . This kind of the nonradiative defects might be in the inner structure of the ZnO nanowires . From the figure 4-28 , the nonradiative defects in the inner structure of the ZnO nanowires were

also not noticeable . And the crystal structure of ZnO may be distorted by the high temperature and long time . From the figure 4-28 , the change of the surface morphology was not noticeable . And the mismatch between the ZnO seeding layer and the aluminum oxide ($AlO_x$) layer makes the Al-doped ZnO nanowires have random direction .

The surface morphology of the Al-doped ZnO nanowires at 650℃ under different thermal process time in the oxygen atmosphere is shown in figure 4-29 . When the thermal process time was from 1 hour to 7 hours , the surface of the ZnO nanowires was repaired by the oxygen ions . From the figure 4-29 , the change of the surface morphology was not noticeable . When the thermal process time was from 1 hour to 7 hours , the nonradiative defects in the Al-doped ZnO nanowires are formed in the oxygen atmosphere . This kind of the nonradiative defects might be in the inner structure of the ZnO nanowires . From the figure 4-29 , the nonradiative defects in the inner structure of the ZnO nanowires were also not noticeable . And the crystal structure of ZnO may be distorted by the high temperature and long time . From the figure 4-29 , the change of the surface morphology was not noticeable . And the mismatch between the ZnO seeding layer and the aluminum oxide ($AlO_x$) layer makes the Al-doped ZnO nanowires have random direction .

Figure 4-30 is the X-ray diffraction pattern of Al-doped ZnO nanowires grown at 550℃ in oxygen atmosphere . Figure 4-31 is the X-ray diffraction pattern of Al-doped ZnO nanowires grown at 600℃ in oxygen atmosphere . Figure 4-32 is the X-ray diffraction pattern of Al-doped ZnO nanowires grown at 600℃ in oxygen atmosphere . From the figure 4-30 , the figure 4-31 and the figure 4-32 , they show the peak of the ZnO(100) , ZnO(002) , ZnO(101) , Si(201) and $AlO_x$ . The peak of Si(201) and $AlO_x$ should originate from the Si substrate and the aluminum thin film . The surface of the aluminum thin film forms the aluminum oxide ($AlO_x$) in high temperature . And the mismatch between the ZnO seeding layer and the aluminum oxide ($AlO_x$) layer makes

the Al-doped ZnO nanowires have the peak of the ZnO(100) and ZnO(101) . But it still maintains the wurtzite structure after the long diffusion time . The intensity of the aluminum oxide ($AlO_x$) signal is very high , so the aluminum oxide (AlOx) signal multiply 0.2 to make the signal of ZnO more obviously . As the diffusion time increases , the (002) peak of ZnO somewhat shifts from 34.46° to 34.52° . It represents that the crystal structure of ZnO may be distorted by the high temperature and long time . The distortion of the structure may result of the heat in the long time or the substitution of aluminum .

### 4.2.4 The various thermal treatment in nitrogen atmosphere

After the growth of ZnO nanowires , the sample is put into the 2-inch ceramic furnace . The carrier gas is nitrogen . The air flow is 10 sccm .The thermal process temperature is 550℃ , 600℃ and 650℃ . The thermal process time is 1 hour , 3 hours , 5 hours and 7 hours .

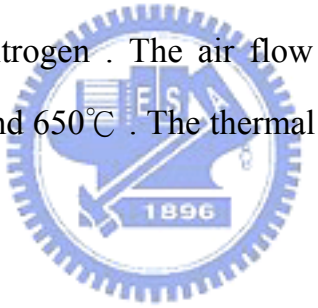

### 4.2.4.1 The optical properties of the Al-doped ZnO nanowires

Figure 4-33 shows the the cathodluminescence (CL) spectra of Al-doped ZnO nanowires at 550℃ under different thermal process time in the nitrogen ambient . From figure 4-33 , the ZnO nanowires still emits a strong emission at 376 nm . And the band gap of the ZnO was still 3.30 eV . The UV peak of the Al-doped ZnO nanowires is at 376 nm and the luminescence is at 575 nm . The luminescence at 575 nm (2.16 eV ) is caused by the deep level [15] . There are many kinds of deep level , like oxygen vacancy ($V_O$), Zinc vacancy ($V_{Zn}$), interstitial zinc ($Zn_i$), interstitial oxygen ($O_i$) and antisite oxygen ($O_{Zn}$) [16-19] . By the ZnO defect`s level diagram [14] in the figure 2-6 , the deep level was the interstitial oxygen ($O_i$) .

When the thermal process time is 1 hour , the intensity of the UV peak is higher than the ZnO nanowires . It is due to that the surface defects may be repaired by the nitrogen ions . The repaired level of the suface defects in nitrogen atmosphere may be higher than that in the oxygen atmosphere . So the intensity of the UV peak in the nitrogen atmosphere is higher than that in the oxygen atmosphere . Although the nitrogen atmosphere may make the oxygen vacancies increase , the reaction equation is shown in equation 4-2, the effect of the surface state is higher than that of the inner state .

$$ZnO \rightarrow V_O + Zn_{Zn} + \frac{1}{2}O_2. \quad \textbf{(eq 4-2)}$$

The peak of the visible light region is lower than the ZnO nanowires . It was shown in figure 4-34 . When the surface defects are repaired in the nitrogen atmosphere , it is not only represented in the UV region , but also represented in the visible light region . So in the visible light region , the intensity of the luminescene can be improved by the repaired surface defects . The heat in the nitrogen atmosphere produce some oxygen vacancies . It also makes the peak of the luminescence higher . But the intensity of the luminescence is the contribution of the surface defects and the heat in the nitrogen atmosphere , so the intensity of the luminescene is lower than the ZnO nanowires . And the luminescence peak position of the Al-doped ZnO nanowires changes from 575 nm to 625 nm (from 2.16 eV to 1.99 eV ) . From the figure 2-6 , the energy level of 2.16 eV was between the Vo level (1.62 eV ) and the $O_i$ level (2.28 eV) . And the energy level of 1.99 eV was also between the Vo level (1.62 eV ) and the $O_i$ level (2.28 eV) . But it is near the Vo level . It may mean that after the thermal process , the quantities of Vo are more than that of Oi . The Oi may replace the Vo after the thermal process .

As the thermal process time increases to 3 hours , the UV peak of the Al-doped ZnO nanowires is higher than 1 hour . It is due to that the surface defects are repaired more completely in the nitrogen atmosphere . But the increasing rage of the UV intensity was

not very much . And the increasing rage of the UV intensity in the oxygen atmosphere is higher than that in the nitrogen atmosphere from 1 hour to 3 hours . It can be represented that the nitrogen ions are harder to decompose than oxygen ions . In the visible light region , the luminescence peak position of the Al-doped ZnO nanowires also shifts from 575nm to 625 nm . But the intensity of the visible light region is higher than that the thermal process time is 1 hour . The thermal process time increases , the oxygen vacancies in the nitrogen atmosphere increase . And the aluminum content in the ZnO nanowires also increase with the diffusion time in the same temperature . They all make the intensity of the luminescene higher than that the thermal process time is 1 hour . When the thermal process time is the range between 1 hour and 3 hours , the UV peak rises slowly , because that the nitrogen molecule doesn`t form the nitrogen ions completely .

When the thermal process time is 5 hours , the intensity of the UV peak is higher than that the thermal process time is 3 hours . It is due to that the surface defects are repaired more completely than 3 hours . The increasing rage of the UV intensity between 1 hour to 3 hours was higher than that between 3 hours to 5 hours . In the visible light region , the more oxygen vacancies are produced by the heat in the nitrogen atmosphere . So the intensity of the luminescene is higher than that the thermal process time is 3 hour .

When the thermal process time is 7 hours , the intensity of the UV peak is higher than that the thermal process time is 5 hours . It is due to that the surface defects are repaired more completely than 5 hours . In the visible light region , the more oxygen vacancies are produced by the heat in the nitrogen atmosphere . So the intensity of the luminescene is higher than that the thermal process time is 5 hours .

Figure 4-35 shows the the cathodluminescence (CL) spectra of Al-doped ZnO nanowires at 600℃ under different thermal process time in the nitrogen atmosphere . When the thermal process is 1 hour , the intensity of the UV peak is higher than the ZnO

nanowires . It is due to that the surface defects is repaired by the nitrogen ions . The peak of the visible light region is lower than the ZnO nanowires . In the visible light region , the intensity of the luminescene can be improved by the repaired surface defects . And the heat in the nitrogen atmosphere produce some oxygen vacancies . They also make the peak of the luminescence higher . It was shown in figure 4-36 . But the intensity of the luminescence is the contribution of the surface defects and the heat in the nitrogen atmosphere , so the intensity of the luminescene is lower than the ZnO nanowires . And the luminescence peak position of the Al-doped ZnO nanowires changes from 575 nm to 625 nm (from 2.16 eV to 1.99 eV ) . From the figure 2-6 , the energy level of 2.16 eV was between the Vo level (1.62 eV ) and the $O_i$ level (2.28 eV) . And the energy level of 1.99 eV was also between the Vo level (1.62 eV ) and the $O_i$ level (2.28 eV) . But it is near the Vo level . It may mean that after the thermal process , the quantities of Vo are more than that of Oi . The Oi may replace the Vo after the thermal process .

As the thermal process time increases to 3 hours , the UV peak of the Al-doped ZnO nanowires is higher than 1 hour . It is due to that the surface defects are repaired more completely in the nitrogen atmosphere . In the visible light region , the luminescence peak position of the Al-doped ZnO nanowires shifts from 575nm to 625 nm . But the intensity of the visible light region is higher than that the thermal process time is 1 hour . When the thermal process time is the range between 1 hour and 3 hours , the UV peak rises slowly , because that the nitrogen molecule doesn`t form the nitrogen ions completely .

When the thermal process time is 5 hours , the intensity of the UV peak is higher than that the thermal process time is 3 hours . It is due to that the surface defects are repaired more completely than 3 hours . In the visible light region , the more oxygen vacancies are produced by the heat in the nitrogen atmosphere . So the intensity of the luminescene is higher than that the thermal process time is 3 hour .

When the thermal process time is 7 hours , the intensity of the UV peak is higher than that the thermal process time is 5 hours . It is due to that the surface defects are repaired more completely than 5 hours . In the visible light region , the more oxygen vacancies are produced by the heat in the nitrogen atmosphere . So the intensity of the luminescene is higher than that the thermal process time is 5 hours .

Figure 4-37 shows the the cathodluminescence (CL) spectra of Al-doped ZnO nanowires at 650℃ under different thermal process time in the nitrogen ambient . When the thermal process is 1 hour , the intensity of the UV peak is higher than the ZnO nanowires . It is due to that the surface defects is repaired by the nitrogen ions . The peak of the visible light region is lower than the ZnO nanowires . In the visible light region , the intensity of the luminescene can be improved by the repaired surface defects . And the heat in the nitrogen atmosphere produce some oxygen vacancies . It also makes the peak of the luminescence higher . It was shown in figure 4-38 . But the intensity of the luminescence is the contribution of the surface defects and the heat in the nitrogen atmosphere , so the intensity of the luminescene is lower than the ZnO nanowires . And the luminescence peak position of the Al-doped ZnO nanowires changes from 575 nm to 625 nm (from 2.16 eV to 1.99 eV ) . From the figure 2-6 , the energy level of 2.16 eV was between the Vo level (1.62 eV ) and the $O_i$ level (2.28 eV) . And the energy level of 1.99 eV was also between the Vo level (1.62 eV ) and the $O_i$ level (2.28 eV) . But it is near the Vo level . It may mean that after the thermal process , the quantities of Vo are more than that of Oi . The Oi may replace the Vo after the thermal process .

As the thermal process time increases to 3 hours , the UV peak of the Al-doped ZnO nanowires is higher than 1 hour . It is due to that the surface defects are repaired more completely in the nitrogen atmosphere . In the visible light region , the luminescence peak position of the Al-doped ZnO nanowires shifts from 575nm to 625 nm . But the intensity of the visible light region is higher than that the thermal process time is 1 hour .

When the thermal process time is the range between 1 hour and 3 hours , the UV peak rises slowly , because that the nitrogen molecule doesn`t form the nitrogen ions completely .

When the thermal process time is 5 hours , the intensity of the UV peak is higher than that the thermal process time is 3 hours . It is due to that the surface defects are repaired more completely than 3 hours . In the visible light region , the more oxygen vacancies are produced by the heat in the nitrogen atmosphere . So the intensity of the luminescene is higher than that the thermal process time is 3 hour .

When the thermal process time is 7 hours , the intensity of the UV peak is higher than that the thermal process time is 5 hours . It is due to that the surface defects are repaired more completely than 5 hours . In the visible light region , the more oxygen vacancies are produced by the heat in the nitrogen atmosphere . So the intensity of the luminescene is higher than that the thermal process time is 5 hours .

The CL intensity ratio of the UV emission to the deep-level emission is shown in figure 4-39 . The figure 4-39 represents the optical properties of ZnO nanowires and the Al-doped ZnO nanowires after the thermal process . The principle of the optical properties is based on the $I_{UV}$ / $I_{DLE}$ ratio . $I_{UV}$ is the intensity of the UV emission and $I_{DLE}$ is the intensity of the deep level emission [14] . In the figure 4-39 , the $I_{UV}$ / $I_{DLE}$ ratio of ZnO nanowires was also 0.73 . It results from the oxygen deficiency in the growth process . At 550℃ as the thermal process time rises from 1 hour to 3 hours , the optical properties are improved not noticeably , because the nitrogen molecule doesn`t form the nitrogen ions completely . When the thermal process time rises from 5 hours to 7 hours , the optical properties rise higher than that the thermal process time was from 1 hour to 3 hours . Because When the thermal process time rises from 5 hours to 7 hours , the nitrogen molecule form the nitrogen ions more completely . The optical properties in nitrogen atmosphere is higher than that in oxygen atmosphere . It may be explained that

the repaired efficiency of the nonradiative defects in nitrogen atmosphere is higher than that in oxygen atmosphere and the non-perfect ZnO structure doesn`t form in the nitrogen atmosphere . At 600℃ as the thermal process time rises from 1 hour to 3 hours , the optical properties are improved not noticeably . When the thermal process time is the range between 1 hour and 3 hours , because the nitrogen molecule doesn`t form the nitrogen ions completely , the optical property is rising slowly . But the optical properties at 600℃ is higher than that at 550℃ . It is because that the quantities of the nitrogen ions at 600℃ is higher than 550℃ . When the thermal process time rises from 5 hours to 7 hours , the optical properties rise higher than that the thermal process time was from 1 hour to 3 hours . Because when the thermal process time rises from 5 hours to 7 hours , the nitrogen molecule form the nitrogen ions more completely . But the optical properties at 600℃ is lower than that at 550℃ . It may be explained that the repaired level of the nitrogen ions can be saturated . And the oxygen vacancies at 600℃ are more than that at 550℃ . At 650℃ as the thermal process time rises from 1 hour to 3 hours , the optical properties are also improved not noticeably . When the thermal process time is the range between 1 hour and 3 hours , because the nitrogen molecule doesn`t form the nitrogen ions completely , the optical property is rising slowly . But the optical properties at 650℃ is higher than that at 600℃ . It is because that the quantities of the nitrogen ions at 650℃ is higher than 600℃ . When the thermal process time rises from 5 hours to 7 hours , the optical properties rise higher than that the thermal process time was from 1 hour to 3 hours . Because when the thermal process time rises from 5 hours to 7 hours , the nitrogen molecule form the nitrogen ions more completely . But the optical properties at 650℃ is lower than that at 600℃ . It may be explained that the repaired level of the nitrogen ions can be saturated . And the oxygen vacancies at 650℃ are more than that at 600℃ .

### 4.2.4.2 The surface morphology and the structure of the Al-doped ZnO nanowires

The surface morphology of the Al-doped ZnO nanowires at 550℃ under different thermal process time in the nitrogen atmosphere is shown in figure 4-40 . When the thermal process time was from 1 hour to 7 hours , the surface of the ZnO nanowires was repaired by the nitrogen ions . From the figure 4-40 , the change of the surface morphology was not noticeable . And the crystal structure of ZnO may be distorted by the high temperature and long time . From the figure 4-40 , the change of the surface morphology was not noticeable .

The surface morphology of the Al-doped ZnO nanowires at 600℃ under different thermal process time in the nitrogen atmosphere is shown in figure 4-41 . When the thermal process time was from 1 hour to 7 hours , the surface of the ZnO nanowires was repaired by the nitrogen ions . From the figure 4-41 , the change of the surface morphology was not noticeable . And the crystal structure of ZnO may be distorted by the high temperature and long time . From the figure 4-41 , the change of the surface morphology was not noticeable .

The surface morphology of the Al-doped ZnO nanowires at 650℃ under different thermal process time in the nitrogen atmosphere is shown in figure 4-42 . When the thermal process time was from 1 hour to 7 hours , the surface of the ZnO nanowires was repaired by the nitrogen ions . From the figure 4-42 , the change of the surface morphology was not noticeable . And the crystal structure of ZnO may be distorted by the high temperature and long time . From the figure 4-42 , the change of the surface morphology was not noticeable .

Figure 4-43 is the X-ray diffraction pattern of Al-doped ZnO nanowires grown at 550℃ in nitrogen atmosphere . Figure 4-44 is the X-ray diffraction pattern of Al-doped ZnO nanowires grown at 600℃ in nitrogen atmosphere . Figure 4-45 is the X-ray diffraction pattern of Al-doped ZnO nanowires grown at 650℃ in nitrogen atmosphere .

From the figure 4-43 , the figure 4-44 and the figure 4-45 , they show the peak of the ZnO (100) , ZnO (002) , ZnO (101) , Si (201) and AlOx . The peak of Si (201) and AlOx should originate from the Si substrate and the aluminum thin film . The surface of the aluminum thin film forms the aluminum oxide ($AlO_x$) in high temperature . And the mismatch between the ZnO seeding layer and the aluminum oxide ($AlO_x$) layer mskes the Al-doped ZnO nanowires have the peak of the ZnO(100) and ZnO(101) . But it still maintains the wurtzite structure after the long diffusion time . The intensity of the aluminum signal is very high , so the aluminum oxide (AlOx) signal multiply 0.2 to make the signal of ZnO more obviously . As the diffusion time increases , the (002) peak of ZnO somewhat shifts from 34.46° to 34.54° . It represents that the crystal structure of ZnO may be distorted by the high temperature and long time . The distortion of the structure results of the heat in the long time and the accrescence of aluminum . In the nitrogen atmosphere , the content of the aluminum is fewer than in the oxygen atmosphere . It can be result that oxygen vacancies in the oxygen atmosphere is fewer than that in the nitrogen atmosphere .

### 4.2.5 The diffusion of Al in the ZnO nanowire under differenet atmospheres

The content of the Al in the ZnO nanowires may be not very much . It is because that the difference of the ionic radius between Al and Zn is more than 15 % . It makes the solid solubility of Al in the ZnO nanowire not very much . As the thermal process time

increases , the Al in the ZnO nanowire may diffuse little far away the Al thin film . The diffusion in different atmosphere may bring about different situation .

Table 4-2 shows the atomic percent of Al in the ZnO nanowires under different thermal process time in oxygen atmosphere in different distance from the Al thin film at 550$^{o}$C . The Al thin film was the datum plane . The x represents the distance from the datum plane of the Al thin film . From the table 4-2 , the content of Al in the ZnO nanowires at the same diffusion distance increase with the thermal process temperature . It is because that the solid solubility of Al into the ZnO nanowires was very low and the diffusion path from the Al thin film to the ZnO nanowires . As the temperature and the diffusion time increase , the quantities of Al arriving in the ZnO nanowires may increase . And the content of Al in the ZnO nanowires at the same thermal process temperature decrease with diffusion distance . The content of Al in the ZnO nanowires may because the temperature and the diffusion time arrive the maximum value , but the Al had been in the ZnO nanowires can diffuse as the thermal process time . Figure 4-46 shows the diffusion of Al into the ZnO nanowires at 550℃ heating 7 hours in oxygen atmosphere . From the figure 4-46 , Cs represents that the atomic percent of Al in the datum plane . Cx represents that the atomic percent of Al in the x distance away from the Al thin film . And the content of the Al in the ZnO nanowire was not very much .

Table 4-3 shows the atomic percent of Al in the ZnO nanowires under different thermal process time in nitrogen atmosphere in different distance from the Al thin film at 550$^{o}$C . The Al thin film was the datum plane . The x represents the distance from the datum plane of the Al thin film . From the table 4-3 , the content of Al in the ZnO nanowires at the same diffusion distance increase with the thermal process temperature . It is because that the solid solubility of Al into the ZnO nanowires was very low and the diffusion path from the Al thin film to the ZnO nanowires . As the temperature and the diffusion time increase , the quantities of Al arriving in the ZnO nanowires may increase .

And the content of Al in the ZnO nanowires at the same thermal process temperature decrease with diffusion distance . The content of Al in the ZnO nanowires may because the temperature and the diffusion time arrive the maximum value , but the Al had been in the ZnO nanowires can diffuse as the thermal process time . Figure 4-47 shows the diffusion of Al into the ZnO nanowires at 550℃ heating 7 hours in nitrogen atmosphere . From the figure 4-47 , Cs represents that the atomic percent of Al in the datum plane . Cx represents that the atomic percent of Al in the x distance away from the Al thin film . And the content of the Al in the ZnO nanowire was not very much .

The content of Al in the ZnO nanowires in the nitrogen atmosphere is higher than that in the oxygen atmosphere . When the thermal process was in the oxygen atmosphere , the surface of the Al thin film formed the aluminum oxide more easily and the structure of the aluminum oxide was better than that in the nitrogen atmosphere . The thick the aluminum oxide and the better structure make the aluminum hard to diffuse to the ZnO nanowires . The source of Al may influence more in the same thermal process environment . And the thermal process in the nitrogen atmosphere produces more oxygen vacancies , so the aluminum have more diffusion path to diffuse .

Figure 4-48 shows the lattice constant c of Al in the ZnO nanowires at 550℃ in oxygen and nitrogen atmosphere . From the figure 4-48 , as the diffusion time increases , the lattice constant c decreases . The lattice constant c decreases from 5.201 Å to 5.192 Å in the oxygen atmosphere . The lattice constant c decreases from 5.201 Å to 5.189 Å in the nitrogen atmosphere . It may result that the content of Al in the ZnO nanowires increases with the diffusion time . And the chang of the lattice constant c in the nitrogen atmosphere is more than that in the oxygen atmosphere at 7 hours . It may result that the content of Al in the ZnO nanowires makes the structure change and the the content of Al in the nitrogen atmosphere is more than that in the oxygen atmosphere .

# Chapter 5 Conclusions

The hydrothermal method provides the simple , cheap and low temperature way to grow ZnO nanowires . Below 100℃ , the ZnO nanowires can be formed .

As the concentration of the chemical solution increases , the density of the ZnO nanowires increases . As the growth time increases , the lengthes of the ZnO nanowires increase . However , the formation time of the ZnO nanowires reguires more than two hours . The pH value is important for the growth environment to grow ZnO nanowires . The hydrothermal method was nonstoichiometric . The cathodluminescence (CL) spectra of the ZnO nanowires shows low UV intensity compared with the visible light intensity .

After the thermal process of the ZnO nanowires , the optical properties were improved . No matter in oxygen or nitrogen atmosphere , the optical properties increase with the annealing temperature . When annealing at 900℃ for 30 min , the $O_{Zn}$ was formed . And in the oxygen atmosphere , the quantities of $O_{Zn}$ were more than that in the nitrogen atmosphere .

By the diffsusion method , the aluminum can be doped in the ZnO nanowires . As the thermal process temperature increases , the content of Al in the ZnO nanowires increases . The solid solubility of Al in the ZnO nanowires was very low . In the nitrogen atmosphere , the content of Al in the ZnO nanowires is more than that in the oxygen atmosphere . It results that more diffusion path was produced in the nitrogen atmosphere . By the diffsusion method , the change of the surface morphology is not noticeable and the lattice constant decreases slightly . The nonradiative defects are easily formed in oxygen

atmosphere . The nitrogen ions repair the surface defects more effectively than the oxygen ions . The shift of the UV peak was not noticeable , because the content of Al in the ZnO nanowires is low and the resolution of the cathodluminescence (CL) spectra is not high enough.

# References


[1] Cao H, Zhao Y G ,ONg H C, Ho S T, Dai J Y, Wu J Y and Chang R P H, 1998 *Appl. Phys. Lett.* ***73*** *3656.*

[2] Li S Y, Lin P, Lee C Y and Tseng T Y , 2004 *J. Appl. Phys*. **95** 3711.

[3] Agashe C,Kluth O, Hupkes J, Zastrow U, Rech B and Wuttig M, 2003 *J.Appl. Phys*. **85** 1911

[4] Li S Y, Lin P, Lee C Y and Tseng T Y , 2003 *J.Cryst. Growth* **247** 357

[5] Heo Y W, Kaufman M, Pruessner K, Norton D P,Ren F, Chisholm M F and Fleming P H ,2003 *Solid-State Electron*. **47** 2269

[6] Morales A M and Leiber C M 1998 *Science* **279** 208

[7] Vayssieres L, Keis K, Hagfeldt A and Lindquist S ,2001 *Chem. Mater.* **13** 4395

[8] Seung Yong Bae, Chan Woong Na, Ja Hee Kang, and Jeunghee Park, 2005 *J. Phys. Chem. B* , **109***,* 2526-2531

[9] 091NCTU0428091-001.ZIP

[10] K. Vanheusden, W.L. Warren, C.H. Seager, D.R. Tallant, J.A. Voigt, B.E. Gnade, *J. Appl. Phys.* 79 (1996) 7983.

[11] Choongmo Kim, Anna Park, K. Prabakar, Chongmu Lee , *Materials Research Bulletin* **41** (2006) 253–259

[12] A. Po¨ppl and G. Vo¨lkel, *Phys. Status Solidi A* ***125***, 571 (1991).

[13] T. Makino, C. H. Chia, N. T. Tuan, Y. Segawa, M. Kawasaki, A. Ohtomo, K. Tamura and H. Koinuma, 2000 *Appl. Phys. Lett.* ***77*** *975*

[14] Jinzhong Wang, Guotong Du, Yuantao Zhang, Baijun Zhao, Xiaotian Yang,Dali Liu , 2004 *Journal of Crystal Growth* **263** 269–272

[15] Wang J, Du G, Zhang Y, Zhao B, Yang X and Liu D, 2004 *J.Cryst. Growth* **263** 269

[16] Jinzhong Wang, Guotong Du, Yuantao Zhang, Baijun Zhao, Xiaotian Yang and Dali Liu, 2004 *Journal of Crystal Growth* **263** 269–272

[17] E.G. Bylander, *J. Appl. Phys*. **49** (1978) 1188.

[18] K. Vanheusden, C.H. Seager, W.L. Warren, D.R. Tallant, J.A. Voiget, *Appl. Phys. Lett.* **68** (1996) 403.

[19] M. Liu, A.H. Kitai, P. Mascher, J. Lumin. **54** (1992) 35.

[20] B. Lin, Z. Fu, Y. Jia, *Appl. Phys. Lett.* **79** (2001) 7.

[21] Jinzhong Wang*, Guotong Du, Yuantao Zhang, Baijun Zhao, Xiaotian Yang, Dali Liu

[22] D. M. Bagnall, Y. F. Chen, Z. Zhu, and T. Yao, *Appl. Phys. Lett.* **70**, 2230

(1997).

[23] E. G. Bylander, *J. Appl. Phys.* **49**, 1188 (1978).

[24] Chin-Ching Lin, Hung-Pei Chen, Hung-Chou Liao, and San-Yuan Chen , *Appl. Phys. Lett.* **86**, 183103 (2005)

[25] J.D. Ye, S.L. Gu, S.M. Zhu, S.M. Liua, Y.D. Zheng, R. Zhang, Y. Shi, H.Q. Yu, Y.D. Ye, *Journal of Crystal Growth* **283** 279–285 (2005)

[26] Takahiro Matsumoto, Hiroyuki Kato, Kazuhiro Miyamoto, Michihiro Sano, and Evgeniy A. Zhukov , *Appl. Phys. Lett*. **81**, 1231 (2002)

[27] Le Hong Quang, Soo Jin Chua, Kian Ping Loh, Eugene Fitzgerald , *Journal of Crystal Growth* **287** 157–161 (2006)

[28] Shou-Yi Kuo, Wei-Chun Chen, Chin-Pao Cheng , *Superlattices and Microstructures* **39** 162–170 (2006)

[29] Chia Ying Lee, Tseung Yuen Tseng, SeuYi Li and Pang Lin, *Nanotechnology* **17** 83–88 (2006)

[30] Chia Ying Lee, Tseung Yuen Tseng, SeuYi Li and Pang Lin, *Nanotechnology* **16** 1105–1111 (2005)

[31] Chia Ying Lee, Tseung Yuen Tseng, SeuYi Li and Pang Lin, *J. Appl. Phys*. **99** 024303 (2006) .

[32] M.Guo et al. , *Journal of solid state chemistry* **178** (2005) 1864-1873

[33] K. Vanheusden, W.L. Warren, C.H. Seager, D.R. Tallant, J.A. Voiget and B. E. Gnade, J. *Appl. Phys.* **79** 7983 (1996) .

[34] Jinmin Wang, Lian Gao, *Solid State Communications* **132** 269–271 (2004) .

[35] G. Shi, C.M. Mo, W.L. Cai, L.D. Zhang , *Solid State Communications* **115** 253-256 (2000) .

[36] K. Vanheusden, W. L. Warren, C. H. Seager, D. R. Tallant, and J. A. Voigt B. E. Gnade , *J. Appl. Phys.* **79** 7983-7990 (1996).

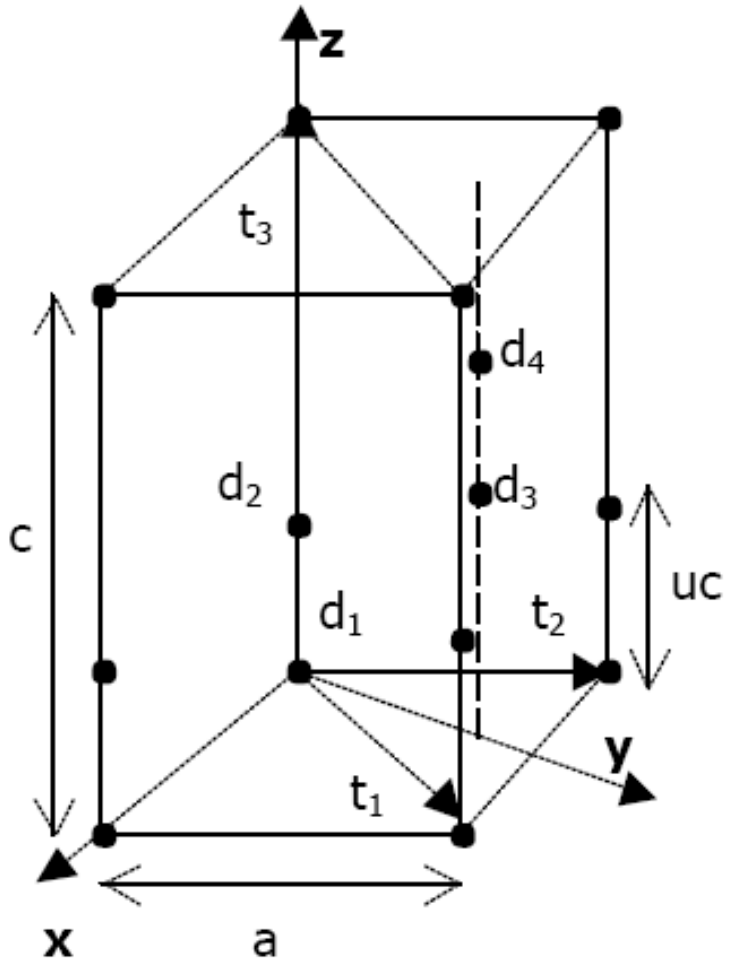


**Figure 2-1 The lattice structure of the ZnO**

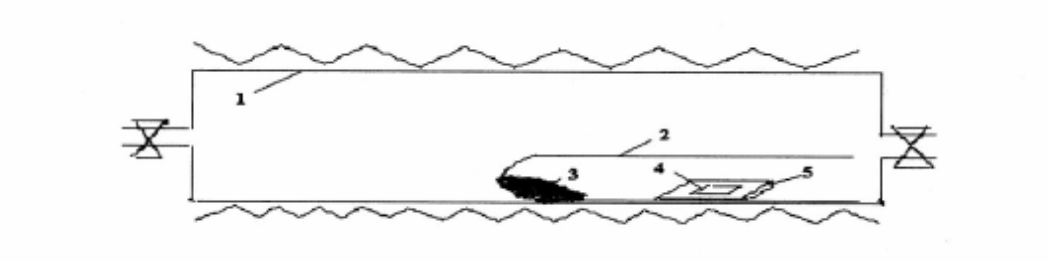


**Figure 2-2 The schematic geometry of ZnO nanowires growth. 1. Furnace tube, 2. slender tube, 3. source, 4. template, 5. alumina supporter**

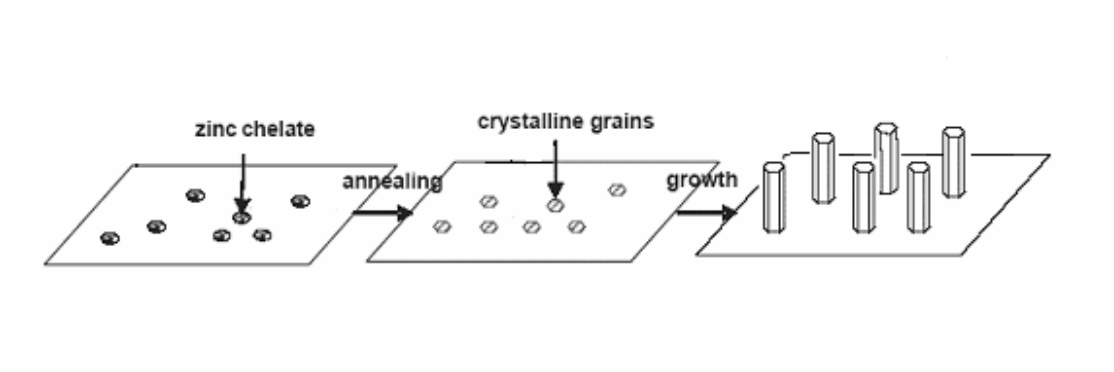


**Figure 2-3 The growth process of the ZnO nanowires by the hydrothermal method**

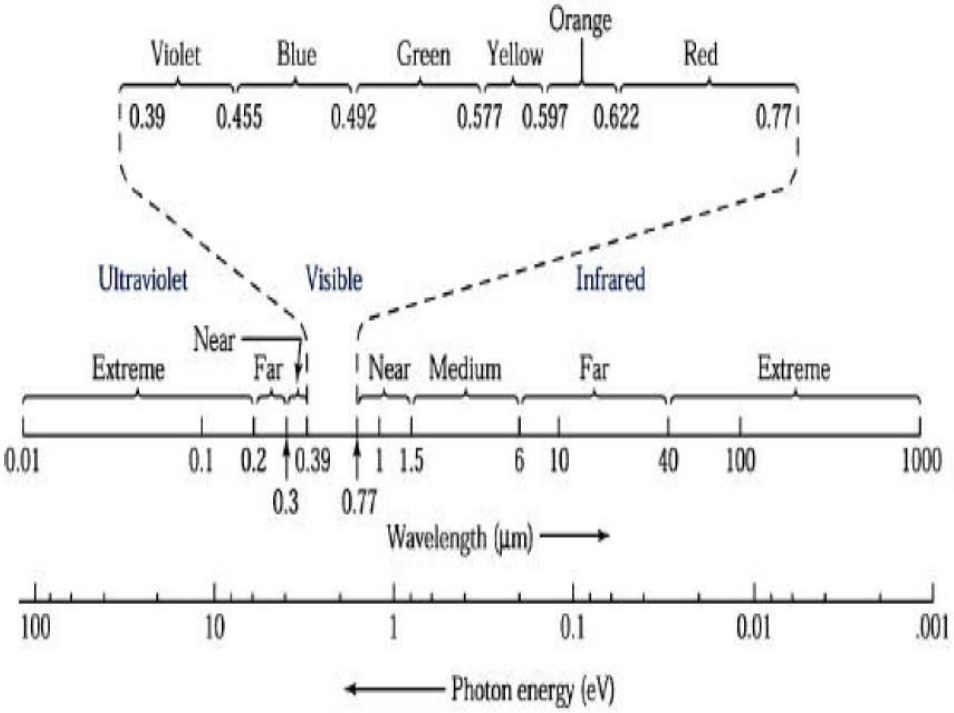


**Figure 2-4 The optical spectrum**

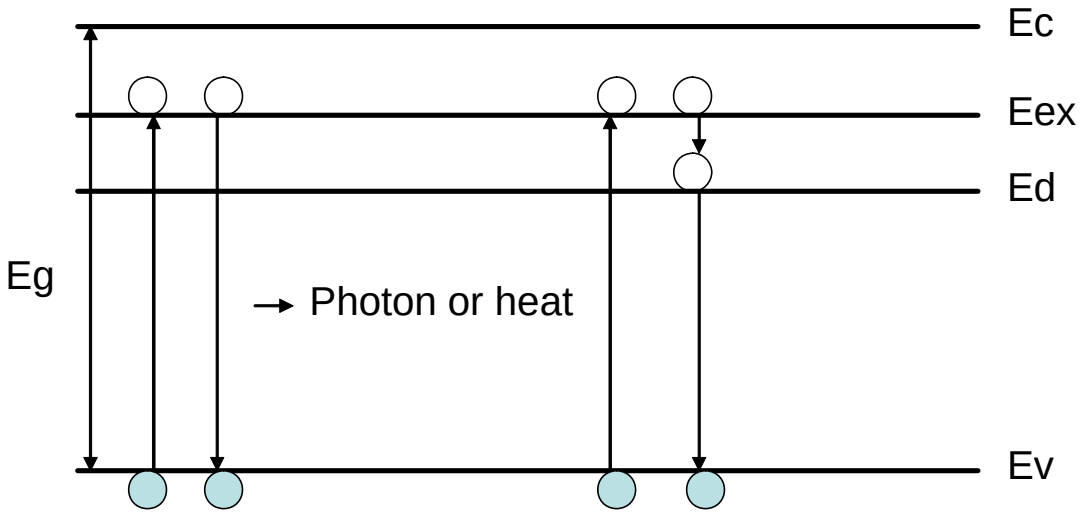


**Figure 2-5 The mechanism of the photoluminescence**

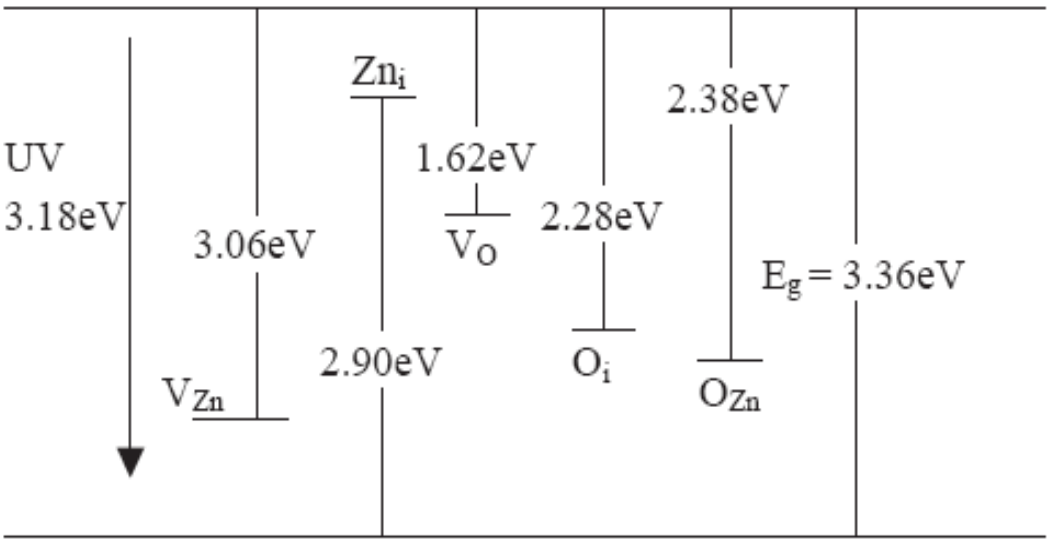


**Figure 2-6 The draft of the calculated defect`s levels in ZnO film**

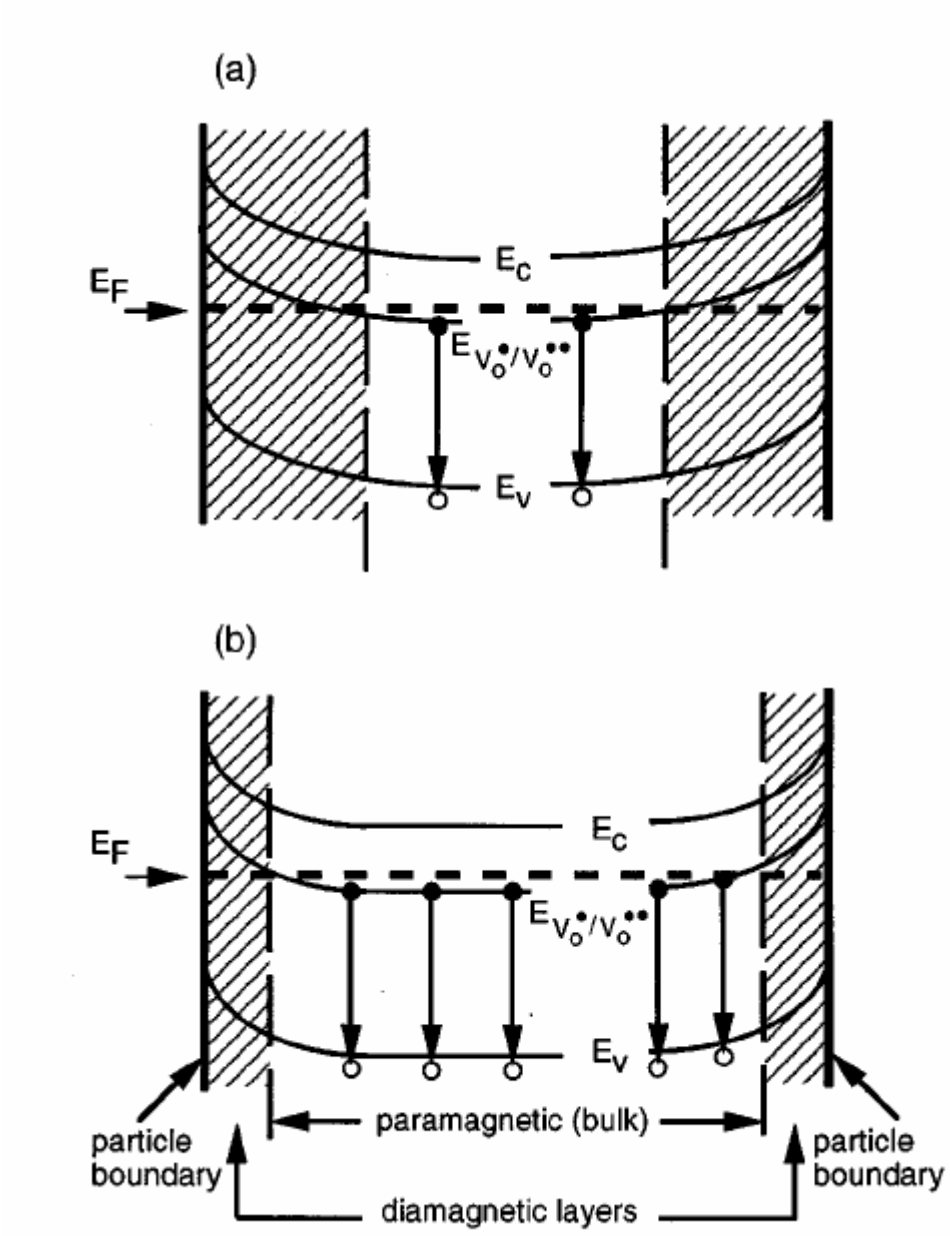


**Figure 2-7 Schematic showing the energy-band diagram of a ZnO grain in cross section. The conduction band (*Ec*), valance band (*Ev*), Fermi level ($E_F$), paramagnetic oxygen vacancy ($VO^{\bullet}$) level, and the diamagnetic $VO^{\bullet\bullet}$ area (hatched) in the grain-boundary depletion region are visualized for a grain with a (a) low and (b) high free-carrier density. The circles and arrows symbolize electron–hole recombination events which emit green light. [10]**

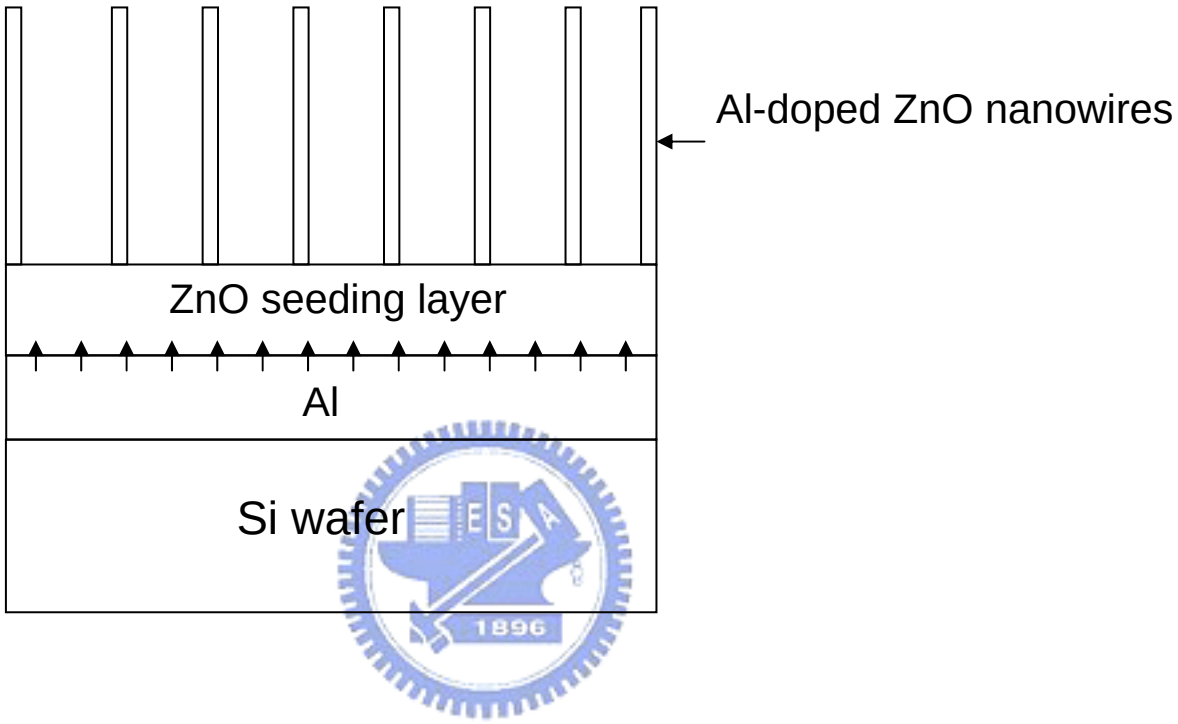


**Figure 3-1 The structure of the Al-doped ZnO nanowires**

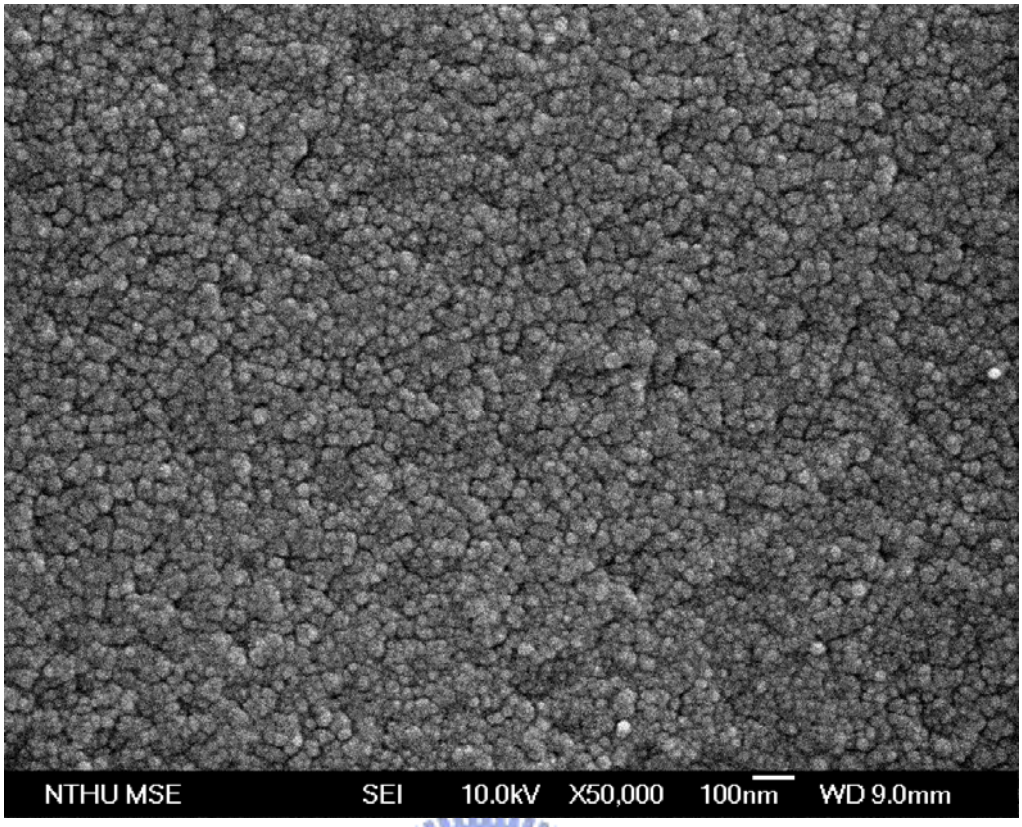


**Figure 4-1 The SEM image of the ZnO seeding layer grown on Si substrate**

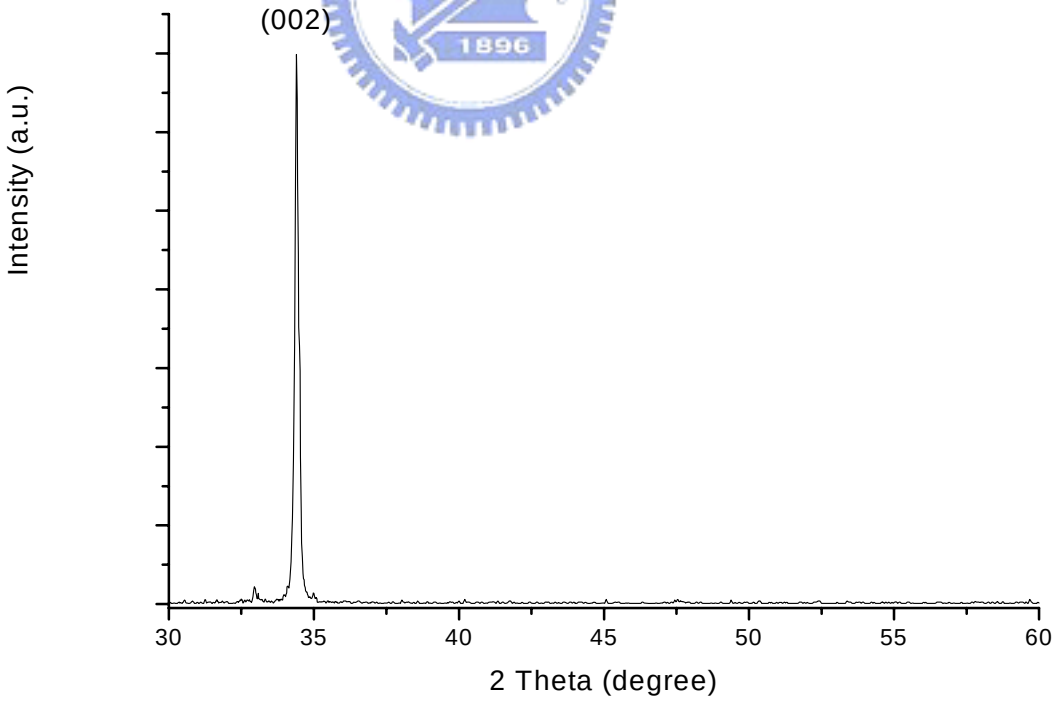


**Figure 4-2 The X-ray diffraction pattern of ZnO seeding layer grown on Si substrate**

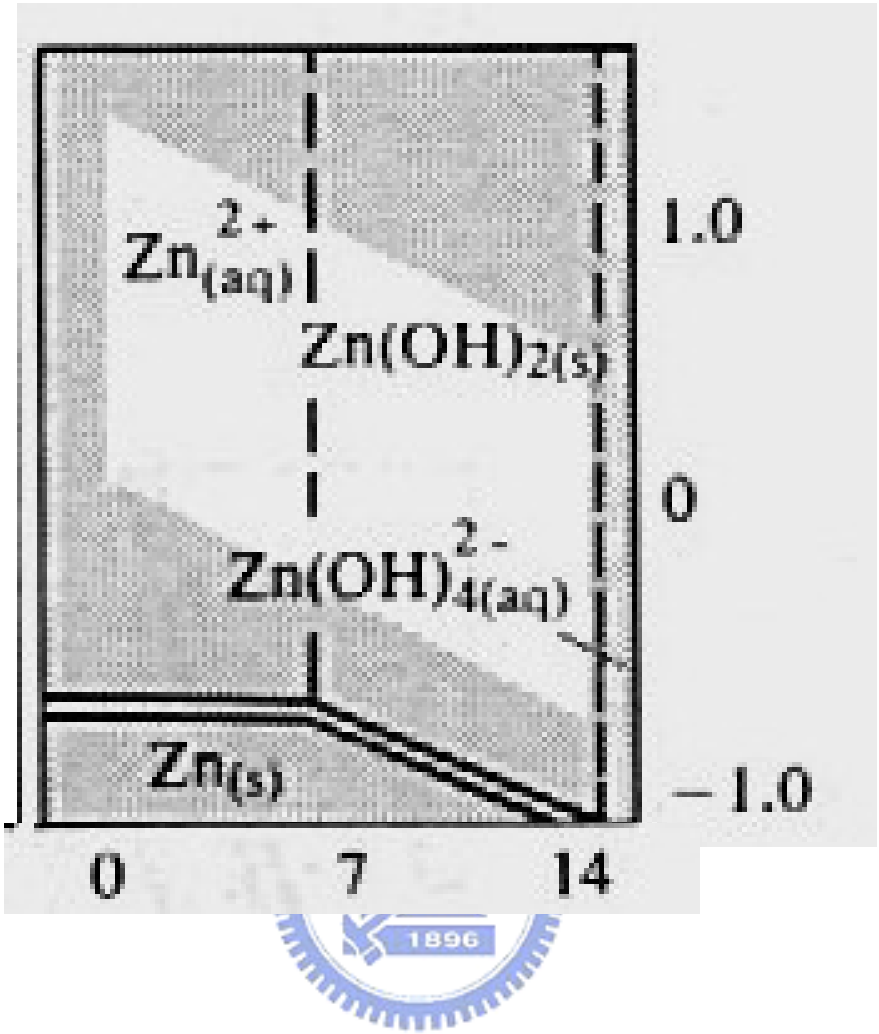


**Figure 4-3 The pourbaix diagram of the $Zn(OH)_2$**

| | 0.08M | 0.10M | 0.12M | 0.14M | 0.16M |
|---|---|---|---|---|---|
| Before growing | pH=6.6 | pH=6.7 | pH=6.6 | pH=6.7 | pH=6.6 |
| After growing 3hr | pH=6.5 | pH=6.4 | pH=6.3 | pH=6.2 | pH=6.1 |

**Table 4-1 The pH value of the chemical solution in different concentration before and after growing**

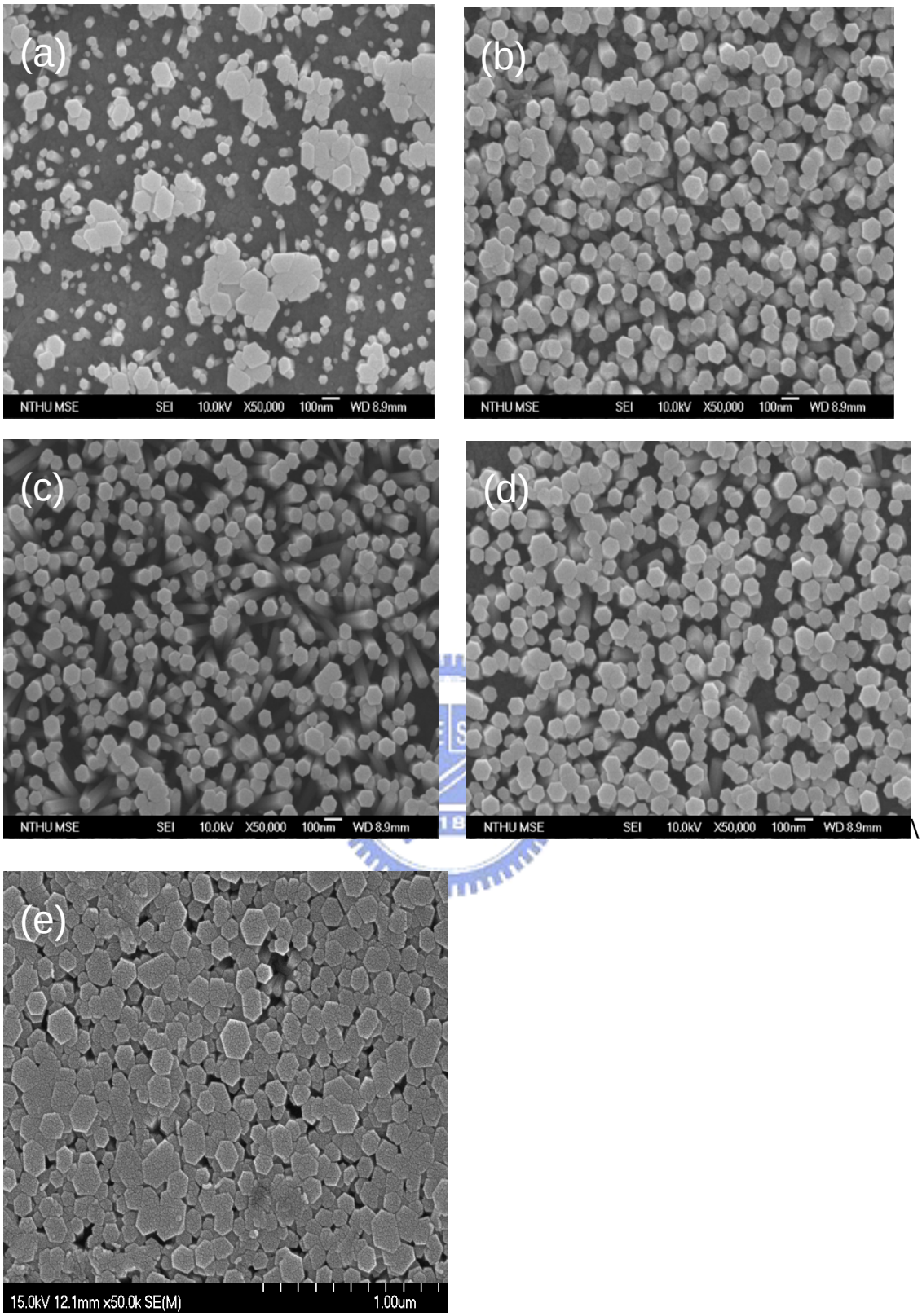


**Figure 4-4 The SEM image of the concentration of the chemical solution was (a) 0.08M (b) 0.10M (c) 0.12M (d) 0.14M (e) 0.16M**

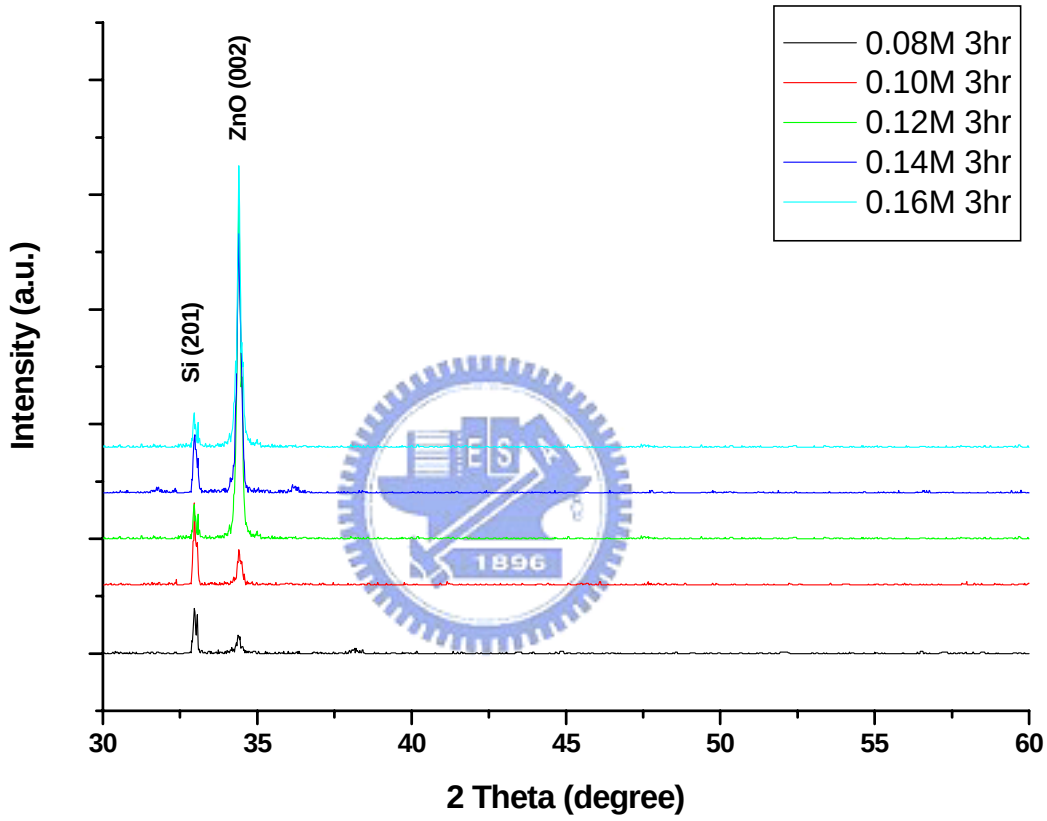


**Figure 4-5 The X-ray diffraction pattern of ZnO nanowires grown on Si wafer in different solution concentraon at the same time**

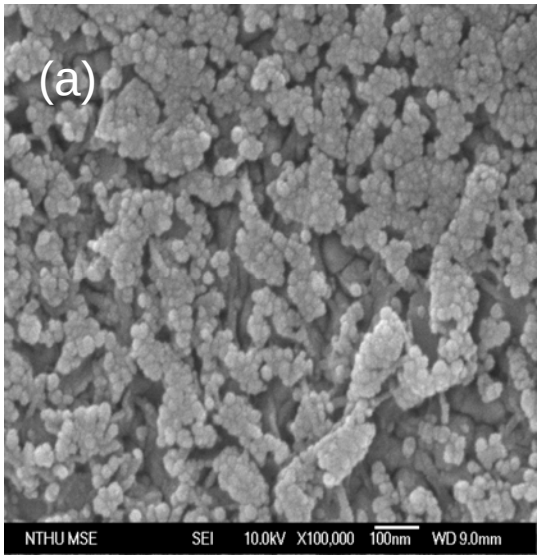
(a)
NTHU MSE SEI 10.0kV X100,000 100nm WD 9.0mm

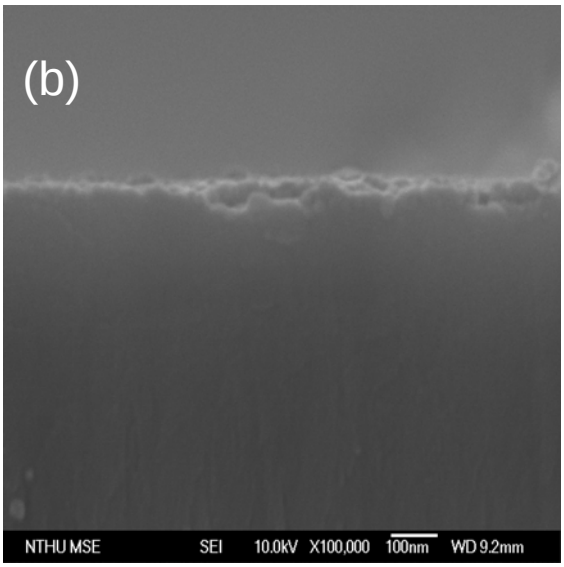
(b)
NTHU MSE SEI 10.0kV X100,000 100nm WD 9.2mm

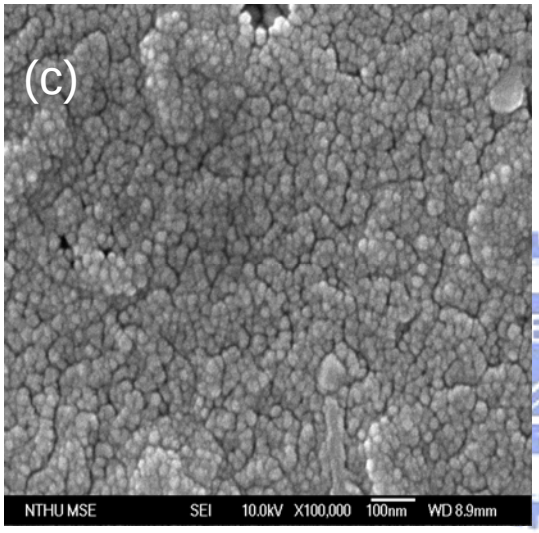
(c)
NTHU MSE SEI 10.0kV X100,000 100nm WD 8.9mm

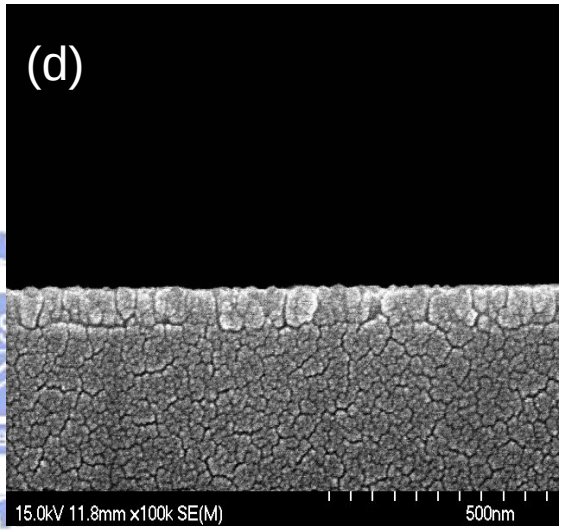
(d)
15.0kV 11.8mm x100k SE(M)
500nm

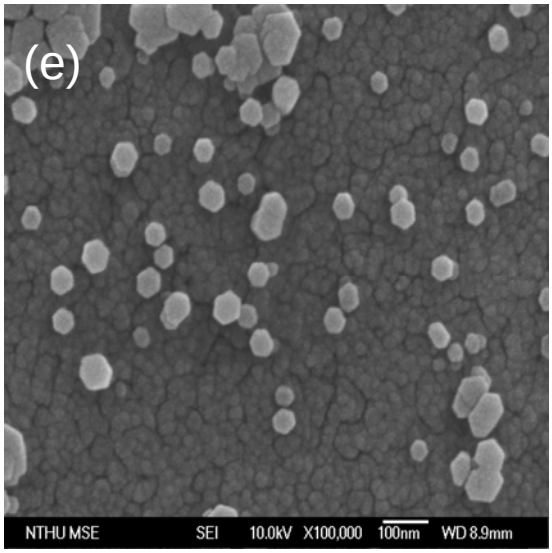
(e)
NTHU MSE SEI 10.0kV X100,000 100nm WD 8.9mm

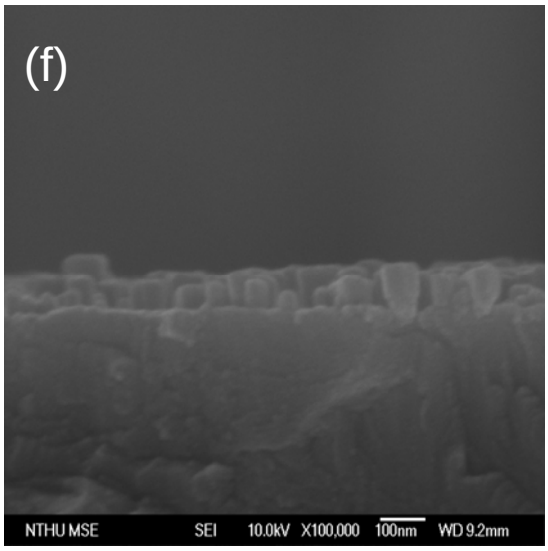
(f)
NTHU MSE SEI 10.0kV X100,000 100nm WD 9.2mm

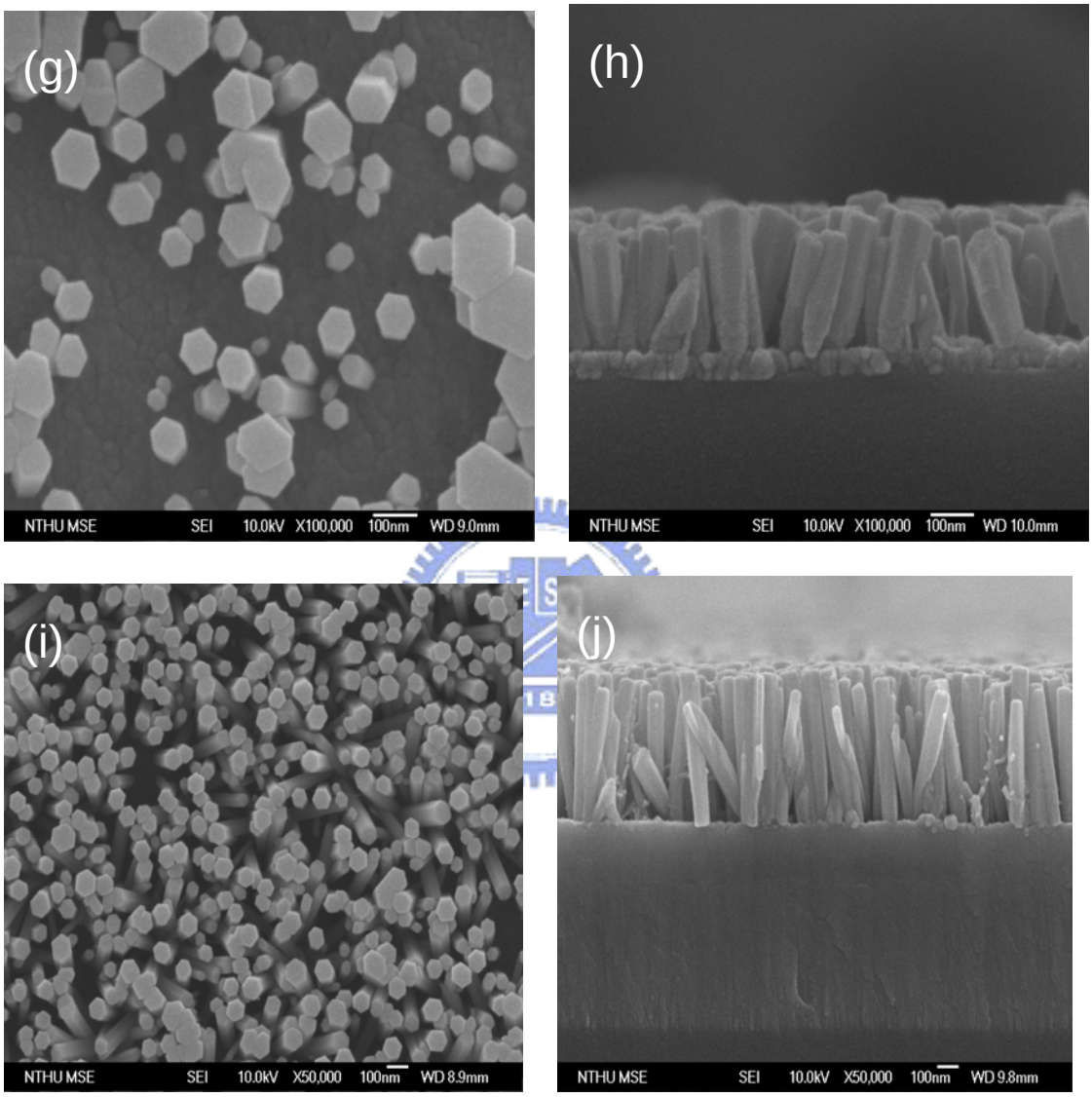


**Figure 4-6 The SEM image of the growth time of ZnO nanowires was (a)(b) 1 hour (c)(d) 1.5 hours (e)(f) 2 hours (g)(h) 2.5 hours (i)(j) 3 hours in the 0.12M**

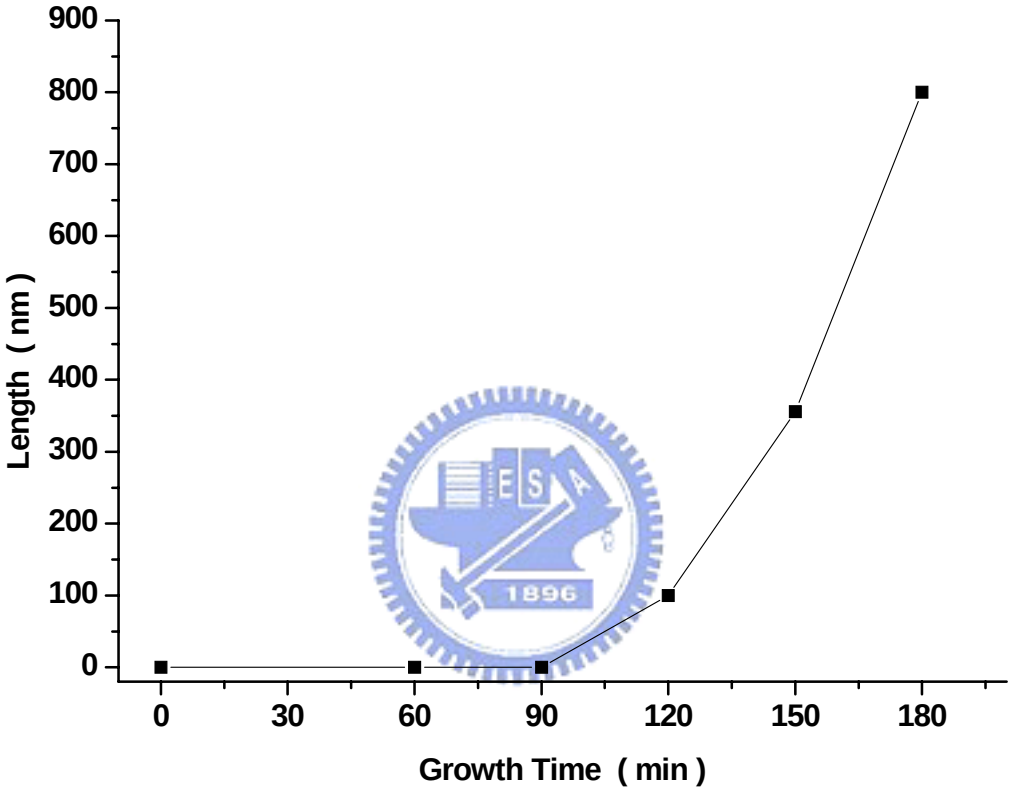


**Figure 4-7 The growth rate of the ZnO nanowires grew on Si wafer**

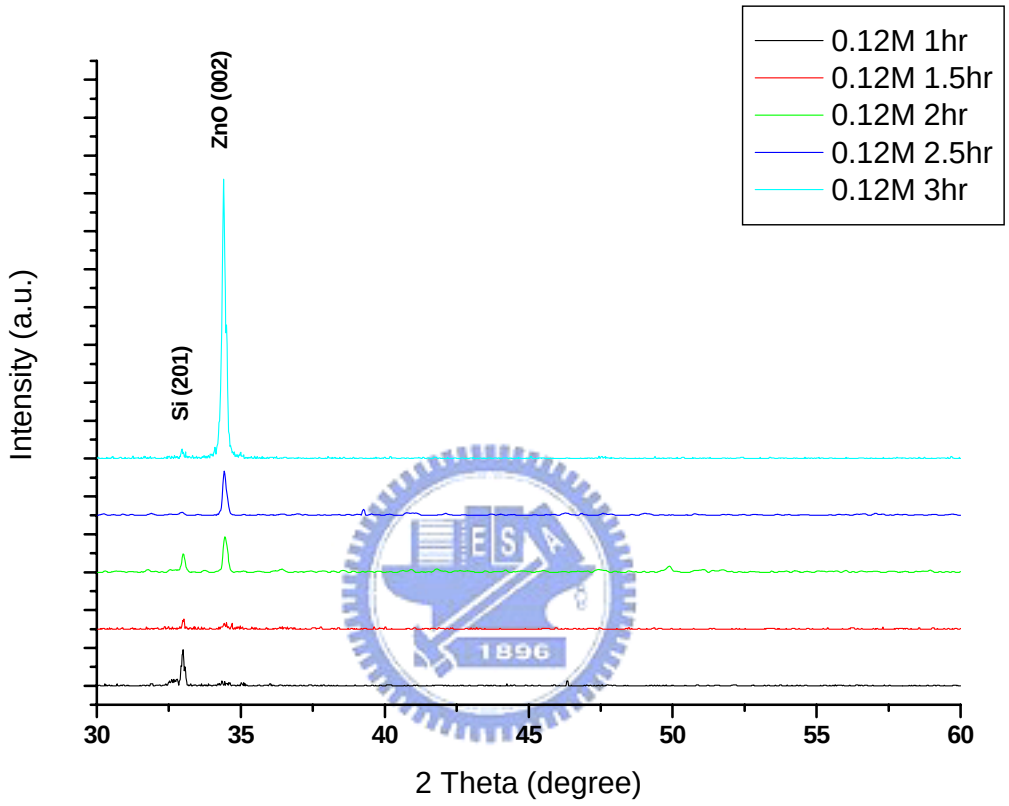


**Figure 4-8 The X-ray diffraction pattern of ZnO nanowires grew on Si wafer at different growth time in the same solution concentration**

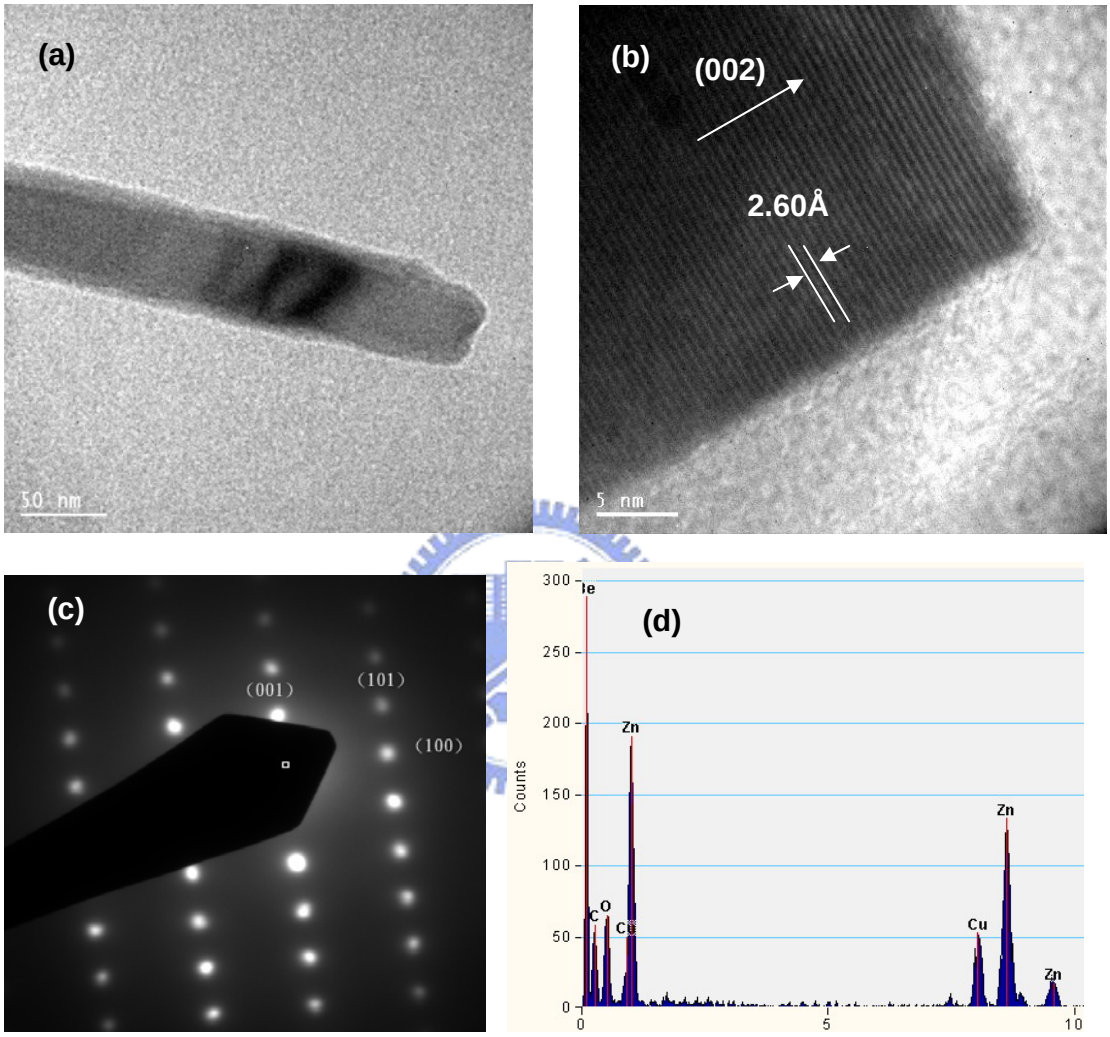


**Figure 4-9 The (a)TEM image (b)HRTEM image (c)SAED (d)EDX spectrum of the ZnO nanowire**

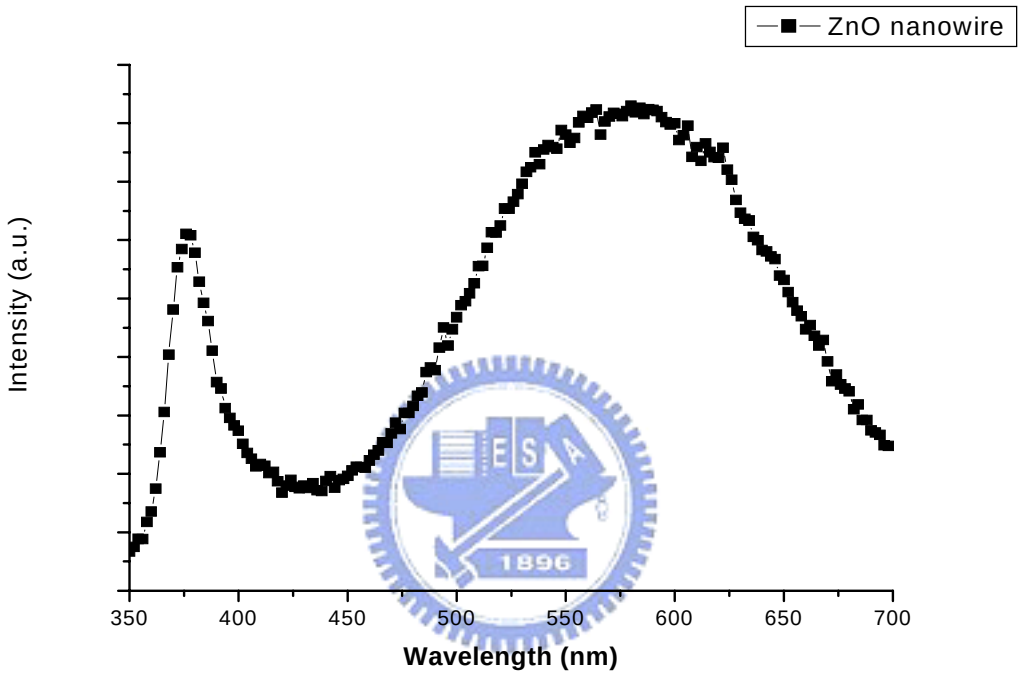


**Figure 4-10 The cathodluminescence (CL) spectra of the ZnO nanowire**

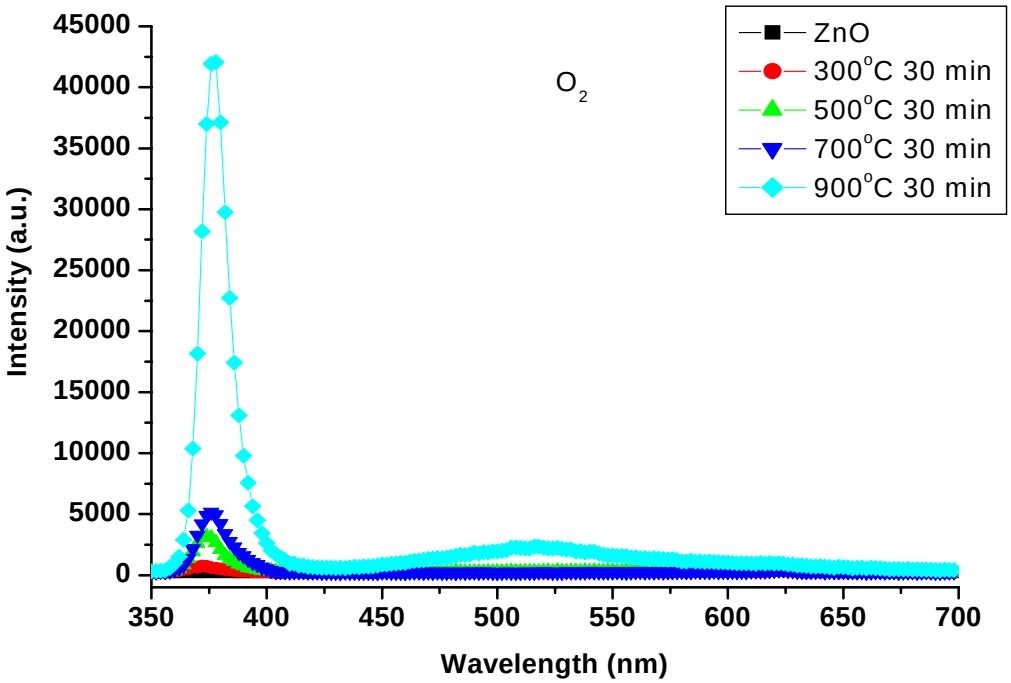


**Figure 4-11 The cathodluminescence (CL) spectra of the ZnO nanowire under the different annealing temperature in oxygen atmosphere**

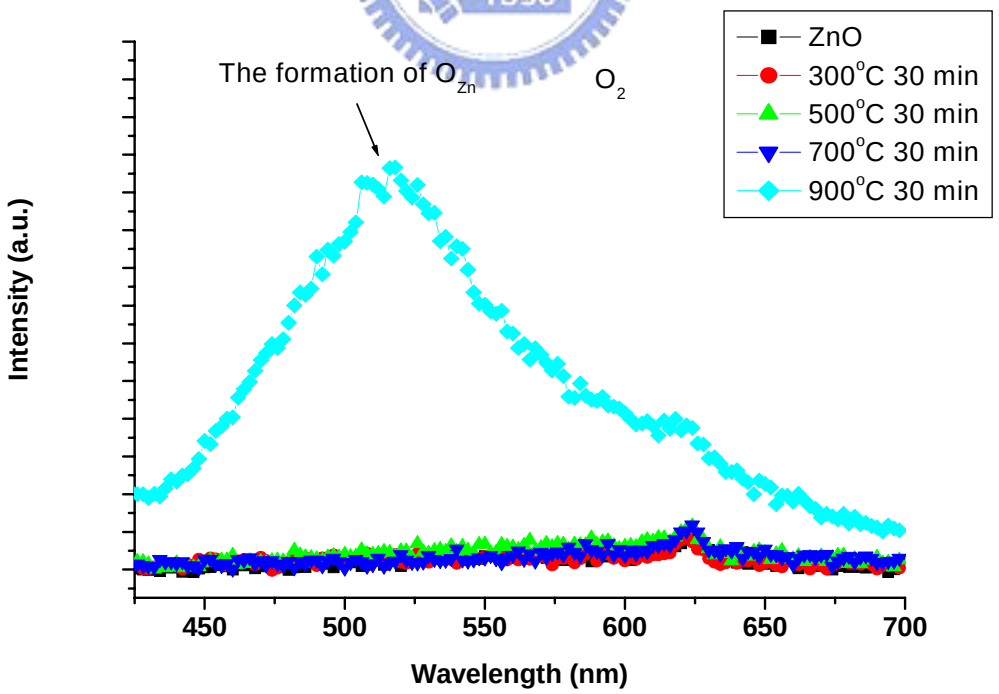


**Figure 4-12 The magnification of Figure 4-11 from 425 nm to 700 nm**

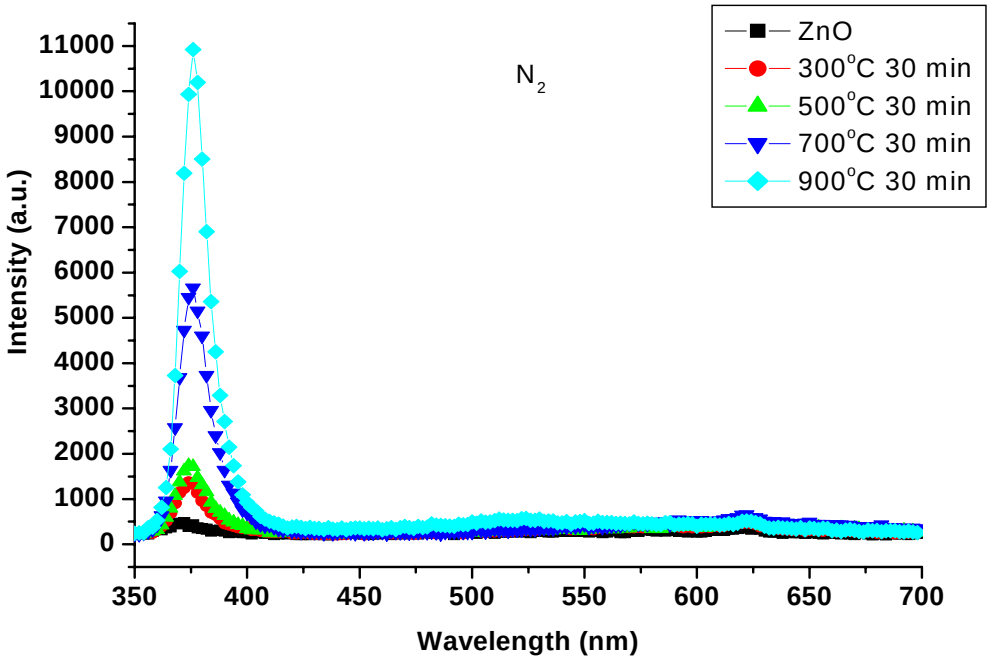


**Figure 4-13 The cathodluminescence (CL) spectra of the ZnO nanowire under the different annealing temperature in nitrogen atmosphere**

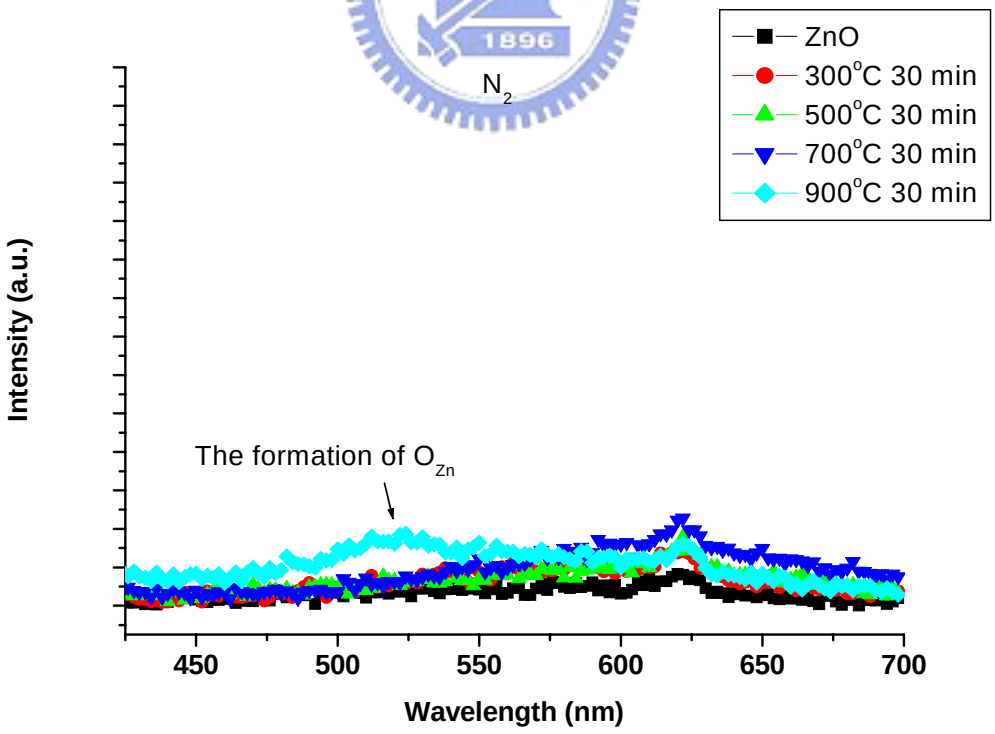


**Figure 4-14 The magnification of Figure 4-14 from 425 nm to 700 nm**

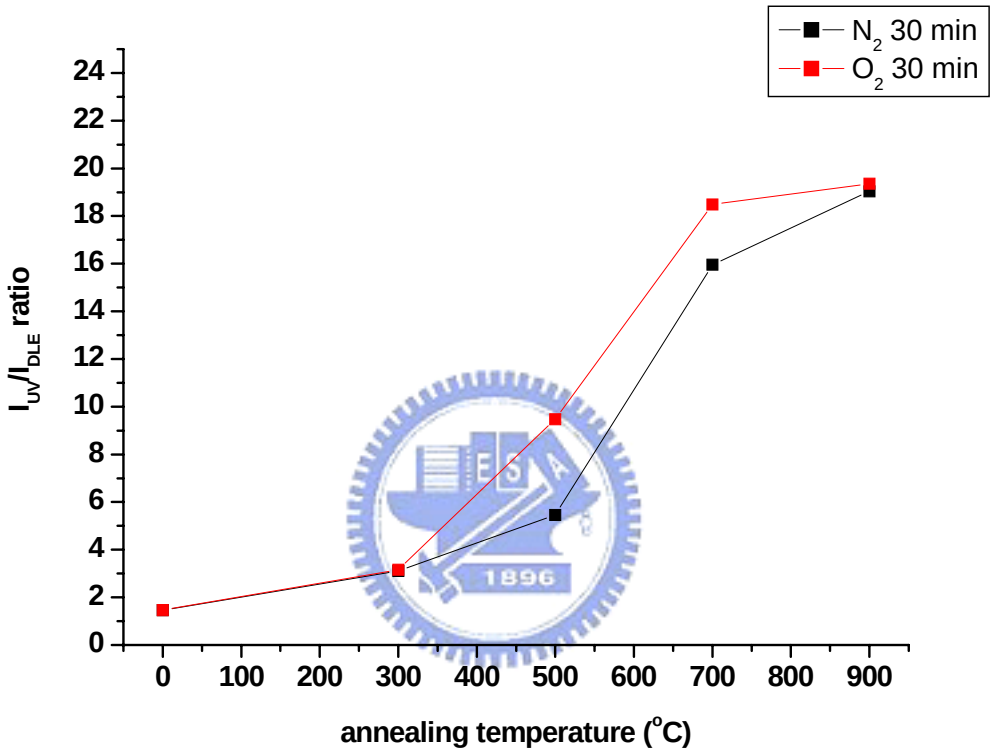


**Figure 4-15 The ratio of $I_{UV}/I_{DLE}$ after annealing in oxygen atmosphere and nitrogen atmosphere**

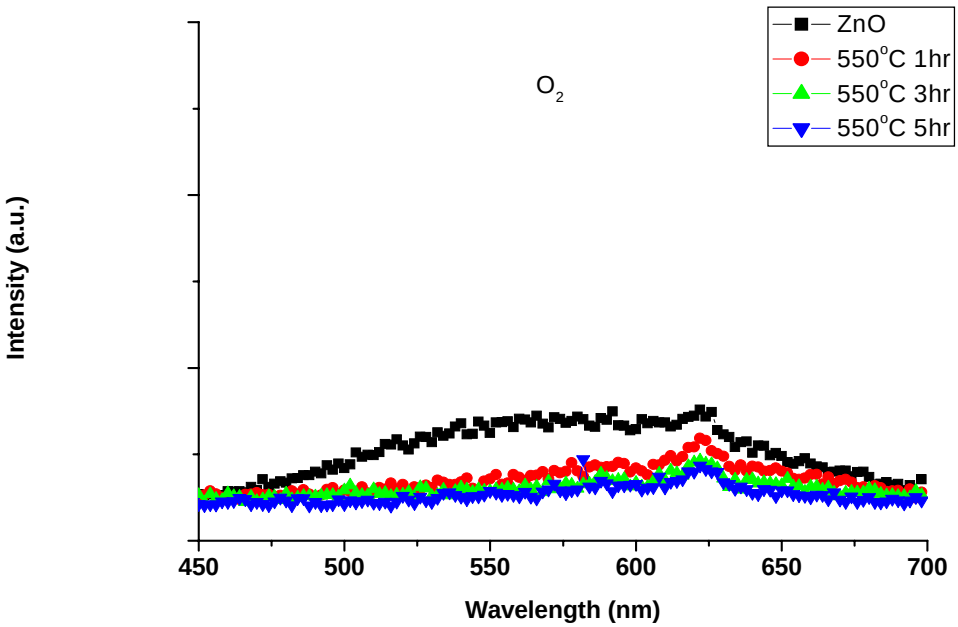


**Figure 4-16 The cathodluminescence (CL) spectra of the ZnO nanowire under the different annealing temperature in oxygen atmosphere**

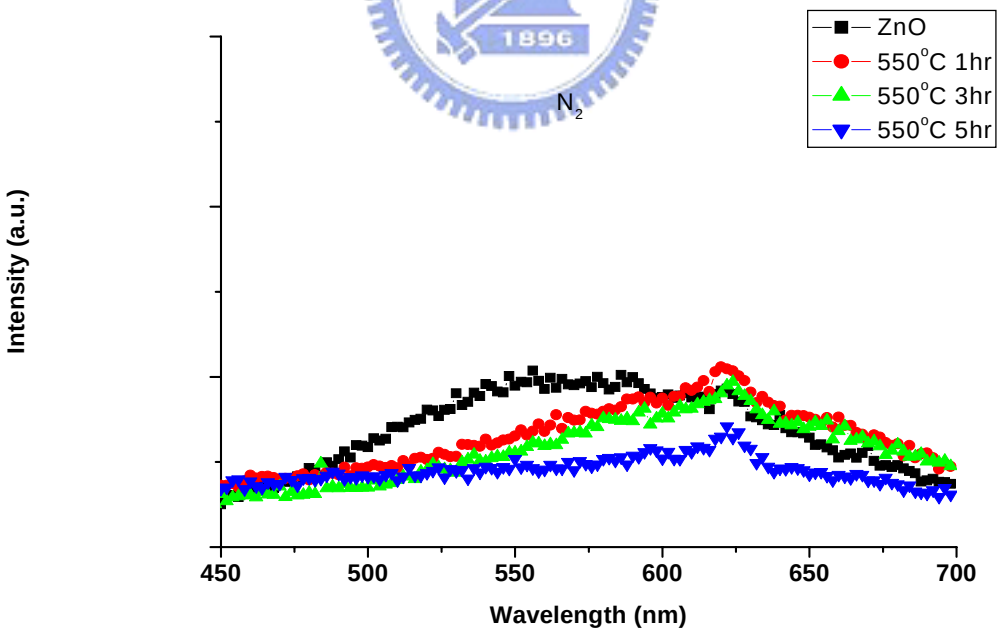


**Figure 4-17 The cathodluminescence (CL) spectra of the ZnO nanowire under the different annealing temperature in nitrogen atmosphere**

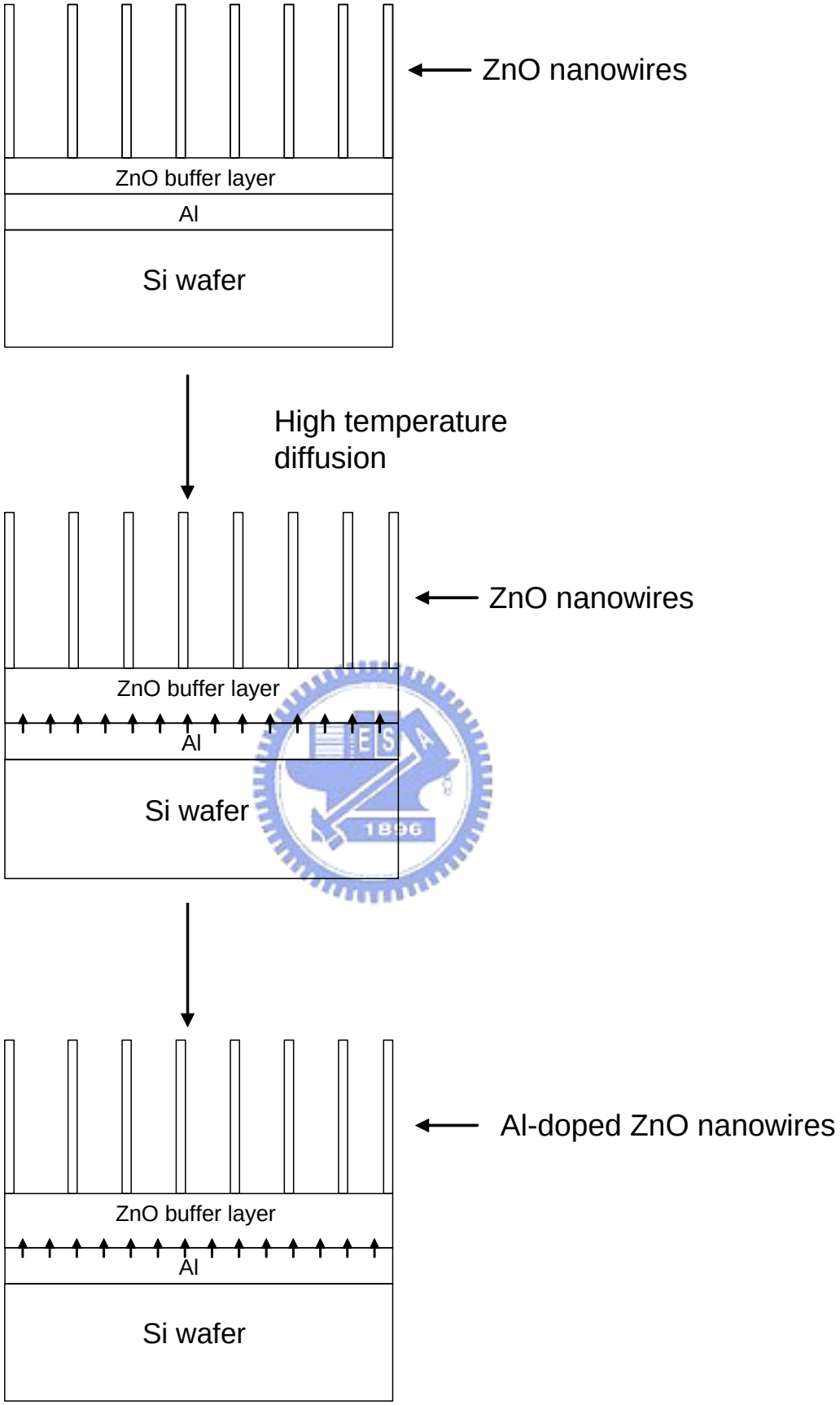


**Figure 4-18 The structure of the Al-doped ZnO nanowires**

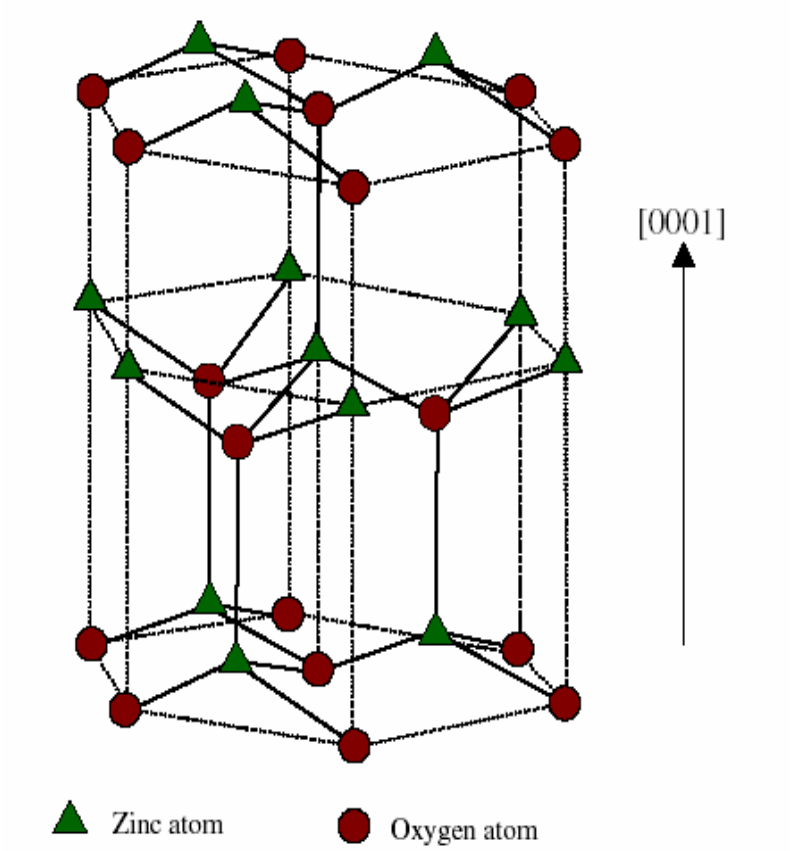


**Figure 4-19 The primitive unit cell of the ZnO structure**

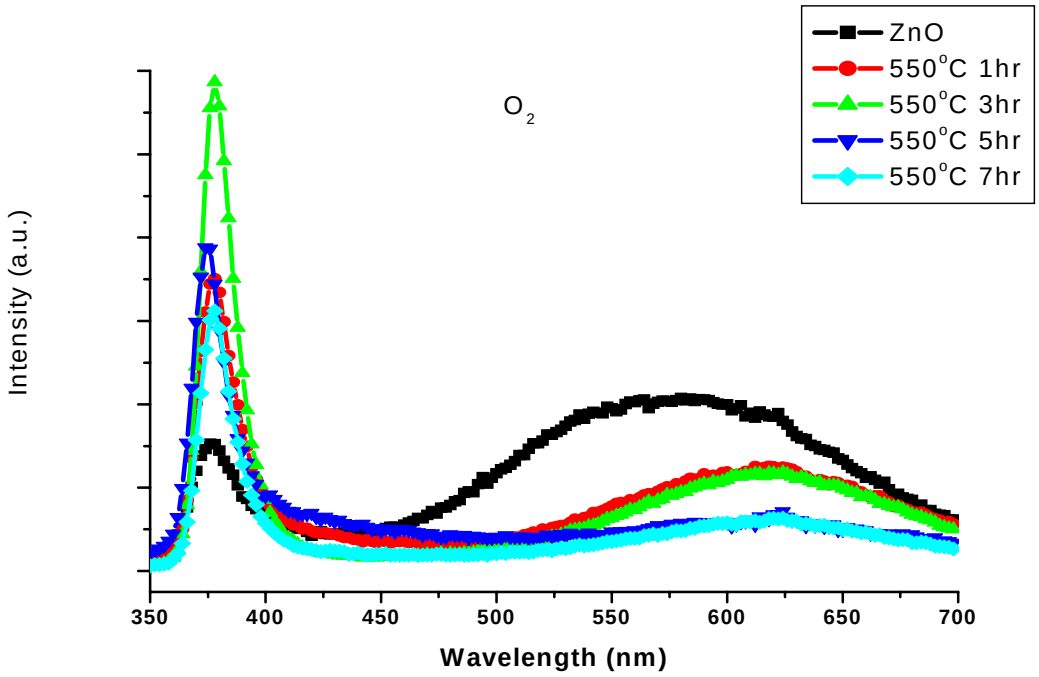


**Figure 4-20 The cathodluminescence (CL) spectra of Al-doped ZnO nanowires at 550℃ under different thermal process time in the oxygen atmosphere**

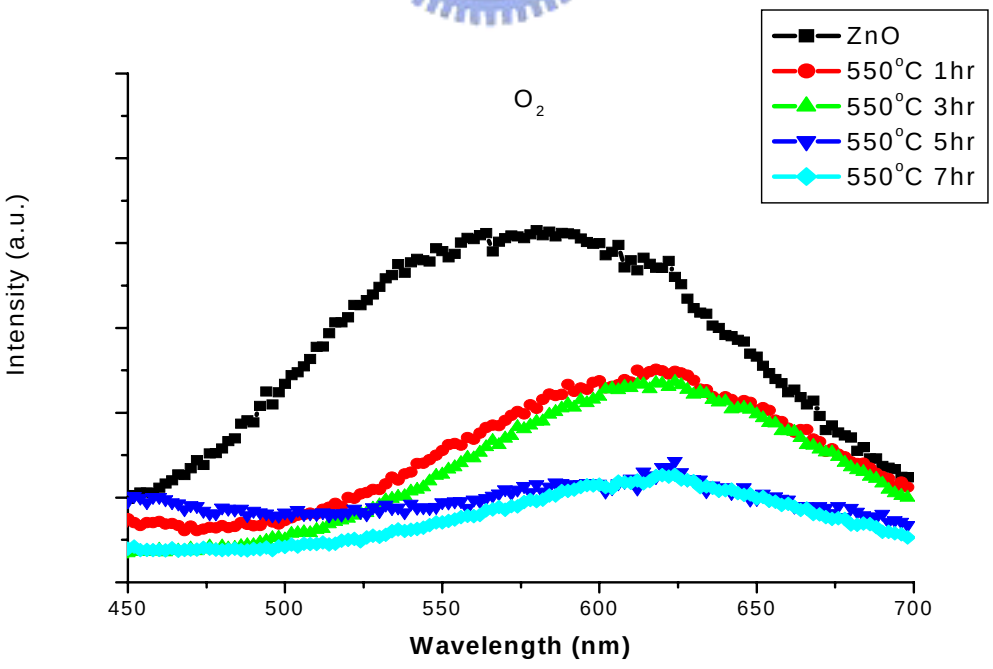


**Figure 4-21 The magnification of Figure 4-20 from 450 nm to 700 nm**

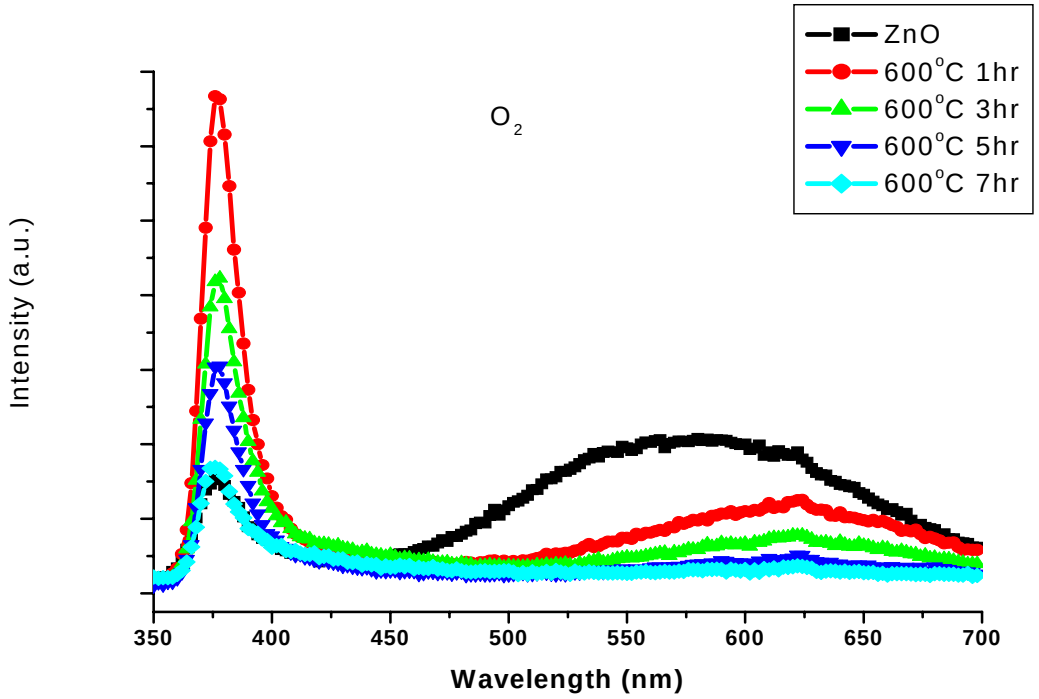


**Figure 4-22 The cathodluminescence (CL) spectra of Al-doped ZnO nanowires at 600℃ under different thermal process time in the oxygen atmosphere**

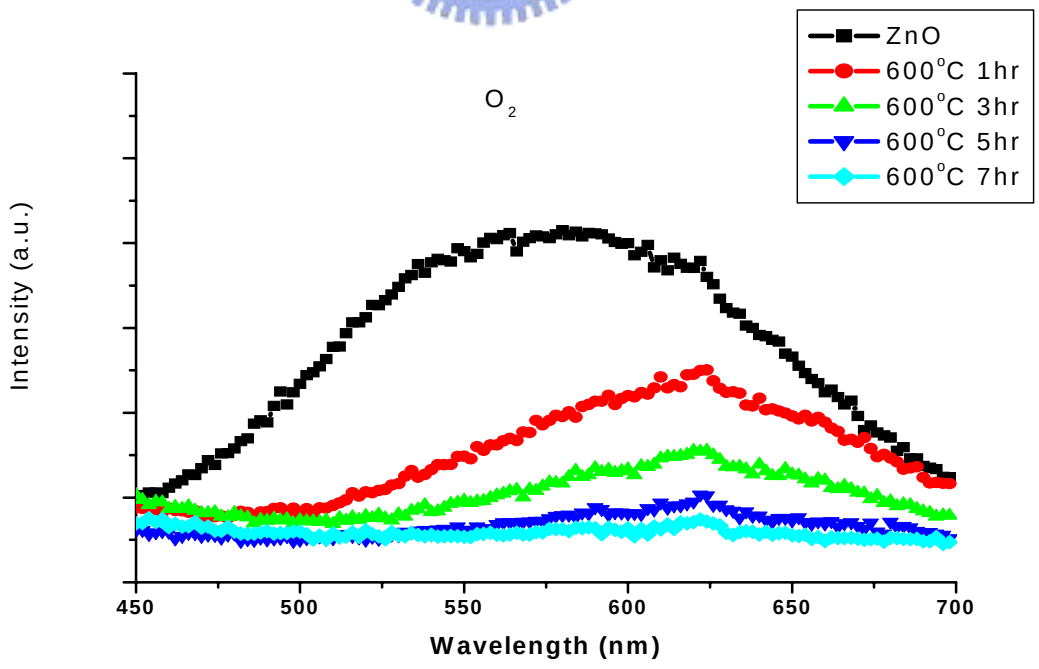


**Figure 4-23 The magnification of Figure 4-22 from 450 nm to 700 nm**

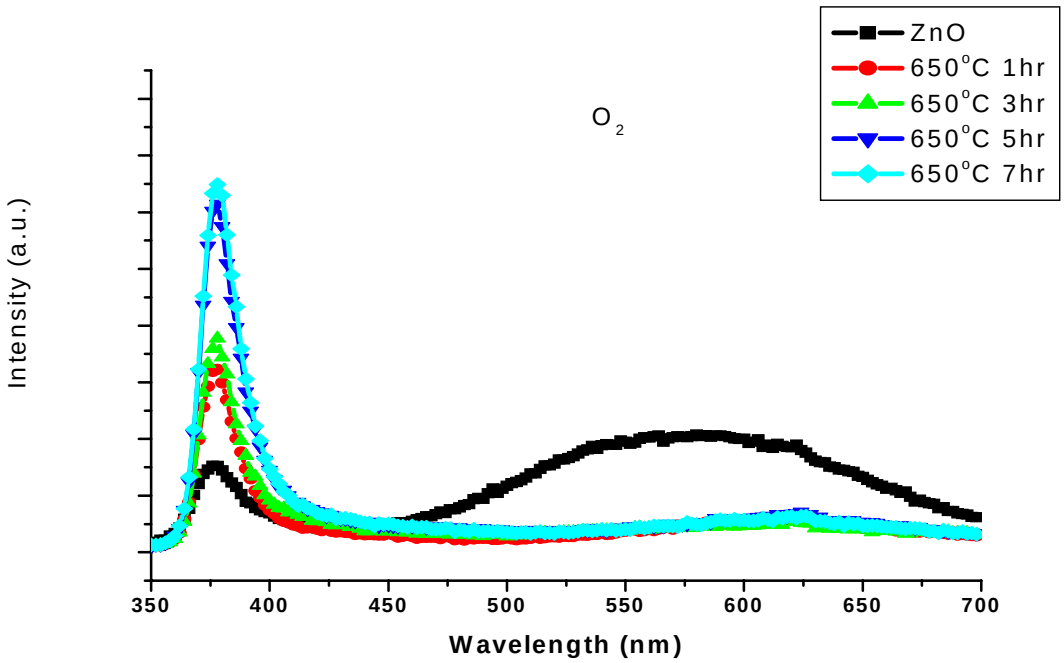


**Figure 4-24 The cathodluminescence (CL) spectra of Al-doped ZnO nanowires at 650℃ under different thermal process time in the oxygen atmosphere**

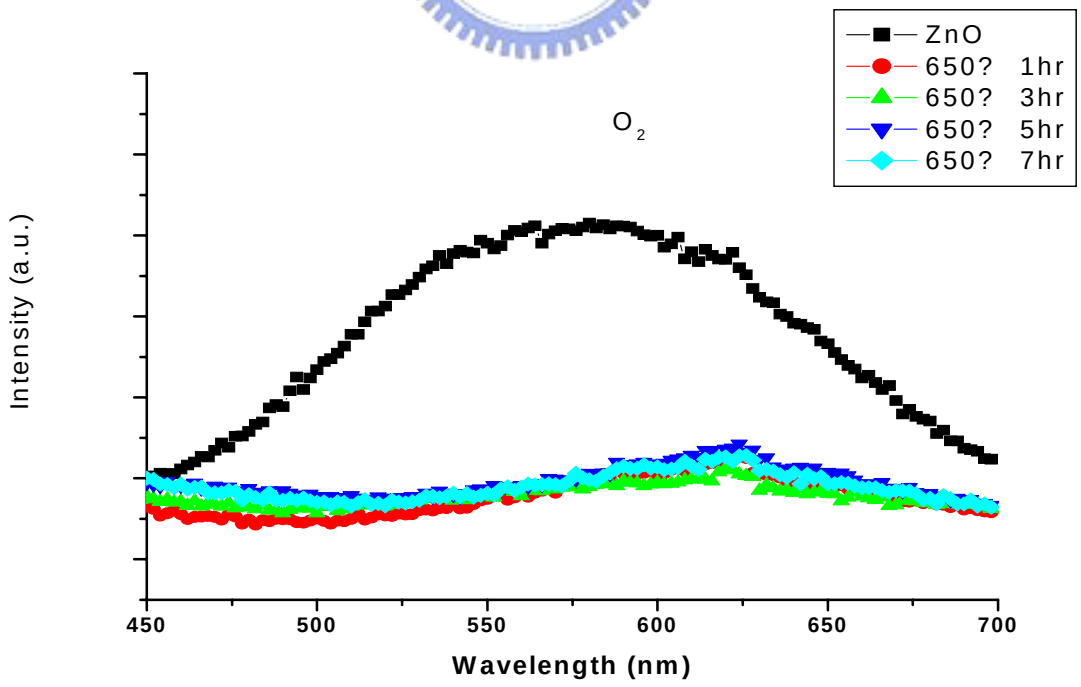


**Figure 4-25 The magnification of Figure 4-24 from 450 nm to 700 nm**

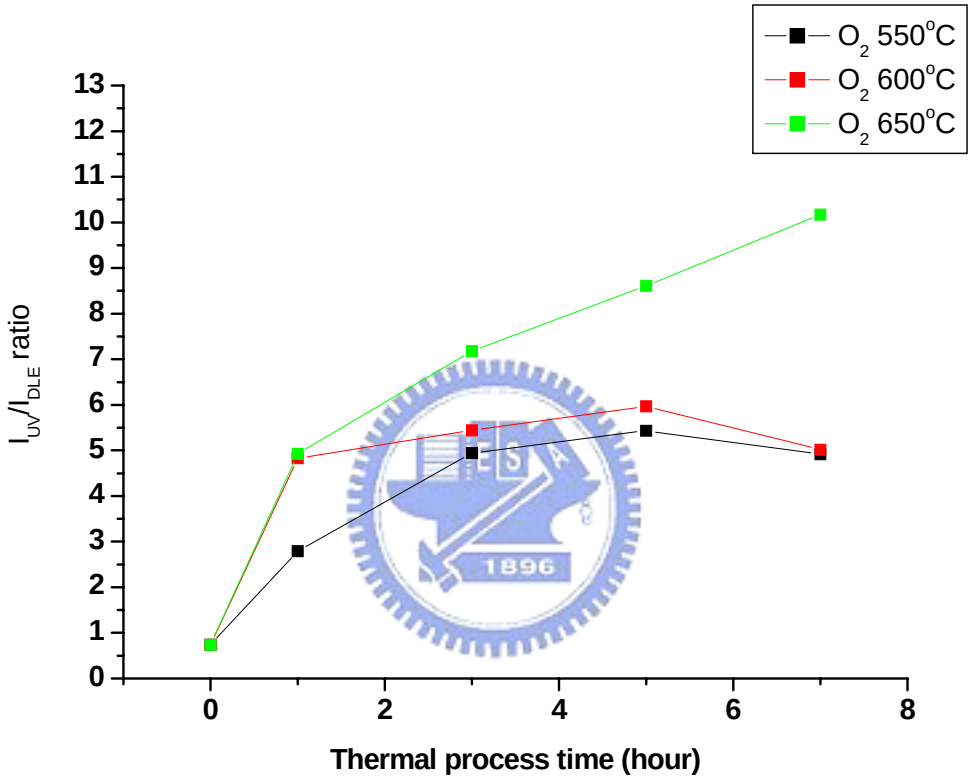


**Figure 4-26 The ratio of $I_{UV}/I_{DLE}$ in oxygen atmosphere at different thermal process temperature**

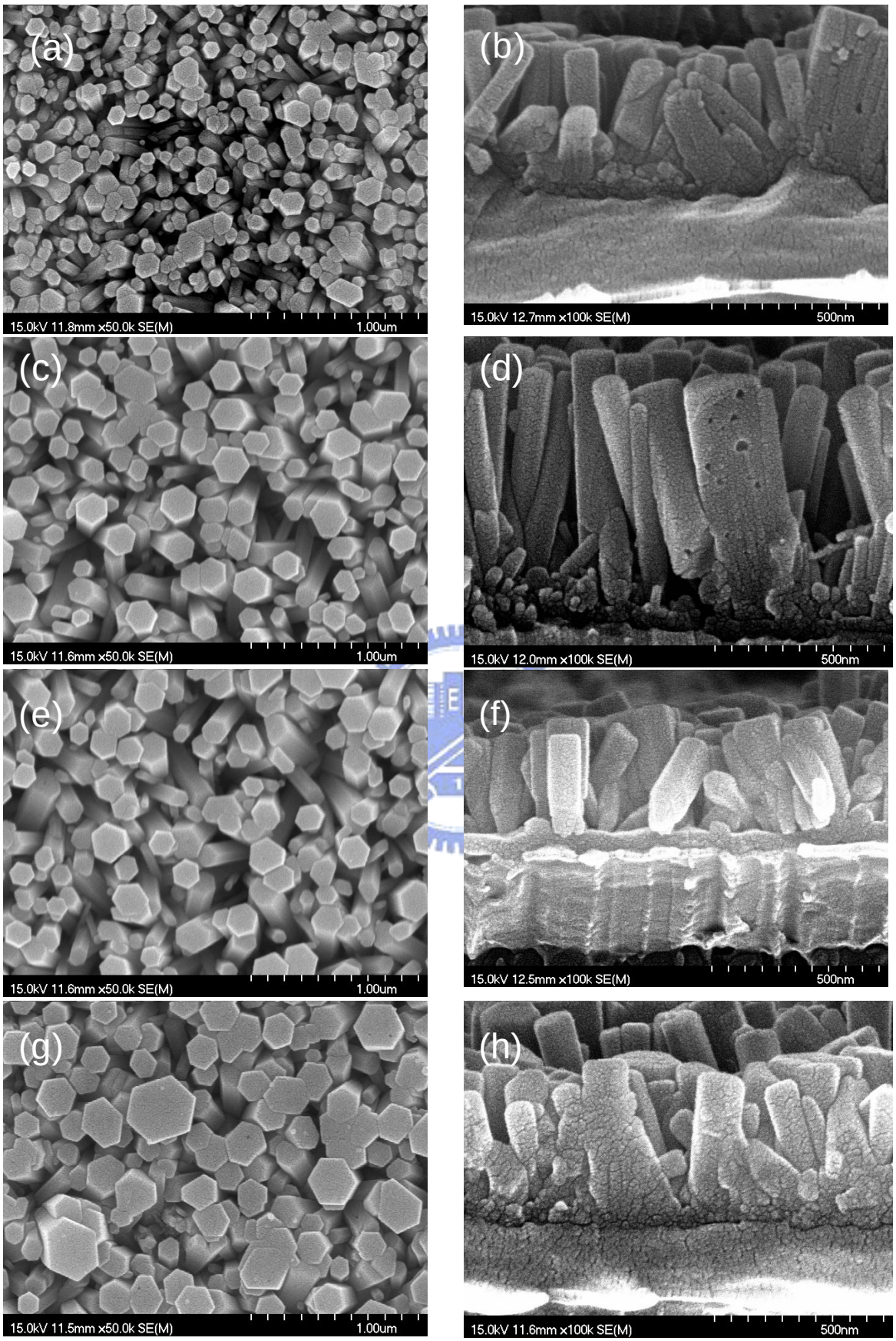


**Figure 4-27 The SEM image of Al-doped ZnO nanowires at 550℃(a)(b) 1 hour (c)(d) 3 hours (e)(f) 5 hours (g)(h) 7 hours in the oxygen atmosphere**

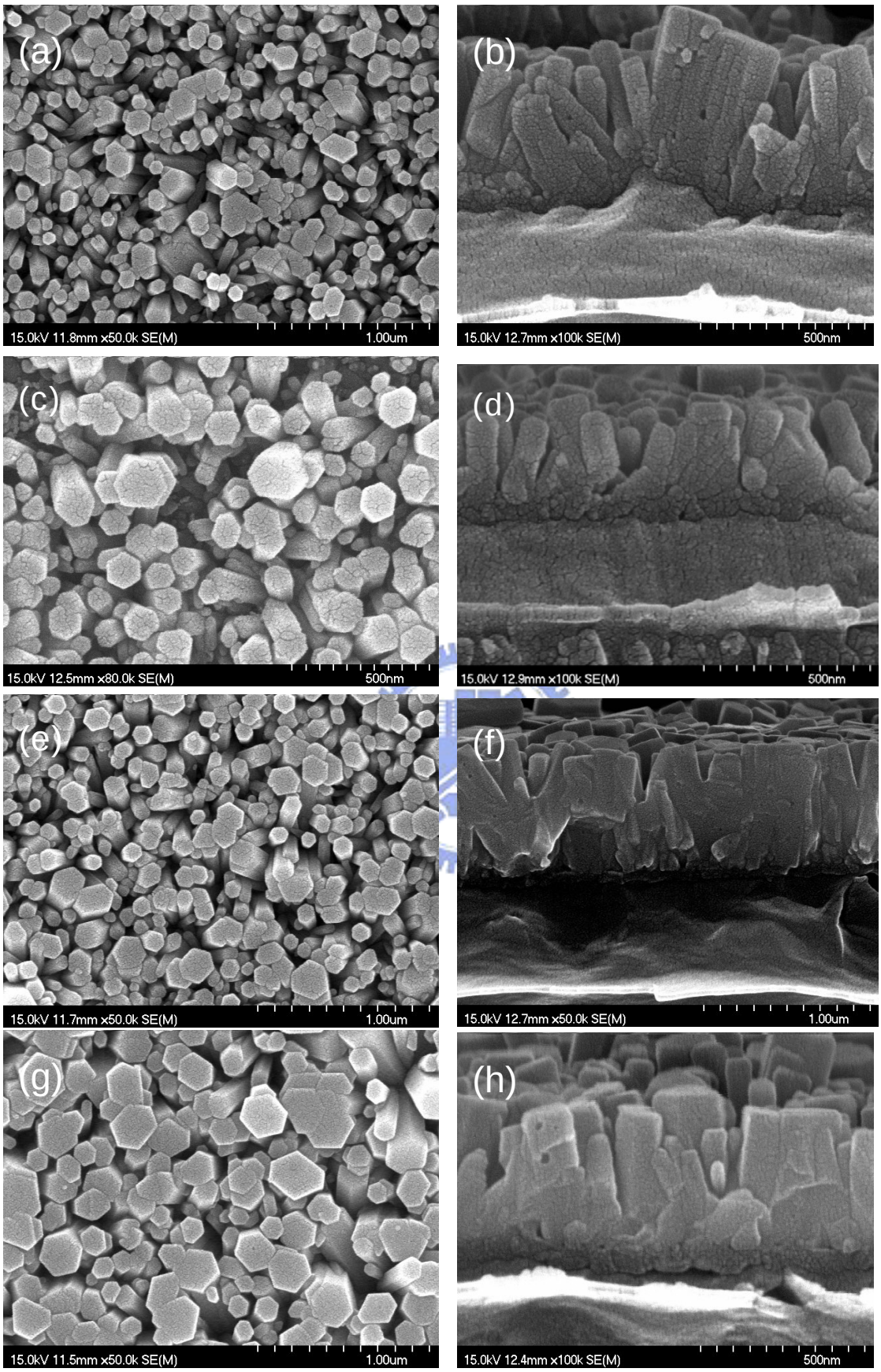


**Figure 4-28 The SEM image of Al-doped ZnO nanowires at 600℃(a)(b) 1 hour (c)(d) 3 hours (e)(f) 5 hours (g)(h) 7 hours in the oxygen atmosphere**

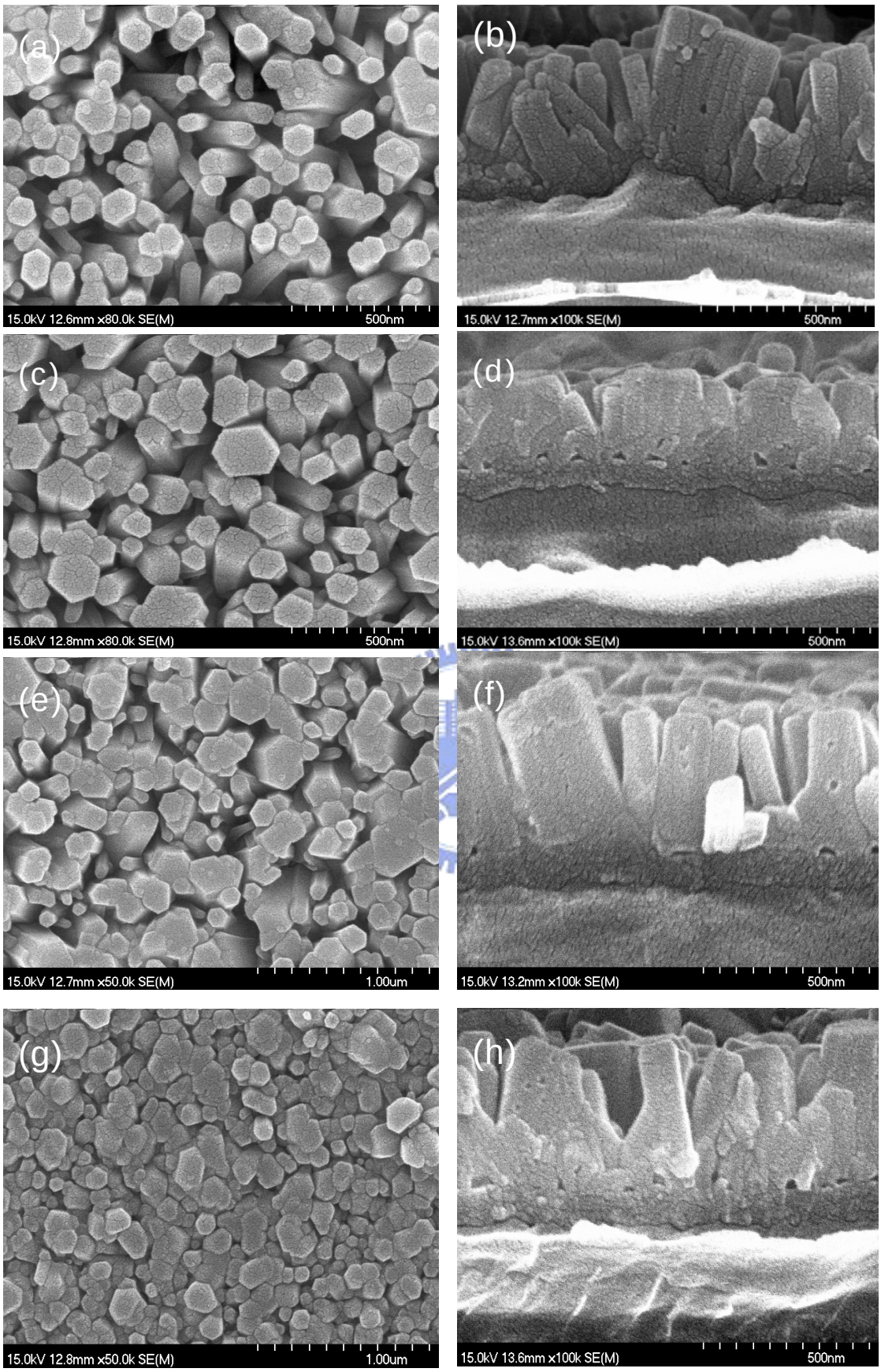


**Figure 4-29 The SEM image of Al-doped ZnO nanowires at 650℃(a)(b) 1 hour (c)(d) 3 hours (e)(f) 5 hours (g)(h) 7 hours in the oxygen atmosphere**

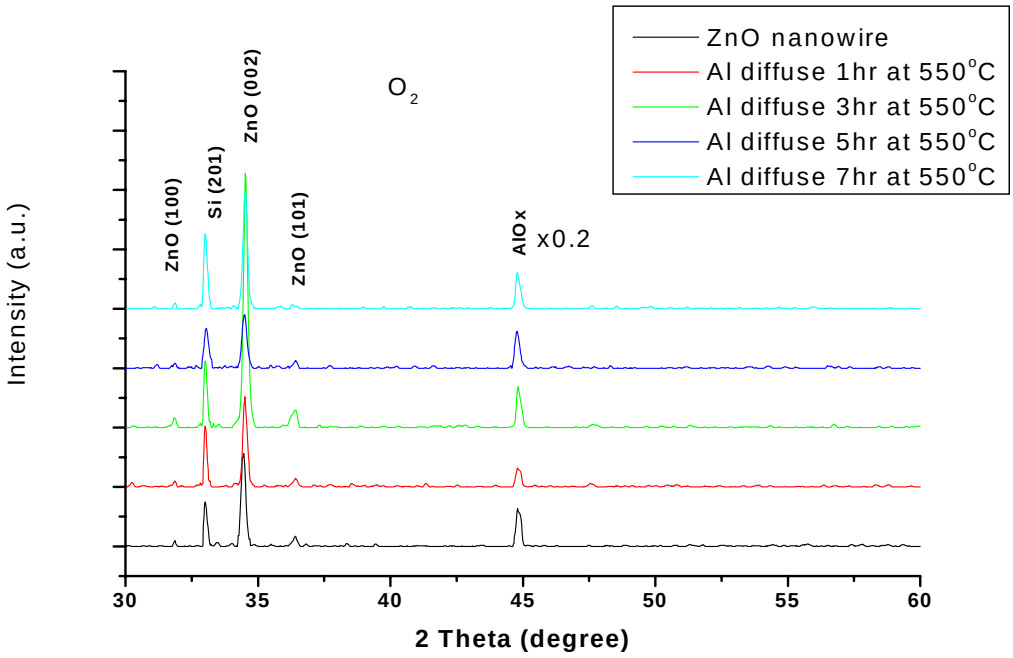


**Figure 4-30 The X-ray diffraction pattern of Al-doped ZnO nanowires grown at 550℃ in oxygen atmosphere**

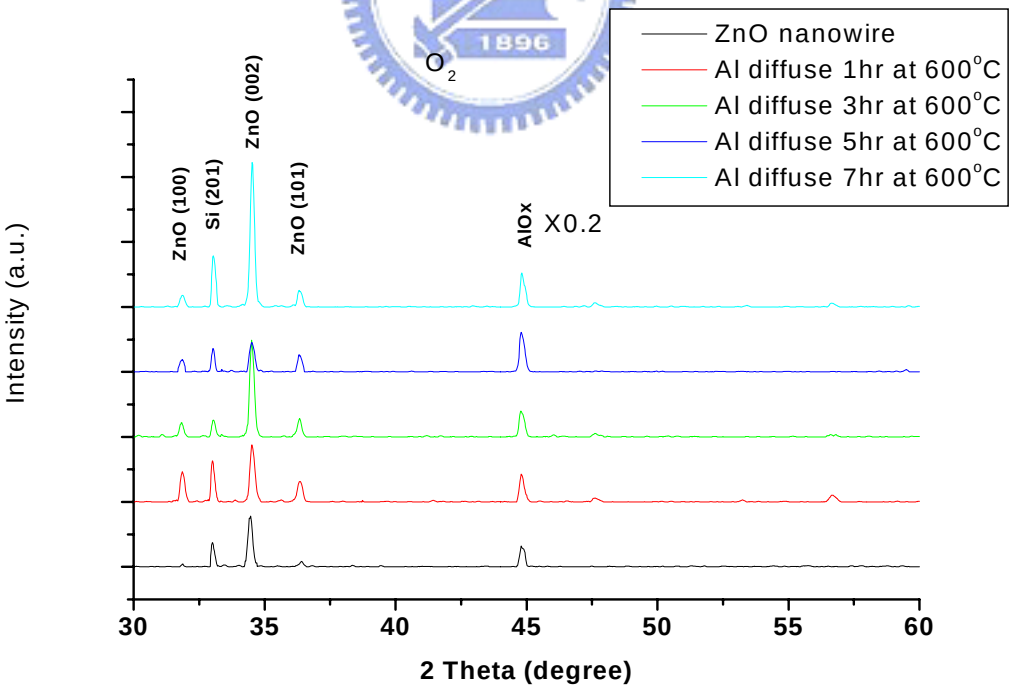


**Figure 4-31 The X-ray diffraction pattern of Al-doped ZnO nanowires grown at 600℃ in oxygen atmosphere**

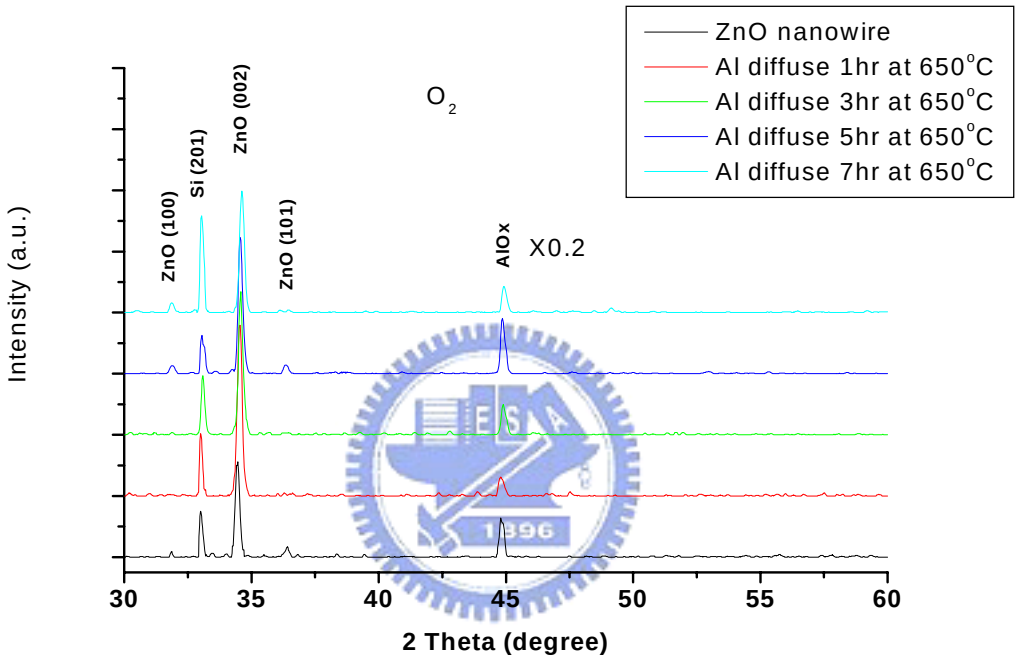


**Figure 4-32 The X-ray diffraction pattern of Al-doped ZnO nanowires grown at 650℃ in oxygen atmosphere**

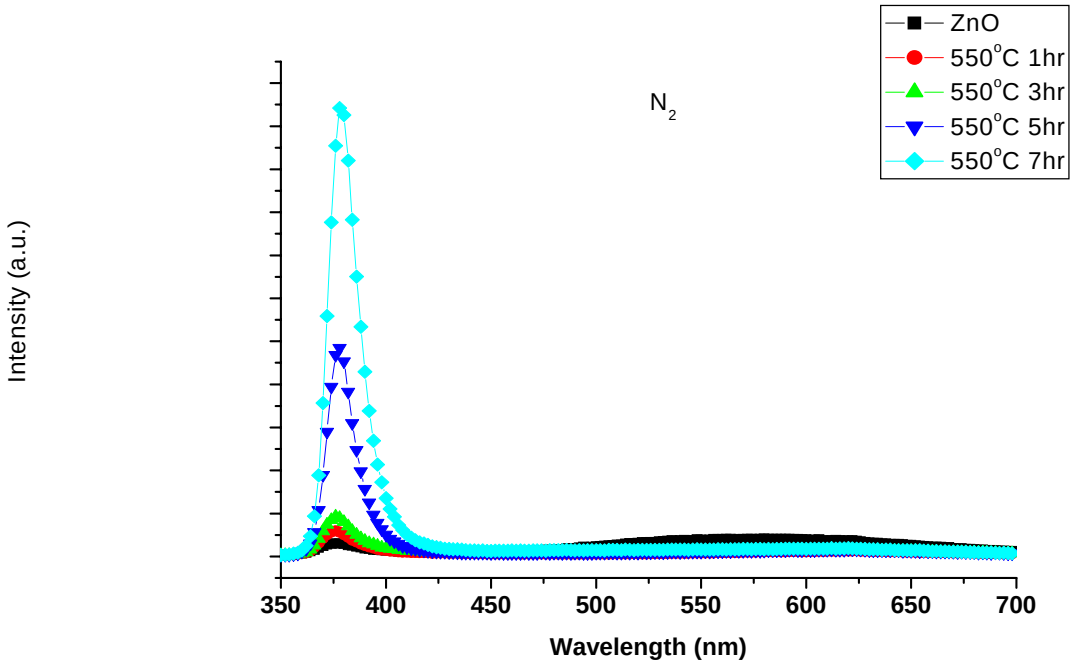


**Figure 4-33 The cathodluminescence (CL) spectra of Al-doped ZnO nanowires at 550℃ under different thermal process time in the nitrogen atmosphere**

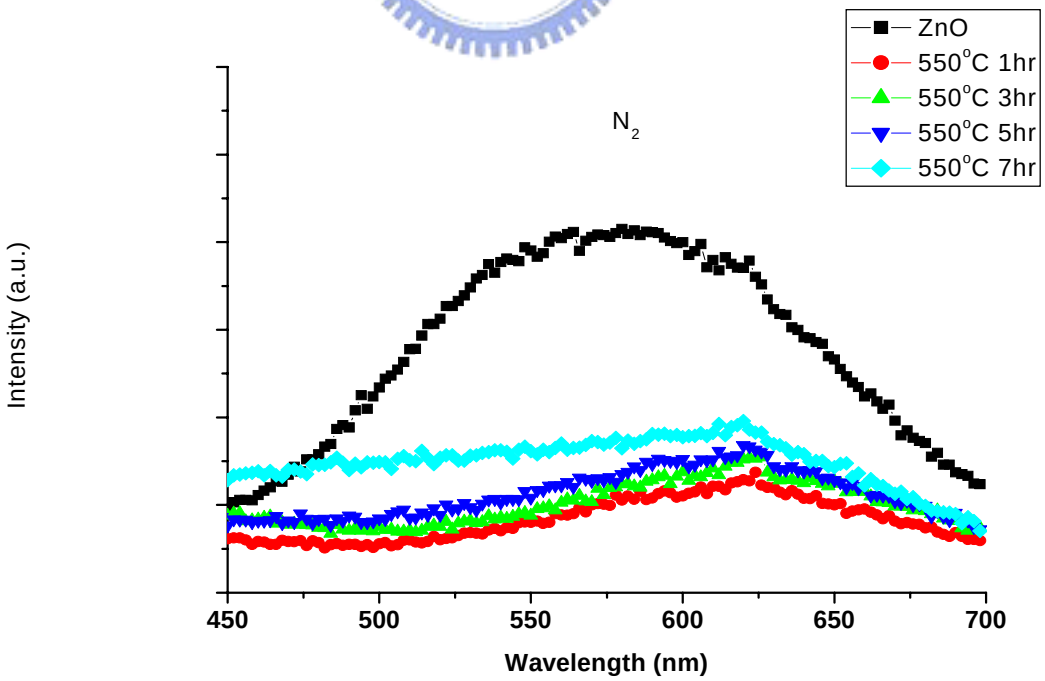


**Figure 4-34 The magnification of figure 4-33 from 450 nm to 700 nm**

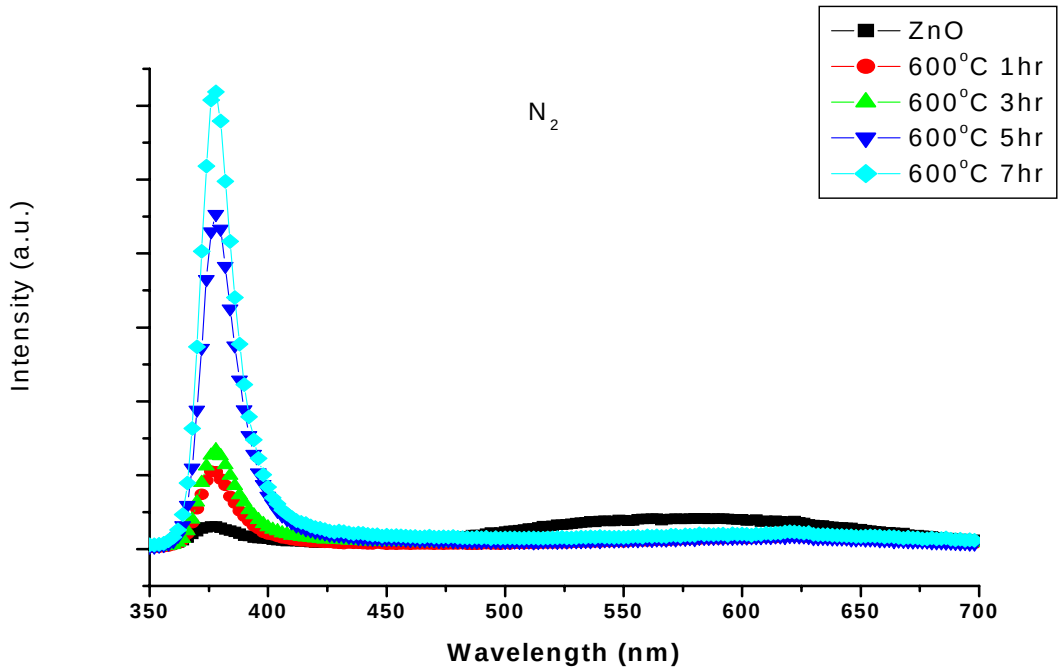


**Figure 4-35 The cathodluminescence (CL) spectra of Al-doped ZnO nanowires at 600℃ under different thermal process time in the nitrogen atmosphere**

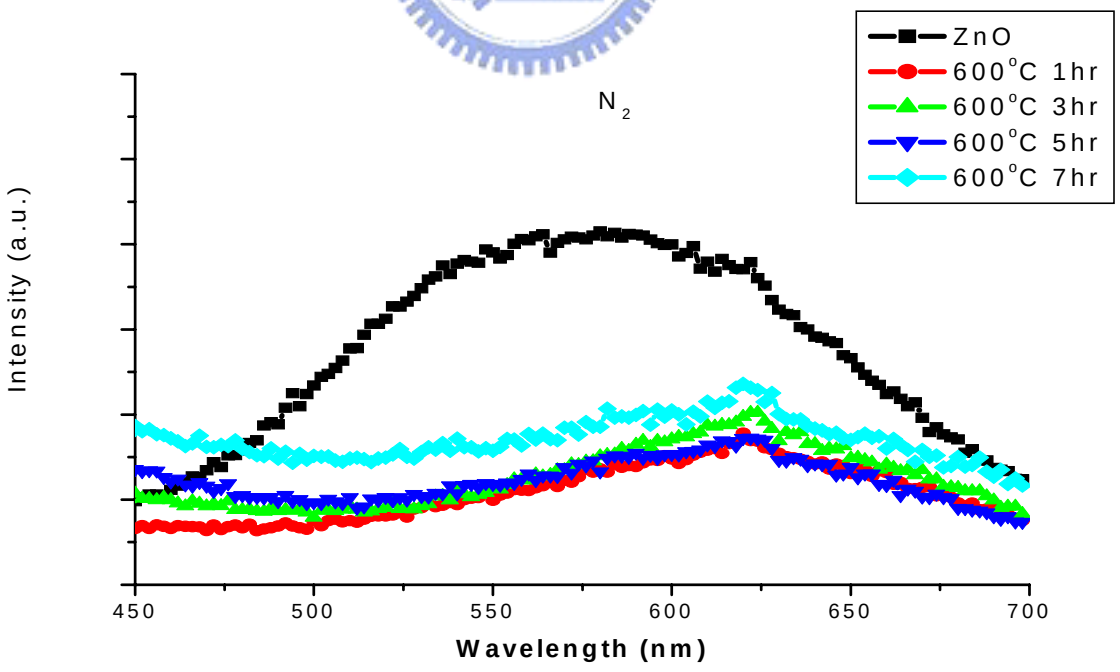


**Figure 4-36 The magnification of figure 4-35 from 450 nm to 700 nm**

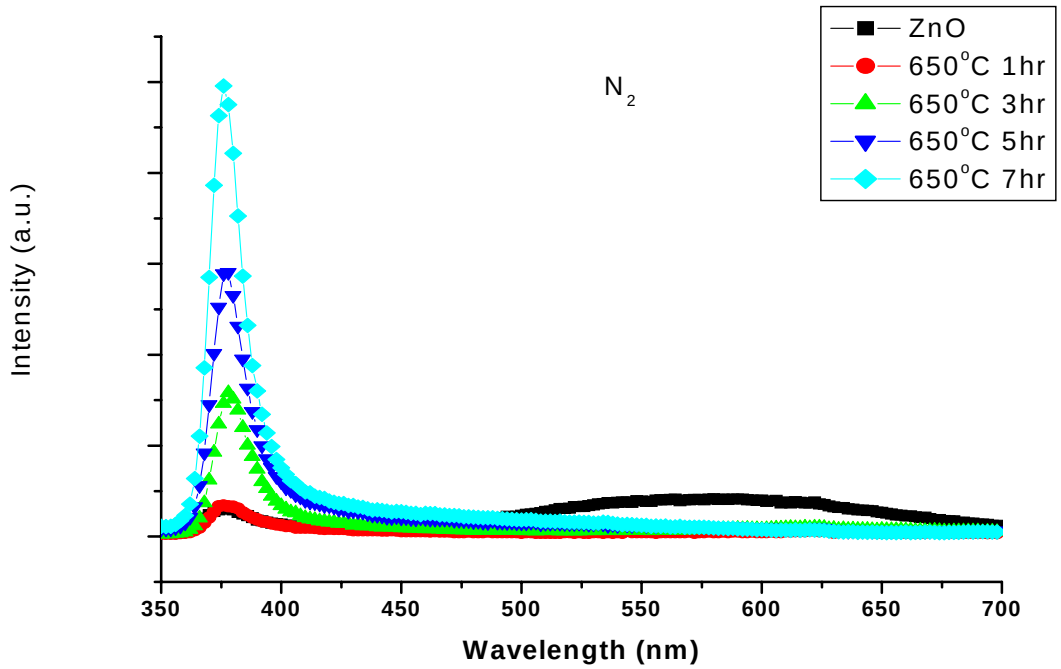


**Figure 4-37 The cathodluminescence (CL) spectra of Al-doped ZnO nanowires at 650℃ under different thermal process time in the nitrogen atmosphere**

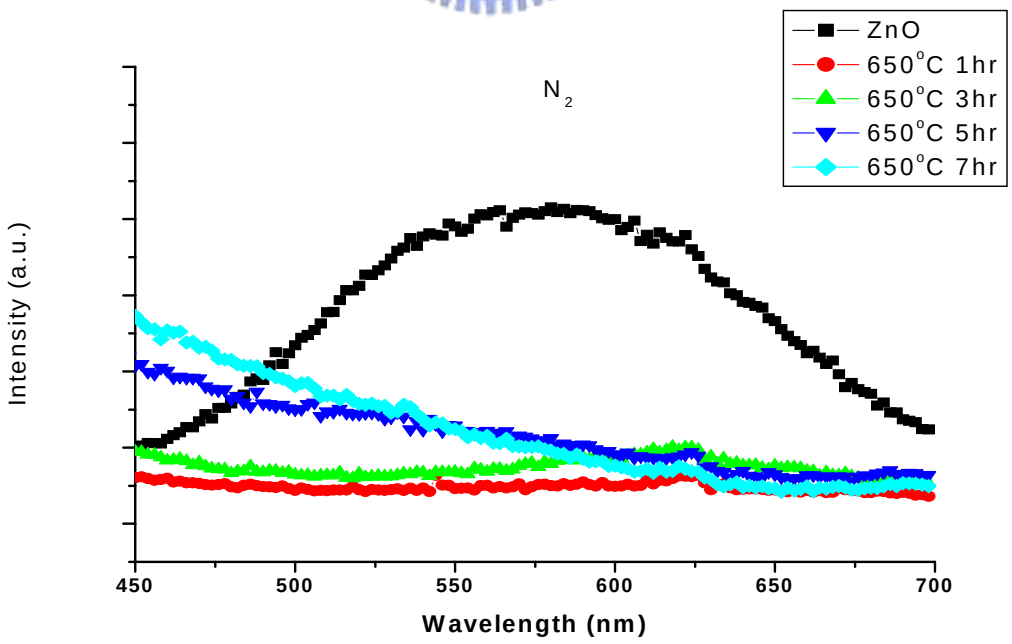


**Figure 4-38 The magnification of figure 4-37 from 450 nm to 700 nm**

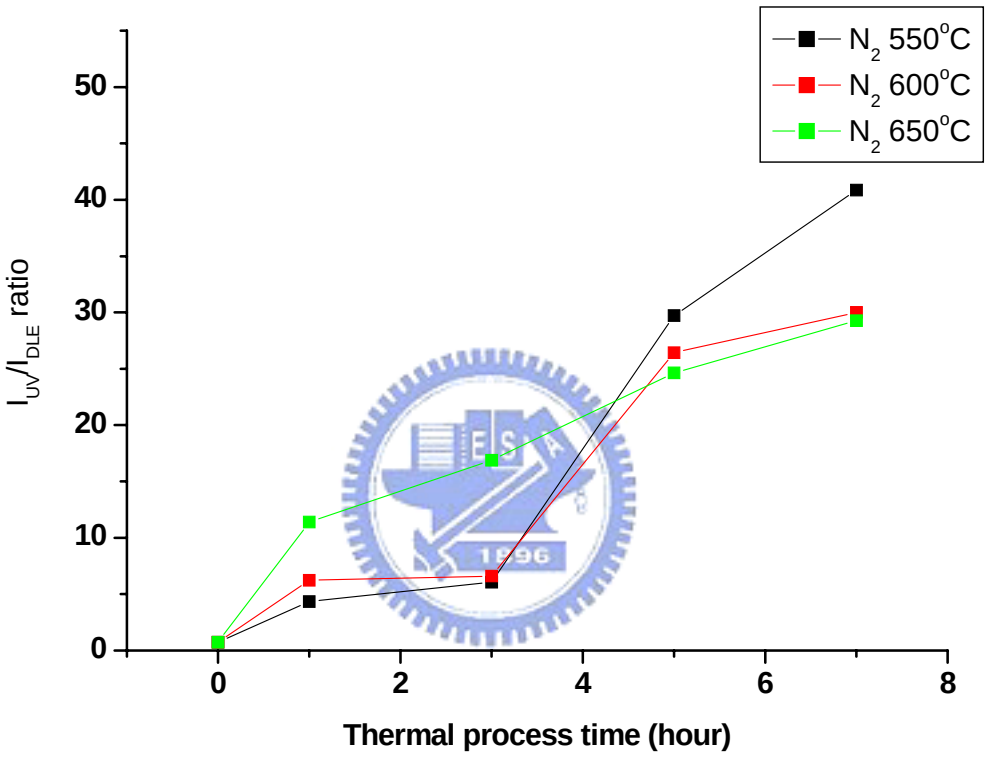


**Figure 4-39 The ratio of $I_{UV}/I_{DLE}$ in nitrogen atmosphere at different thermal process temperature**

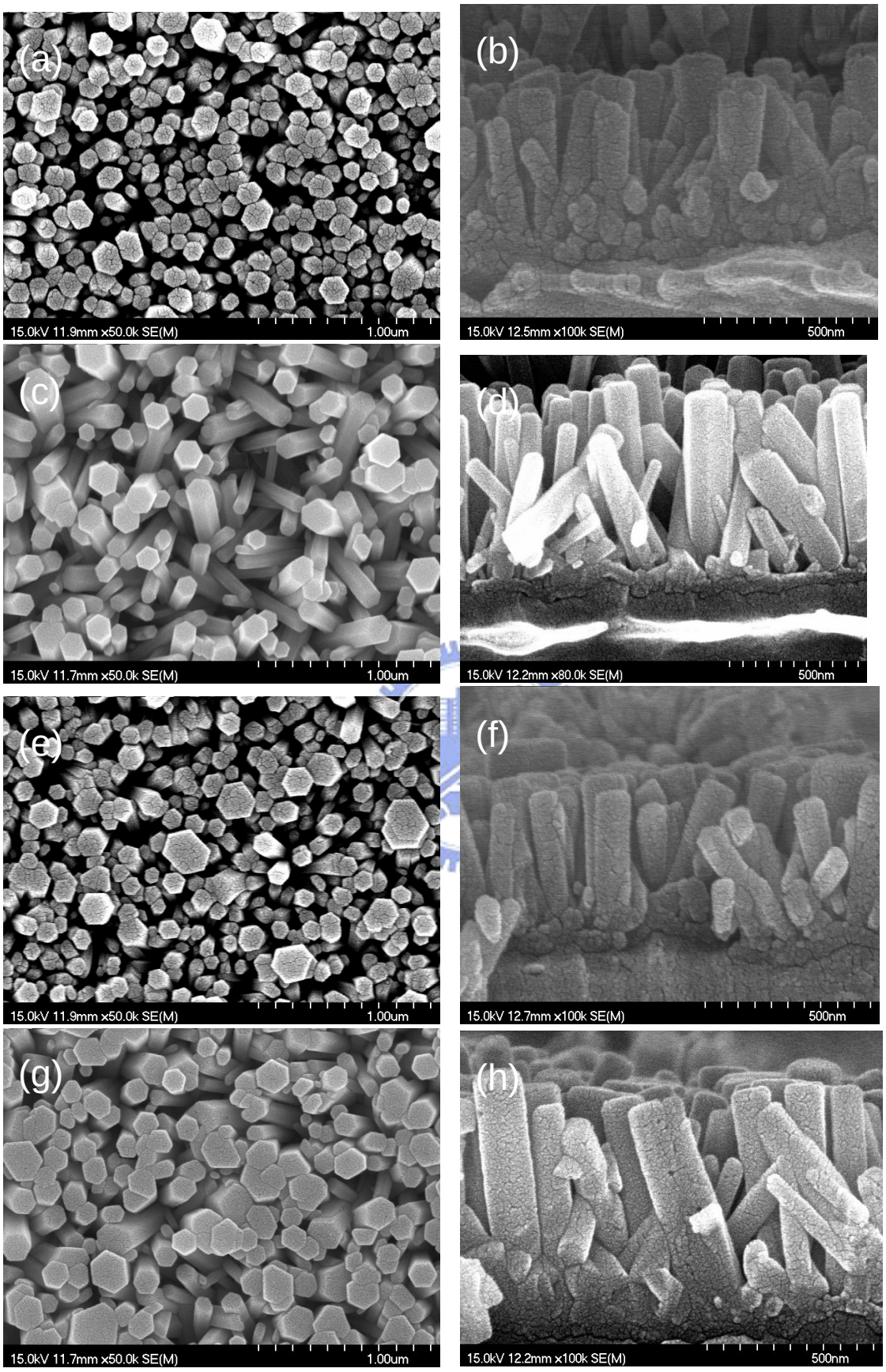


**Figure 4-40 The SEM image of Al-doped ZnO nanowires at 550℃(a)(b) 1 hour (c)(d) 3 hours (e)(f) 5 hours (g)(h) 7 hours in the nitrogen atmosphere**

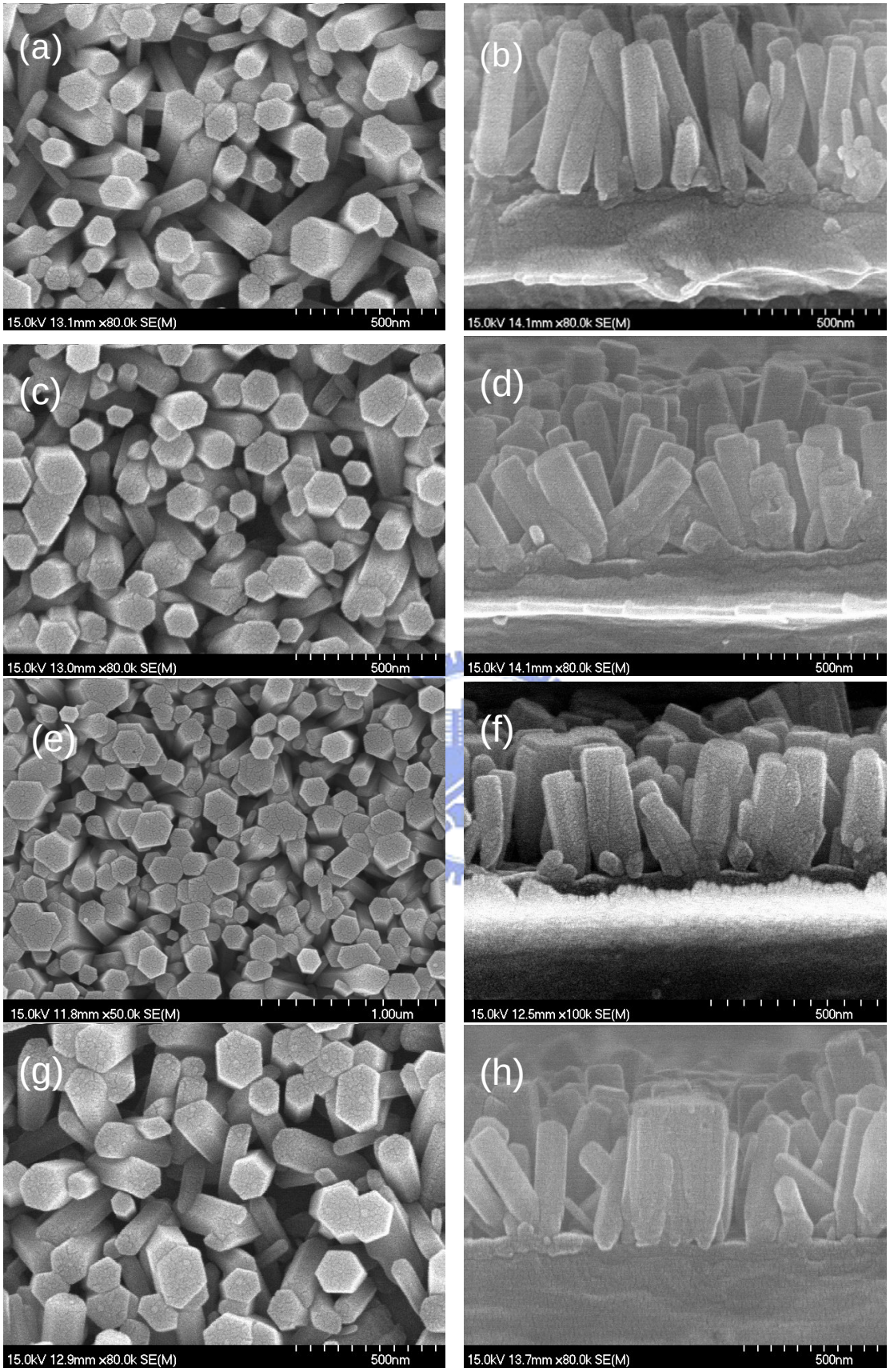


**Figure 4-41 The SEM image of Al-doped ZnO nanowires at 600℃(a)(b) 1 hour (c)(d) 3 hours (e)(f) 5 hours (g)(h) 7 hours in the nitrogen atmosphere**

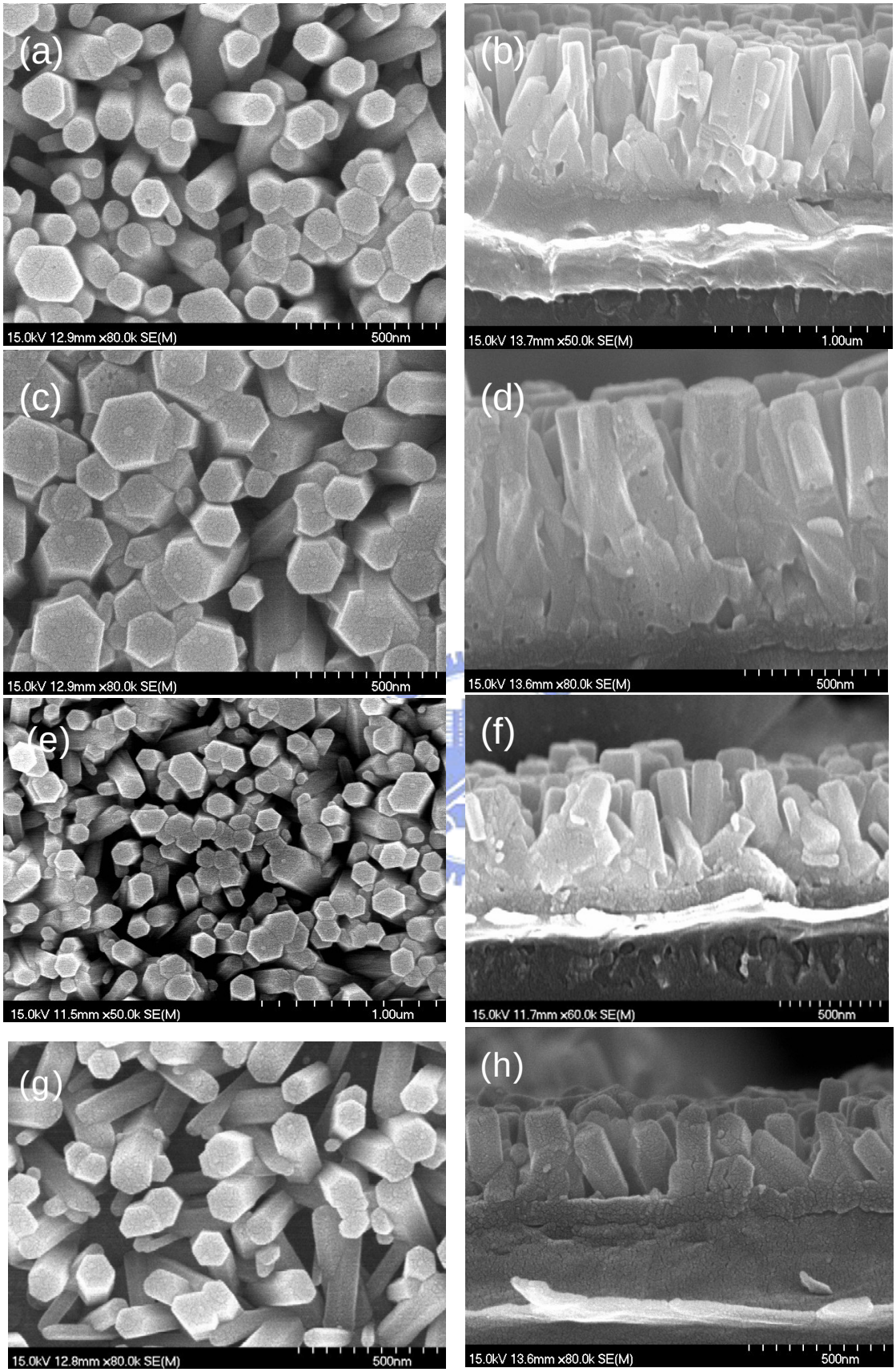


**Figure 4-42 The SEM image of Al-doped ZnO nanowires at 650℃(a)(b) 1 hour (c)(d) 3 hours (e)(f) 5 hours (g)(h) 7 hours in the nitrogen atmosphere**

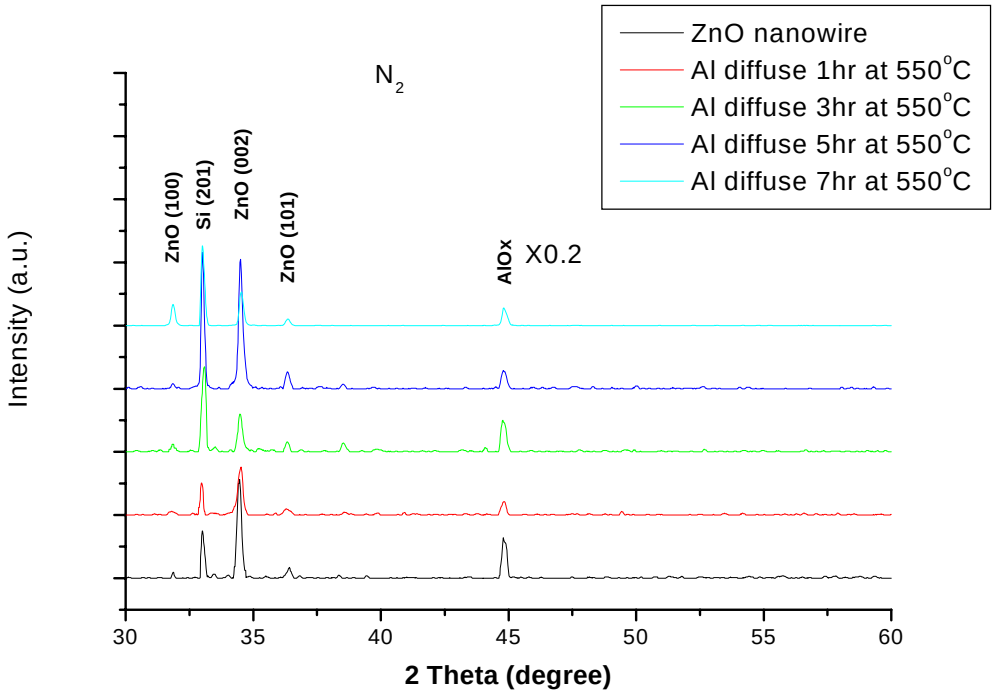


**Figure 4-43 The X-ray diffraction pattern of Al-doped ZnO nanowires grown at 550℃ in nitrogen atmosphere**

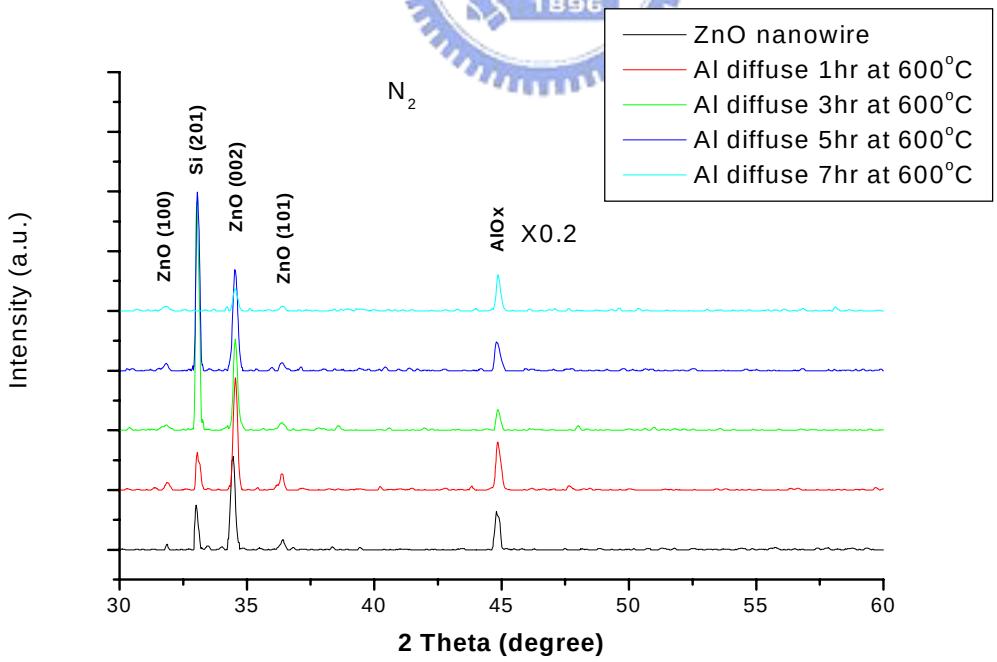


**Figure 4-44 The X-ray diffraction pattern of Al-doped ZnO nanowires grown at 600℃ in nitrogen atmosphere**

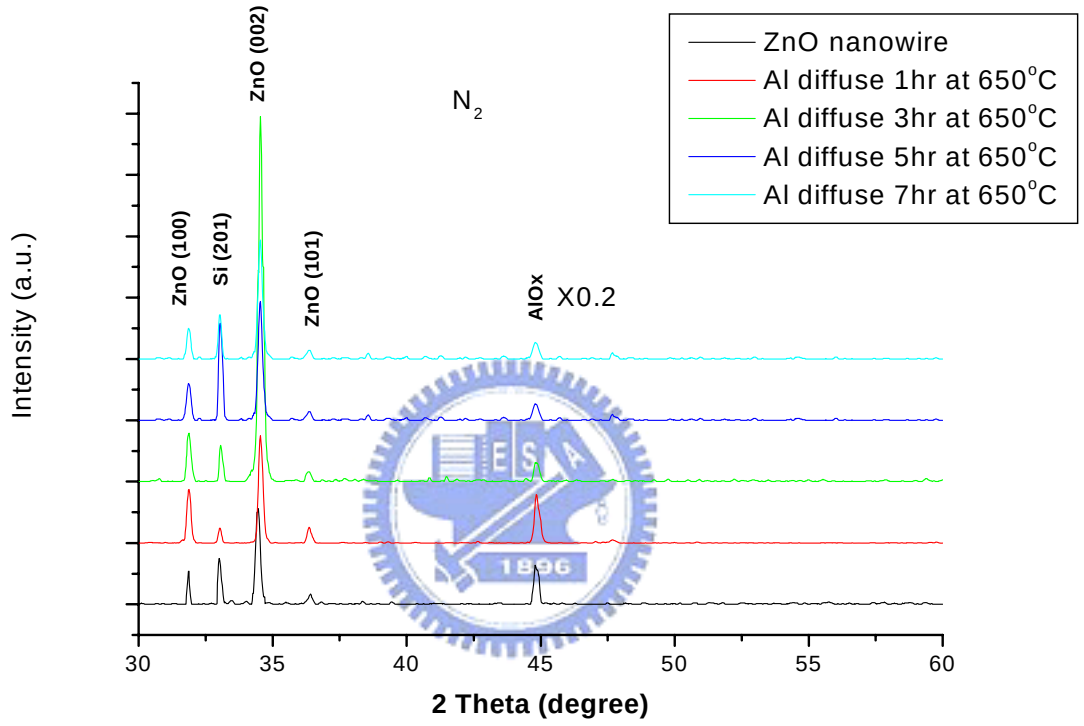


**Figure 4-45 The X-ray diffraction pattern of Al-doped ZnO nanowires grown at 650℃ in nitrogen atmosphere**

| Dffusion time | At.% of Al in the ZnO nanowires at X=50nm | At.% of Al in the ZnO nanowires at X=125nm | At.% of Al in the ZnO nanowires at X=200nm | At.% of Al in the ZnO nanowires at X=275nm | At.% of Al in the ZnO nanowires at X=350nm |
|---|---|---|---|---|---|
| 0 hour | 0 | 0 | 0 | 0 | 0 |
| 3 hours | 0.33 | 0.23 | 0.10 | 0.06 | 0.02 |
| 5 hours | 0.46 | 0.28 | 0.20 | 0.10 | 0.08 |
| 7 hours | 0.54 | 0.31 | 0.23 | 0.17 | 0.16 |

**Table 4-2 The atomic percent of Al in the ZnO nanowires under different thermal process time in oxygen atmosphere in different distance from the Al thin film at 550°C**

| Dffusion time | At.% of Al in the ZnO nanowires at X=50nm | At.% of Al in the ZnO nanowires at X=125nm | At.% of Al in the ZnO nanowires at X=200nm | At.% of Al in the ZnO nanowires at X=275nm | At.% of Al in the ZnO nanowires at X=350nm |
|---|---|---|---|---|---|
| 0 hour | 0 | 0 | 0 | 0 | 0 |
| 3 hours | 0.39 | 0.28 | 0.17 | 0.13 | 0.11 |
| 5 hours | 0.63 | 0.33 | 0.22 | 0.18 | 0.15 |
| 7 hours | 1.1 | 0.81 | 0.46 | 0.24 | 0.18 |

**Table 4-3 The atomic percent of Al in the ZnO nanowires under different thermal process time in nitrogen atmosphere in different distance from the Al thin film at 550°C**

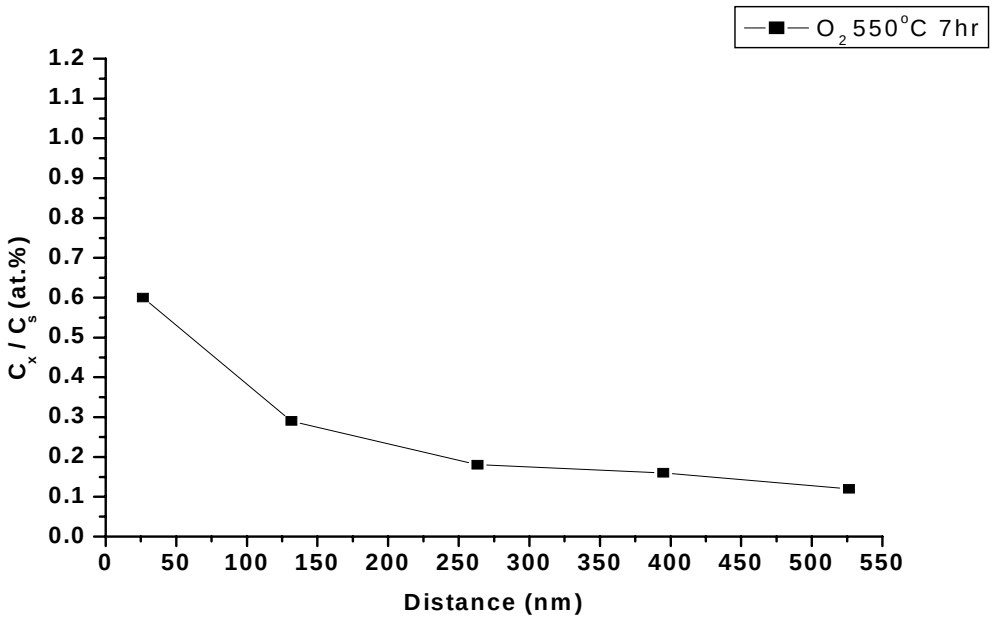


**Figure 4-46 The diffusion of Al into the ZnO nanowires at 550℃ heating 7 hours in oxygen atmosphere**

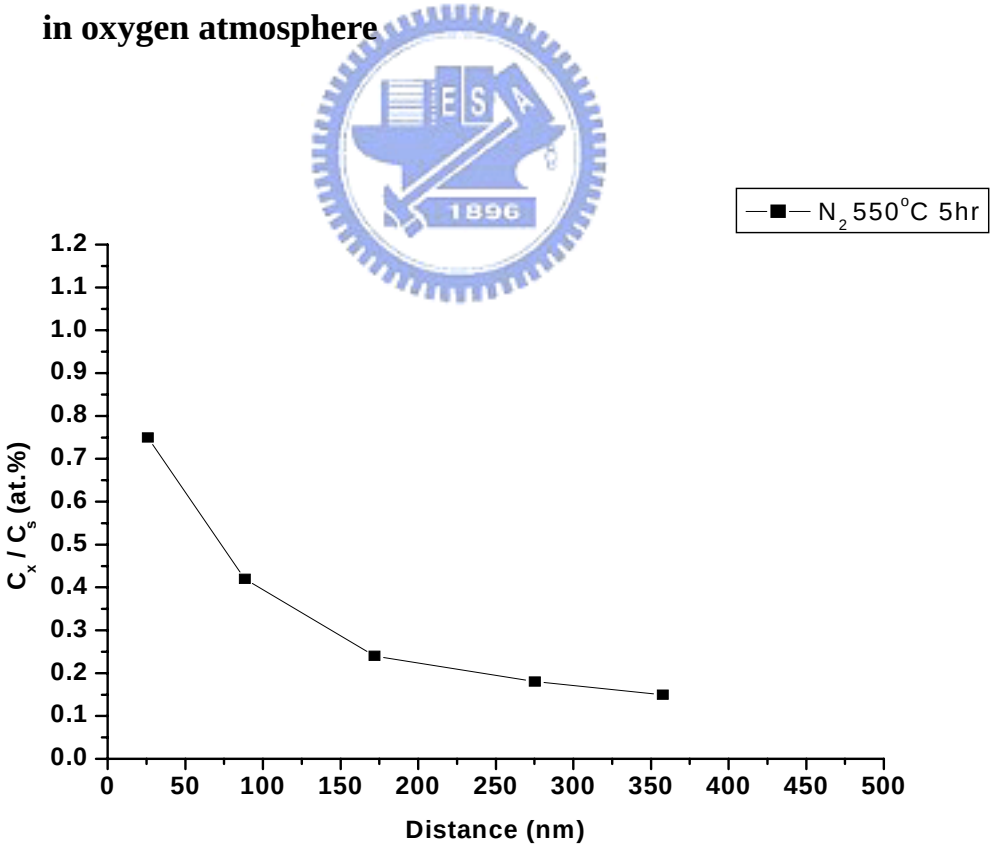


**Figure 4-47 The diffusion of Al into the ZnO nanowires at 550℃ heating 5 hours in nitrogen atmosphere**

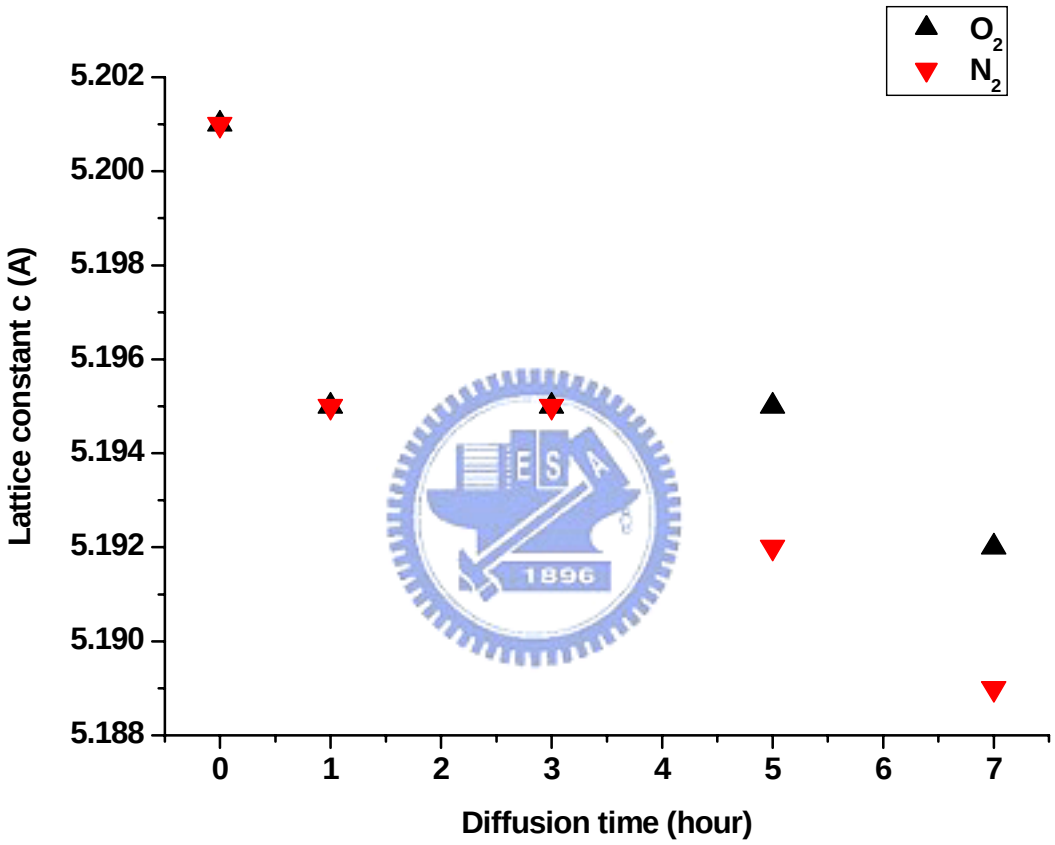


**Figure 4-48 The lattice constant of Al in the ZnO nanowires at 550℃ in oxygen and nitrogen atmosphere**